

ORIGIN OF MEGA-GOLD PLACER DEPOSITS IN THE LIGHT
OF DATA ON THE BUKON JEDEH DEPOSIT, LIBERIA,
AND ON THE TARKWA DEPOSIT, GHANA.

by

Isaac O. Boadi

Submitted in Partial Fulfillment of
the Requirements for the degree of
Doctor of Philosophy

NEW MEXICO INSTITUTE OF MINING AND TECHNOLOGY

Socorro, New Mexico

December, 1991

PROJECT SUMMARY

This dissertation has emerged from studies on two gold deposits in West Africa. The origin of mega-gold placer deposits was addressed by studying a Cenozoic placer deposit in Bukon Jedeh, eastern Liberia, and a Proterozoic paleo-placer deposit in Ghana (Fig. 1). The literature on mega-gold placer deposits is enormous. Nonetheless, several fundamental aspects of this class of gold deposits, particularly those pertaining to their genesis, are poorly understood. The sources of gold in mega-placers, the nature of their source terranes and their overall higher content of gold when compared with modern placers remain enigmatic. In the Witwatersrand basin, South Africa, and the Tarkwa basin, Ghana, where these deposits are extensively mined and also studied, the deposits are hosted by mature sedimentary units in which clues on the nature of source terranes and sources of gold are invariably obscured. It is quite clear from the extensive nature of the auriferous units in the basins, that gold was deposited by numerous streams draining large catchment areas with anomalous levels of gold.

The Bukon Jedeh deposit, covered in Part I of this dissertation, was studied because it represents a primitive and relatively undisturbed placer deposit in which there are abundant clues on the nature of source rocks and processes involved in its formation. The deposit which was determined

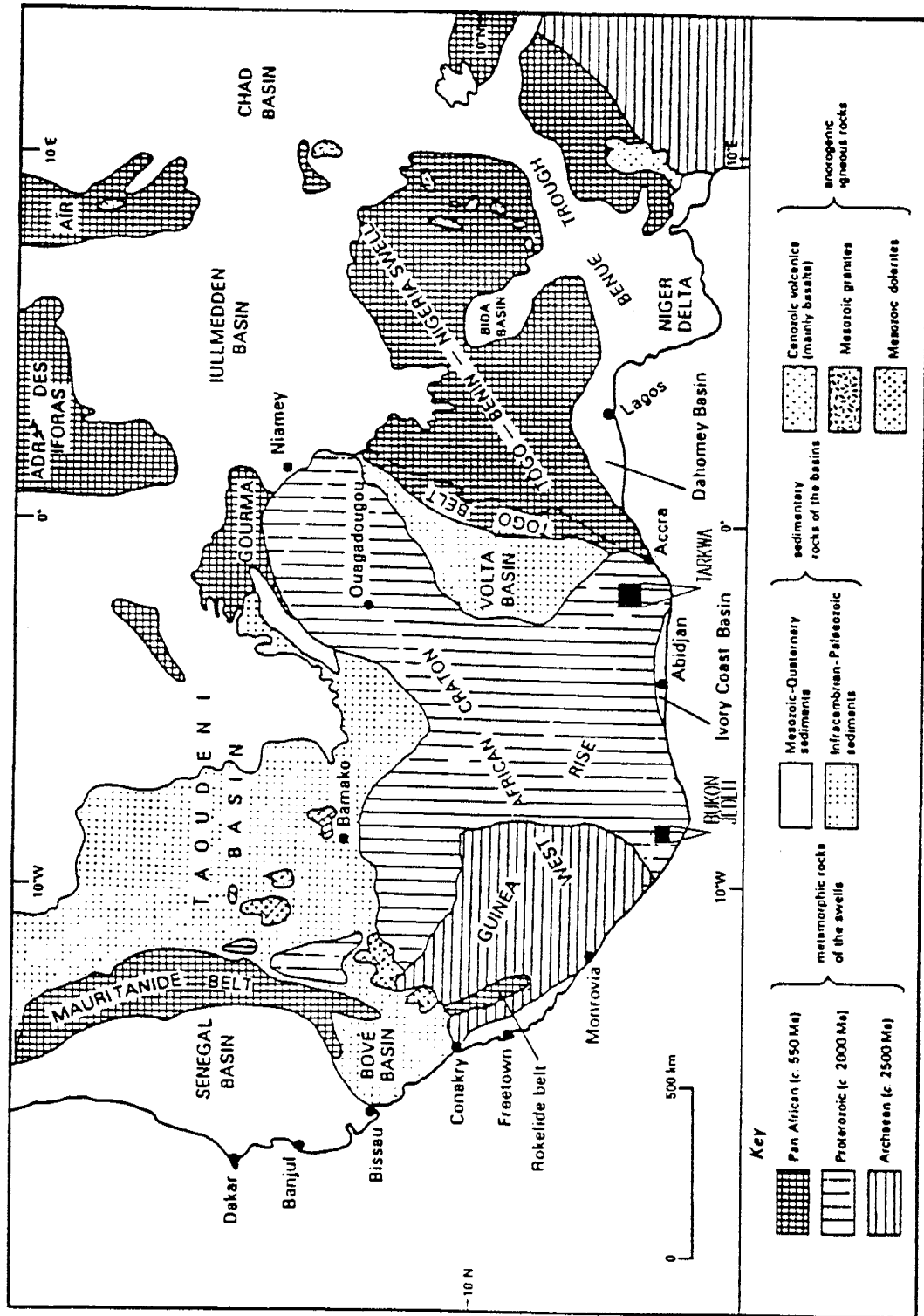


Fig. 1. Regional geologic Map of West Africa showing location of Bukon Jedeh and Tarkwa deposits (after Wright et al., 1985).

in this study to have formed in situ during chemical weathering of underlying bedrock, is a source of gold for numerous smaller placer deposits within alluvial plains of streams that originate from Bukon Jedeh. The district has dimensions exceeding 50 sq. km. The origin of gold in the Bukon Jedeh deposit bears relationship to the source of gold in major paleoplacer deposits because it provides an example of terranes over which large surficial deposits with elevated concentrations of gold may develop during chemical weathering. These surficial deposits would supply auriferous sediments to multiple streams discharging into adjacent basins in event of an uplift. The morphology, grade and size distribution of gold in laterite profiles, and the minor and trace element chemistry of gold nuggets and grains from the Bukon Jedeh deposit were studied to determine processes leading to the formation of this deposit. Protore of the lateritic deposit was studied and serves as an example of the type of primary mineralization likely to be present in the source terranes of paleoplacer deposits. Petrographic and geochemical data on bedrock in Bukon Jedeh are presented and provide constraints on lithologic packages and tectonic settings that contain broadly disseminated low grade gold mineralization envisaged to be present in source areas of major paleoplacer deposits.

The nature of source terrane and origin of gold in the Tarkwa paleoplacer deposit is covered in Part II of the

dissertation. The Tarkwa basin occurs within the same Proterozoic greenstone succession present in Bukon Jedeh. The occurrence of large, low grade primary mineralization in Bukon Jedeh rocks thus suggests that fertile source terranes necessary to provide gold for mega-placers do exist in the Proterozoic greenstone belts of West Africa. The distribution of gold in sedimentary units within the Tarkwa basin was studied. Immature sediments in the basin have grades that are comparable to average gold contents of the surficial deposit in Bukon Jedeh. The distribution of gold, and high content of angular volcanic fragments in the immature sediments show they have experienced minimal reworking since they were deposited in the basin. They are therefore interpreted to represent direct erosional products of material in source area that was being eroded. Analysis of volcanic fragments from the immature sediments show derivation of the sediments from source rocks with low grade disseminated gold mineralization. Sedimentological factors responsible for concentrating gold to the levels observed in mega-placers were investigated: the effect of reworking (packing and sorting) on gold content of mega-placers is addressed. Geochemical data on the volcanic fragments, petrography of the auriferous sediments, and minor and trace element chemistry of gold from the Tarkwa basin all indicate that processes in the source area of the Tarkwa deposit are similar to those involved in the formation of the lateritic deposits.

Data presented on the two deposits covered in this dissertation provide a documentation on source rocks, and a spectrum of processes that operate in source areas and within sedimentary basins to generate mega-gold placer deposits.

ACKNOWLEDGEMENT

This study was made possible by grants from the Rockefeller Foundation (African Dissertation Internship Award RF 88038, #52), the New Mexico State Mining and Mineral Resources Research Institute, a Charles F. Park, Jr award and a Fellowship from Mr Kenneth A. Ross Jr., owner of Bentley Mines, Liberia. Anton and Anita Budding, and the Geological Society of America also provided extra financial assistance. All of my sponsors are duly acknowledged for their support to this study and their continued committment to scientific research.

Dr. David Norman, chairman of my advisory committee, travelled to Ghana and Liberia to visit with me in the field. His input in this study has been considerable and is much appreciated. Dr. Philip Kyle, Dr. Andrew Campbell and Dr. James Robertson are all gratefully acknowledged for their participation in the study, and their critical review of the dissertation. Dr Kyle and his graduate student, Grazyna Zreda, are acknowledged for their help in the acquisition of the neutron activation data on gold samples from Ghana and Liberia. Mr. G. O. Kesse, director of the Ghana geological survey, provided considerable logistic support for the field work in Ghana. He is acknowledged for that and also for his thorough review of the dissertation. The assistance of Dr. William Chavez and Dr. Brian Patrick on the petro-

graphic aspects of this study is very much appreciated.

Geologists at various mining companies in Ghana assisted in this study. B. Nunoo, A. Tsiriku and W. Shamo (TGF Co.), J. Amanor, W. Gyapong (AGC), (Mintah and his colleagues (PGF Co.) are duly acknowledged. R. S Nartey and Peter Pshorr assisted in the field work in Ghana and in Liberia, respectively. The Liberian Lands and Mines Ministry granted permission for rock, soil and gold samples to be exported out of Liberia for analysis.

Isotopic analysis for this study was conducted at Dr. Douglas Brookins geochronology laboratory at the University of New Mexico, Albuquerque, with much help from Mike Ward. Other geochemical analysis were performed at facilities at the New Mexico Bureau of Mines and Mineral Resources in Socorro. The drafting staff at the Bureau is credited with the figure on the model presented in this dissertation for the formation of mega-gold placers.

My office mate, Ingar Walder and I spent endless hours discussing our individual research topics. I learned a great deal from our discussions, particularly on the evolution of ore fluids during magma generation. I have enjoyed the companionship and support of other students in geoscience to whom I extent my profound appreciation.

I would like to thank the Chairman of the Geoscience Department, Dr. John Schlue, and the secretaries: Pat., Connie and Nancy for helping to make my stay at Tech a pleasant and memorable one. The same feeling of gratitude is conveyed to the Dean of graduate school, Dr. Alan Smoke and his secretary, Mrs Mary Finley.

TABLE OF CONTENT

	Page
PREFACE	i
ACKNOWLEDGEMENT	vi
TABLE OF CONTENT	ix
LIST OF FIGURES	xi
LIST OF TABLES	xiii
PART I	1
ABSTRACT	2
INTRODUCTION	5
Regional Geology	6
Previous work	9
BEDROCK GEOLOGY	10
Metamorphic rocks	10
Intrusive rocks	18
Structure and metamorphism	18
ROCK GEOCHEMISTRY	22
GOLD MINERALIZATION	37
Alluvial gold	37
Lateritic gold	38
Bedrock mineralization	59
Gold composition	62
DISCUSSION	74
Tectonic setting	74
Timing of primary mineralization	74
Nature of primary mineralization	75
Origin of lateritic deposits	79
Source of alluvial gold	90
CONCLUSIONS	91
REFERENCES	94
APPENDIX 1-A	100
APPENDIX 1-B	104
APPENDIX 1-C	105
APPENDIX 1-D	109
APPENDIX 1-E	114
APPENDIX 1-F	117
PART II	118
ABSTRACT	119
INTRODUCTION	122
Regional geology	127
Birimian Supergroup	127
Tarkwaian Group	128
Gold deposits	132
Source area problem	136
Methods of investigation	138
GEOLOGY OF THE BANKET FORMATION	140
Stratigraphy, composition and texture	140
Detrital heavy minerals	152
Sphericity and Oblate-prolate indices	152
GEOLOGY OF THE KAWERE FORMATION	159

GOLD MINERALIZATION IN BANKET SEDIMENTARY UNITS	160
Gold composition	172
LITHIC FRAGMENTS	178
Petrography	178
Geochemistry	183
Rb-Sr isotopic systematics	190
DISCUSSION	197
Source of gold	197
Composition and nature of source terrane	197
Nature of mineralization in source area	199
Placer formation and concentration of gold	200
Model	202
CONCLUSIONS	206
REFERENCES	208
APPENDIX 2-A	214

LIST OF FIGURES

<u>Figure</u>	<u>Page</u>
1.2 Location of a) Bukon Jedeh, b) major shear zones ...	7
1.3 Geologic Map of the Bukon Jedeh area ...	12
1.4 Photomicrograph of a) pyroxene-bearing gneiss, b) XRD spectra of graphite ...	15
1.5 Modal classification of granitoids ...	20
1.6 TiO ₂ versus (Fe ₂ O _{3T} +MgO) plot of samples of the garnet-bearing gneiss from Bukon Jedeh ...	25
1.7 Zr/TiO ₂ versus Nb/Y plot of samples of the Pyroxene-bearing gneiss and amphibolite from Bukon Jedeh ...	27
1.8 Ab-An-Or plot of granitoid samples from Bukon Jedeh ...	29
1.9 Al ₂ O ₃ /(Na ₂ O+K ₂ O+CaO) versus Al ₂ O ₃ /(Na ₂ O+K ₂ O) plot of granitoid samples from Bukon Jedeh ...	31
1.10 Rb versus (Y+Nb) tectonic discrimination diagram	33
1.11 CaO+MgO-SiO ₂ /10-Na ₂ O+K ₂ O ternary plot of rocks from Bukon Jedeh ...	35
1.12 Photographs of alluvial and lateritic gold ...	39
1.13 Soil profiles ...	46
1.14 Histograms of gold grades in Bukon Jedeh laterite and bedrock ...	48
1.15 Contour of gold values in laterite ...	51
1.16 SEM and XRD spectra ...	55
1.17 Simplified geologic map of study area with locations of bedrock samples and their gold grades ...	60
1.18 (a) Photomicrograph of mineralized bedrock sample with the assemblage py, py and cpy, (b) photomicrograph of bedrock sample from Bukon Jedeh showing sulphide phases along selvages within graphite ...	63

1.19a	Ag-Sc plot of alluvial/lateritic gold	...	70
1.19b	Ag-Sb plot " " "	...	72
1.20	Sulphide speciation and gold mobility	...	82
2.1	Geologic map of south western Ghana	...	125
2.2	Geologic map of the Tarkwa basin	...	130
2.3	Generalized stratigraphic column of the Banket Formation showing the reef zones	...	134
2.4	Distribution of immature and mature sedimentary units of the Banket in the Tarkwa basin	...	141
2.5	Photographs of Banket sediments at Iduapriem and Teberebie	...	143
2.6	Photographs of mature banket sediments at Akoon, Apinto and Fanti	...	148
2.7	Photomicrograph showing gold associated with detrital hematite and zircon in West Reef	...	153
2.8	Sphericity versus Oblate-Prolate Index diagram	...	157
2.9	Photograph of Kawere conglomerate	...	160
2.10	Detailed stratigraphic column and gold content of the Banket Formation at Iduapriem, Teberebie and Akoon	...	163
2.11	Histogram of gold value in Banket sediments	...	166
2.12	Histogram showing gold grades in (a) loose and compact reefs at Akoon Apinto and Fanti areas, (b) well sorted versus poorly sorted reefs	...	169
2.13a	Ag-Sc plot of Tarkwa paleoplacer gold	...	174
2.13b	Ag-Sb plot of Tarkwa paleoplacer gold	...	176
2.14	Photomicrographs of thin sections of Birimian rocks	...	180
2.15	Zr/TiO ₂ versus Nb/Y variation diagram	...	185
2.16	Rb-SR isochron plots	...	193
2.17	Schematic illustration of genetic model	...	204

LIST OF TABLES

1.1	Mineralogy of Bukon Jedeh rocks	... 14
1.2	Selected geochemical data on supracrustal and intrusive rocks from Bukon Jedeh	... 23
1.3	Instrumental neutron activation analysis of gold sample from Liberia	... 67
2.1	Oblate - prolate index diagram	... 155
2.2	Instrumental neutron activation analysis of gold samples from Ghana	... 173
2.3	Selected geochemical data on Birimian rocks and volcanic fragments from the Banket Formation	... 184
2.4	INAA data on lithic fragments for Au, Ag, etc	... 187
2.5	Rb - Sr isotopic analysis	... 192

PART I

BUKON JEDEH GOLD DEPOSITS, LIBERIA,
WEST AFRICA

ABSTRACT

Bedrock in Bukon Jedeh is Proterozoic and comprises mainly of pyroxene- and garnet-bearing gneisses, amphibolites, granitoids and gabbroic intrusives. Mineralogy, texture and geochemical analysis indicate protoliths of pyroxene- and garnet-bearing gneisses to be volcanic and volcanoclastic rocks of intermediate composition. The amphibolite is similarly indicated to have a protolith of basalt to basaltic andesite composition. Granitoid samples have the mineralogy and chemistry of I-type granitoids that formed in volcanic arc setting. Mineral assemblages indicate upper amphibolite to granulite facies metamorphism.

Lateritic and primary gold mineralization occur in Bukon Jedeh associated with an ENE - WSW trending chain of hills covering a terrane about 3 km by 50 km. Lateritic gold is present in clay-rich soils, 0.2 to 2 m thick, and in underlying deeply weathered bedrock at grades of 0.04 to 6 ppm. Grain-size of gold decreases down the profile. Over 70% of the gold from the soils exceed 1 mm in diameter. Nuggets up to 20 mm in diameter are common, particularly in the top ferruginous zone where they are associated with iron oxides and graphite. In saprolite, gold grains range from 100 microns to 1 mm in diameter. Gold nuggets and grains in the laterite have angular crystalline and concretionary shape,

and are indicated by instrumental neutron activation analysis to contain less than 4 wt. % Ag, and minor to trace amounts of Hg, Sc, Zr, Th, Hf and rare earth elements. Gold from mesothermal vein deposits contain greater than 20 wt. % Ag, minor to trace amounts of Hg and Sb. Bedrock assays indicate anomalous to ore-grade levels of gold (0.05 to 8 ppm) in all of the different rocks represented in Bukon Jedeh. Primary mineralization is broadly disseminated and associated with pyrite, pyrrhotite, chalcopyrite and minor arsenopyrite. Petrographic data on mineralized rocks indicate primary gold is minute to sub-microscopic in size.

Lateritic deposits at Bukon Jedeh formed from refractory primary ores during weathering of underlying bedrock. They differ from other lateritic deposits by the coarseness of their gold grains and common occurrence of gold nuggets. Gold is of secondary origin and formed in situ by dissolution and reprecipitation of primary gold grains liberated in the weathering zone. Metastable sulphur species generated by oxidation of sulphide minerals in the weathering zone, and organic acids formed by decay of organic litter were the probable species responsible for the dissolution and remobilization of gold. Indicated molecular to micron grain size of primary gold also facilitated dissolution of gold and promoted the formation of gold nuggets in the lateritic soils. Alluvial gold, hosted by gravel deposits on a network

of drainages in Bukon Jedeh, was derived from lateritic deposits by erosional processes.

Primary gold in bedrock is enigmatic lacking structural or distinct lithologic controls. Textural data indicate mineralization occurred prior to or during metamorphism. Mineralization is thought to be syngenetic and formed within carbon-bearing sediments and volcanics, with redistribution of ore minerals during regional metamorphism.

Introduction

Gold in laterite is a new class of ore deposits about which there is limited published data. Lateritic gold deposits represent low grade but readily accessible sources of gold. Until about a decade ago, these deposits were considered uneconomic owing to their low gold content. However, with increasing availability of effective and relatively inexpensive metallurgical processes for the treatment of lateritic ores (Kennedy, 1989), this class of gold deposits has become an important source of gold and is the focus of numerous exploration programmes in Australia, Africa, South America and India (Butt, 1988; Freyssinet et al., 1989 (a and b); Bowell et al., 1991; Davy and El-Ansary, 1986; Santosh and Omana, 1991). By far the largest, and perhaps, the most extensively studied of these deposits is the Boddington deposit in Western Australia with published reserves of 60 million metric tons of ore at an average grade of 1.6 g/metric ton (Roth et al., 1991).

The Bukon Jedeh gold deposits in eastern Liberia, West Africa, belong to this class of gold deposits. A typical profile of the laterite hosting the Bukon Jedeh deposits consists of thinly developed soils over deeply weathered and graphite-bearing bedrock. The laterite contains extensive low grade ore and has been worked by small-scale Liberian miners for over six decades. Although they share several

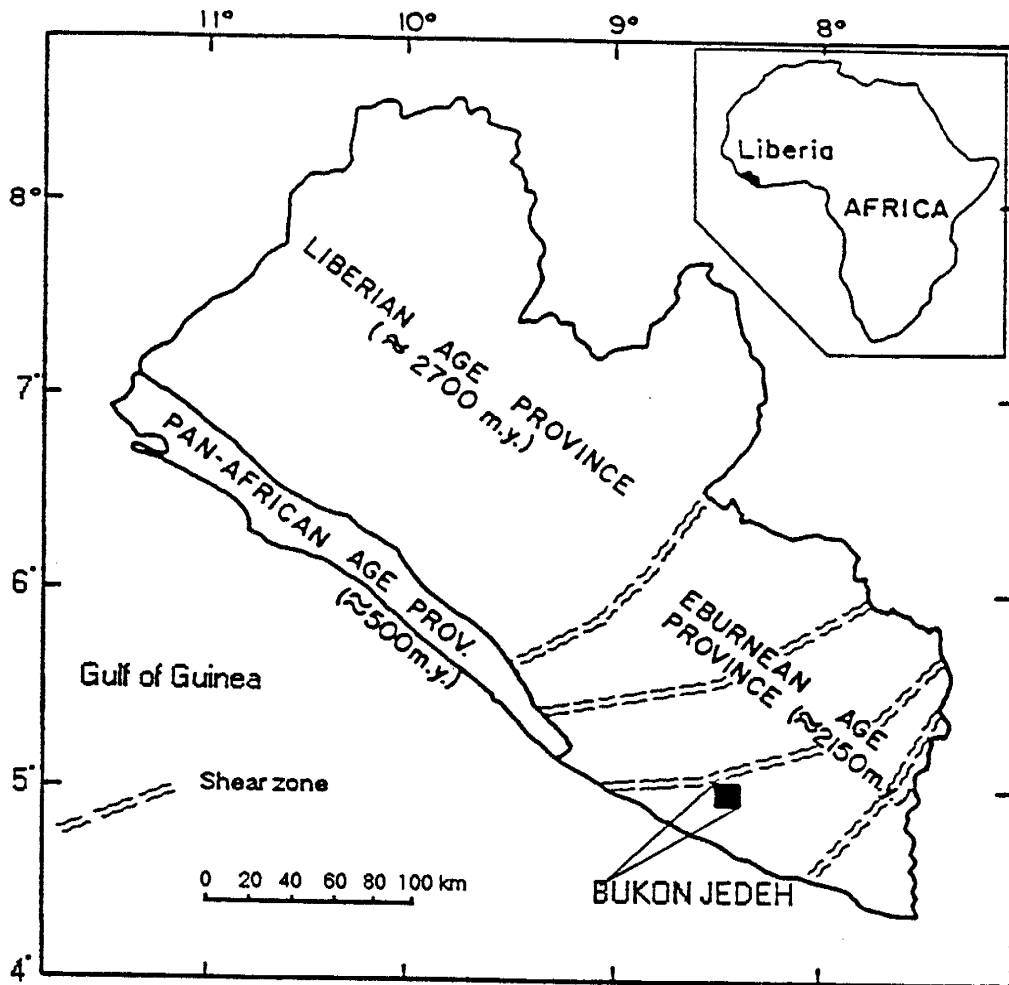
common features with the Boddington and other lateritic gold deposits, the grade, size distribution and geochemistry of gold at Bukon Jedeh are unique.

The local geology, and geochemistry of bedrock and ore minerals were studied to determine the nature of source rocks and its gold content, and the processes that formed the lateritic gold deposits in Bukon Jedeh.

Regional Geology

Liberia is underlain mostly by crystalline Precambrian rocks that are a part of the West African craton (Fig. 1.2). Bukon Jedeh lies within the Eburnean age province (2.15 Ga). Precambrian basement rocks are cut by a swarm of NW-SE trending diabase dikes of Jurassic age which intrude along a system of faults related to the opening of the Atlantic Ocean (Tysdal, 1977; Wright et al, 1985). Several major NNE to NE trending faults and shear zones characterized by broad zones of mylonites occur in Proterozoic rocks of eastern Liberia (Fig. 1.2). These have evidence of left lateral strike-slip movement (Tysdal, 1977; Brock et al., 1977) and mark lithotectonic contacts of highly diversified terranes suggesting that they represent suture contacts resulting from the closure of small back arc and inter-arc basins (Wright et al., 1985).

FIG. 1.2 Age province map of Liberia (modified from Tysdal and Thorman, 1983) showing major shear zones in the Eburnean (Proterozoic) province, and the location of the Bukon Jedeh area.



The Bukon Jedeh gold deposit is located adjacent to and immediately south of the Dugbe shear zone, one of the NE-SW trending shear systems. The terrane north of the structure consists of leucocratic gneisses and is characterized by a widespread occurrence of iron formations consisting of oxide and silicate facies. In Bukon Jedeh just south of this structure, there are no iron formations. Rather, graphitic units and manganese formations characterize this terrane (Tysdal, 1977). Major rock types in this area include gneisses, amphibolites, quartzites, granites and ultramafic intrusives.

Previous work

Gold mineralization in Bukon Jedeh was mentioned by Griethuysen (1971) and Tysdal (1978). Both note the anomalous concentration of gold in that area and refer to the mineralization as placers originating from small quartz veins. Molybdenum anomalies in the Bukon Jedeh area are reported to be in close spacial association to gold mineralization (Griethuysen (1971). Boadi and Norman (1990) and Boadi et al., (in prep.) report the occurrence of nuggets in lateritic soils and extensive low grade gold occurrences in both soils and bedrock.

BEDROCK GEOLOGY

Rock units within an area approximately 18 sq. km in size were mapped at a scale of 1:10,000. Bedrock in the area consists of gneisses and amphibolites that are intruded by granitoids and meta-gabbro. Petrographic study of 40 thin sections and corresponding hand specimens of these rock units was conducted. All thin sections examined indicated a fresh or unaltered mineralogy and showed no visible indications of alteration subsequent to crystallization.

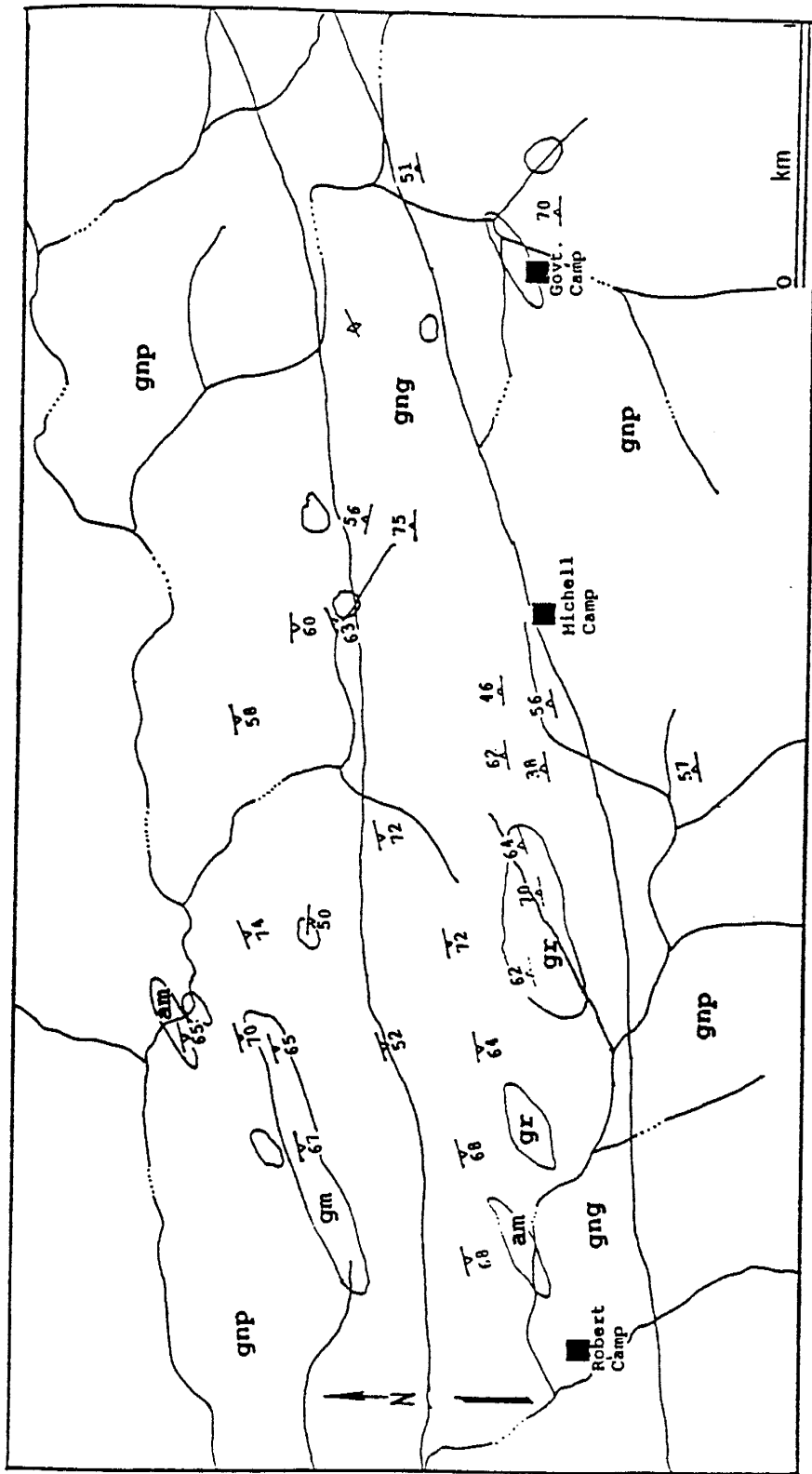
Metamorphic rocks

Bukon Jedeh gneisses are subdivided into pyroxene-bearing, and garnet-bearing gneisses (Fig. 1.3). Both units contain disseminated micaceous, carbonaceous matter (Fig 1.4a) with good X-ray diffraction patterns for graphite (Fig. 1.4b). The garnet-bearing gneiss contains a distinct megascopic banding that commonly characterize para-gneisses. Quartz veins, a few centimeters to several meters wide, occur along foliation planes within garnet-bearing gneiss. The veins are laterally persistent and have been traced along strike for more than 100 meters in areas of good exposure. The pyroxene-bearing gneiss is strongly foliated, although much less heterogeneous as compared with the garnet-bearing gneiss. Both gneisses are medium to coarse-grained in thin section and have a granoblastic texture consisting of quartz and

plagioclase crystals with large poikiloblasts of pyroxene or garnet (Table 1.1). Potassic feldspar is rare in the pyroxene-bearing gneiss and occurs only as antiperthitic intergrowths within the plagioclase. Perthitic and antiperthitic intergrowths are also common in the feldspars of the garnet-bearing gneisses. The mineralogical composition and texture of the gneisses suggest they are products of volcanic and volcanoclastic rocks of mafic to intermediate composition.

Small lenticular bodies of medium grained amphibolite occur within the gneisses (Fig. 1.3, Table 1.1). An absence of modal quartz in the amphibolite suggests a basaltic protolith.

FIG. 1.3 Geologic map of Bukon Jedeh.



LEGEND

Supracrustals	Intrusives	Symbols
Pyroxene-bearing gneiss	Granitoid	contact
Garnet-bearing gneiss	Meta-gabbro	64 strike and dip of foliation
Amphibolite		stream

Table 1.1 Mineralogy of Bukon Jedeh rocks given in vol % of constituent minerals.

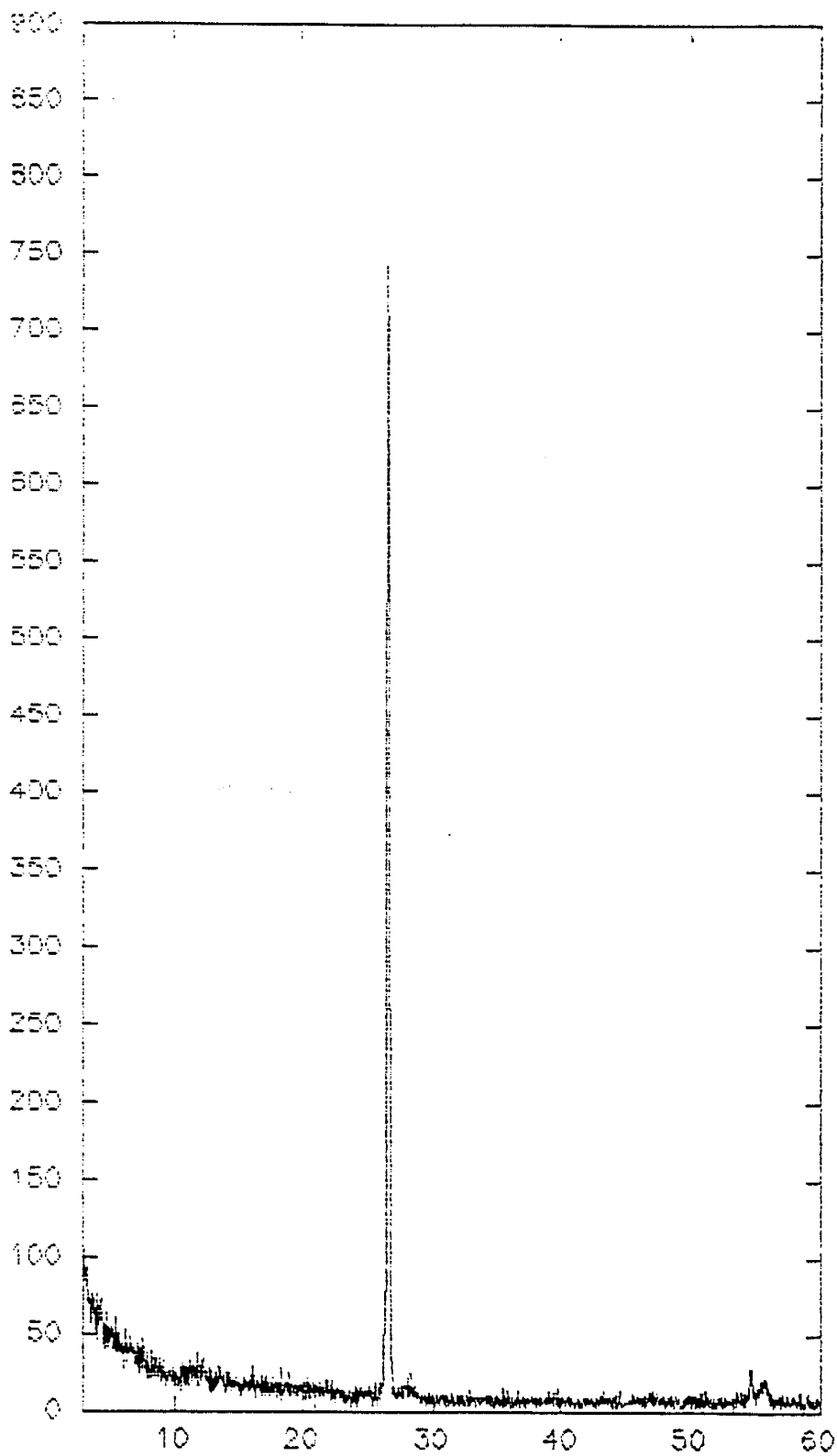
Rock unit	Mineralogy (%)									
	Qtz	Plg	KF	Bio	Opx	Cpx	Hbl	Garnet	S ²⁻	
Px-gneiss	20-30	30-40		10-15	5-15	10-20	0-10		2-5	
Gnt-gneiss	20-40	20-40	0-35	15-25				5-20	2-5	
Amphibolite	<3	35-40		<3		20-30	30-35		2-5	
Meta-gabbro		15-20			15-20	25-30	20-25		2-5	
Granitoid	25-35	15-50	5-35	5-10		0-15	0-10			

FIG. 1.4 a) Photomicrograph of pyroxene-bearing gneiss with graphite and sulphide, b) X-ray diffraction spectra of graphite from bedrock.



(a)

Counts



2θ

Intrusive rocks

Granitic intrusive rocks occur as small lenses within the gneisses. They are generally massive or possess only a weak foliation, are pyroxene-bearing and may contain up to 15% hornblende (Table 1.1). On a Quartz - K-rich alkali Feldspar - Plagioclase plot after Streckeisen (1976), the granitoids plot in the fields of granite, granodiorite and tonalite (Fig. 1.5). A small lense of coarsely crystalline metagabbro intrudes into the gneisses (Fig. 1.3). Photomicrographs of the different rock types from Bukon Jedeh are in Appendix 1-B.

Structure and metamorphism

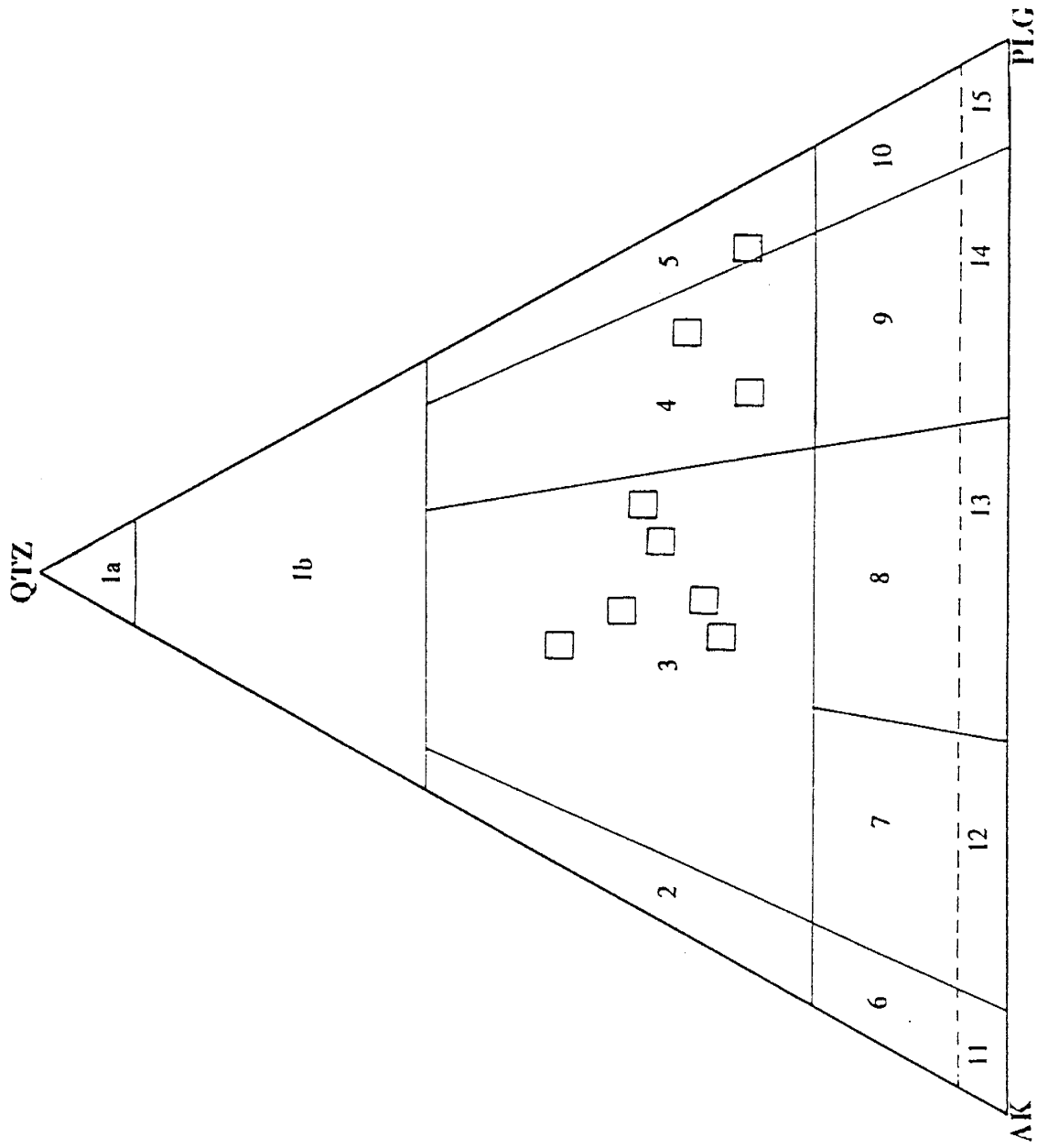
Rocks in the Bukon Jedeh area are folded into a synform with the axis trending E to ENE. Dominant foliation in the rocks is marked by the alignment of phyllosilicates, hornblende and pyroxene, and parallels the axis of the synform.

Perthitic and anti-perthitic textures in feldspars commonly observed in thin sections of the gneisses indicate high grade metamorphic conditions for the Bukon Jedeh rocks (Dymek and Schiffries, 1987). Mineral assemblages plagioclase + clinopyroxene + orthopyroxene + quartz + biotite +/- hornblende +/- garnet and plagioclase + microcline + quartz + garnet + biotite identified in the gneisses, and the assemblages plagioclase + clinopyroxene + hornblende and

plagioclase + clinopyroxene + orthopyroxene + hornblende in the mafic units (Table 1.1) indicate an upper amphibolite to granulite facies metamorphism (Best, 1982). Microtextures observed in thin section indicating the co-existence of strained and unstrained minerals suggest pre-, syn-, and post kinematic growth of metamorphic minerals resulting from multiple episodes of deformation in the rocks.

FIG. 1.5 Classification of granitoids using modal composition in vol. % (normalized). After Streckeisen, 1976.

Modal analysis are in appendix 1-B. The fields on figure are 1a) Quartzolite, 1b) quartz-rich granitoids, 2) alk. feldspar granite, 3) granite, 4) granodiorite, 5) tonalite, 6) alk. feldspar quartz syenite, 7) quartz syenite, 8) quartz monzonite, 9) quartz monzodiorite, 10) quartz diorite, 11) alk. feldspar syenite, 12) syenite, 13) Monzonite, 14) Monzodiorite, 15) Diorite.



ROCK GEOCHEMISTRY

Thirty one geochemical analyses were made of Bukon Jedeh rocks (Appendix 1-C; 1-F). Representative analyses are shown in Table 1.2. Results of the analyses show that the garnet-bearing gneisses have significant amounts of normative corundum (2.5 to 5 wt %) which is consistent with a sedimentary protolith. Analyses of pyroxene-bearing gneiss and amphibolites show little or no normative corundum. These units are assigned volcanic protoliths.

The garnet-bearing gneiss exhibits a major element chemistry quite similar to sandstones of Paleozoic turbidite sequence deposited in arc related basins. On a TiO_2 versus $(Fe_2O_{3T} + MgO)$ tectonic discrimination diagram (Bhatia, 1983), samples of this rock unit plot in, or closest to, the fields of oceanic- and continental-island arcs (Fig. 1.6). On a Zr/TiO_2 versus Nb/Y plot after Winchester and Floyd (1977), most samples of the pyroxene-bearing gneiss plot in the andesite field, one plots in the field of subalkaline basalt and another in the dacite field. Amphibolite samples plot in the fields of basalts and basaltic andesite (Fig. 1.7).

Plotting the results of analyses of granitoids on a normative Ab-An-Or ternary diagram indicated that they have a granodiorite to tonalite compositions (Fig. 1.8). However,

Table 1.2. Selected geochemical data on supracrustal and intrusive rocks from Bukon Jedeh (ggn: garnet-bearing gneiss; am: amphibolite; mg: metagabbro; pgn: pyroxene-bearing gneiss and gr: granitoid).

%	IB-35ER ggn	-11BR ggn	-18CR am	-26BR mg	-9DR1 pgn	-11DR pgn	-16CR3 gr
SiO ₂	64.83	61.31	48.03	50.69	61.97	64.72	59.13
TiO ₂	0.64	0.64	1.15	0.36	0.75	0.47	1.09
Al ₂ O ₃	16.38	16.69	14.43	6.50	15.02	13.41	16.57
Fe ₂ O ₃	6.10	6.07	13.48	9.95	7.90	6.08	6.31
MnO	0.07	0.14	0.21	0.17	0.10	0.17	0.09
MgO	2.54	3.24	6.77	16.89	3.09	2.14	2.56
CaO	2.16	2.80	9.95	13.55	5.28	8.64	6.19
Na ₂ O	3.73	3.99	3.44	0.81	3.34	1.34	5.23
K ₂ O	2.26	2.35	0.91	0.37	1.42	0.22	1.25
P ₂ O ₅	0.13	0.10	0.09	0.04	0.22	0.10	0.25
LOI	0.26	0.93	0.48	0.70	0.14	1.62	0.52
Total	99.11	98.25	98.95	100.03	99.24	98.91	99.18

(ppm)

Pb	12	15	10				
Th							
Rb	124	83	11	6	42	5	33
U							
Sr	361	444	268	78	479	678	740
Y	21	21	27	21	21	23	23
Zr	144	145	71	32	153	175	183
Nb	10	9	7	3	7	6	17
Mo	1	1	1	1	1	1	1
Ga	22	21	20	9	18	16	19
Zn	93	96	107	53	77	65	73
Cu	23	63	80	112	21	27	69
Ni	38	52	98	183	49	40	61
Zr/TiO ₂	0.02	0.02	0.01	0.01	0.02	0.04	0.02
Nb/Y	0.48	0.43	0.26	0.14	0.33	0.26	0.74

CIPW MINERAL NORMS (wt. %)

Q	24.80	17.01			20.04	36.21	8.29
C	4.25	2.82					
Or	13.57	14.33	5.53	2.22	8.52	1.34	7.52
Ab	32.07	34.84	25.05	6.96	28.68	11.70	45.05
An	10.03	13.66	21.83	13.21	22.12	30.89	18.37
Ne			2.63				
Di			23.35	43.78	2.46	10.46	9.15
Hy	10.96	13.04		21.74	12.61	5.40	6.04
Ol			16.10	9.08			
Mt	2.79	2.82	3.04	2.24	3.61	2.82	2.89
Il	1.24	1.25	2.24	0.69	1.45	0.92	2.11
Ap	0.31	0.24	0.21	0.09	0.52	0.24	0.59

results of some analyses fall in fields of granite and trondhjemite. All granitoid analyses indicate a low amount of normative corundum and an overall major element chemistry consistent with I-type intrusives (Chappell and White, 1974) (Fig. 1.9). The granitoids are indicated to be metaluminous to slightly peraluminous in character (Shand, 1947) and plot in the volcanic arc field on a tectonic discrimination diagram using Rb versus (Y+Nb) (Fig. 1.10).

Major element chemistry of the metavolcanic-, meta-sedimentary- and intrusive rocks are compared on a $\text{CaO}+\text{MgO}-\text{SiO}_2/10-\text{Na}_2\text{O}+\text{K}_2\text{O}$ ternary plot (after Taylor and McLennan, 1985) (Fig. 1.11). The volcanic and intrusive rocks define a linear trend that suggests derivation of the two from a single evolving magma chamber. Major element chemistries of the pyroxene- and garnet-bearing gneisses are similar which suggest local derivation of the metasediments from the metavolcanic rocks with minimal reworking or dilution. SiO_2 content of the metasediment is low and precludes any significant granitic component to its composition.

FIG. 1.6 TiO_2 versus $(\text{Fe}_2\text{O}_3\text{T} + \text{MgO})$ tectonic setting discrimination plot of samples of the Bukon Jedeh gneiss (after Bhatia, 1983). The fields A, B, C and D represent, respectively, island arc, continental arc, active continental margin and passive margin.

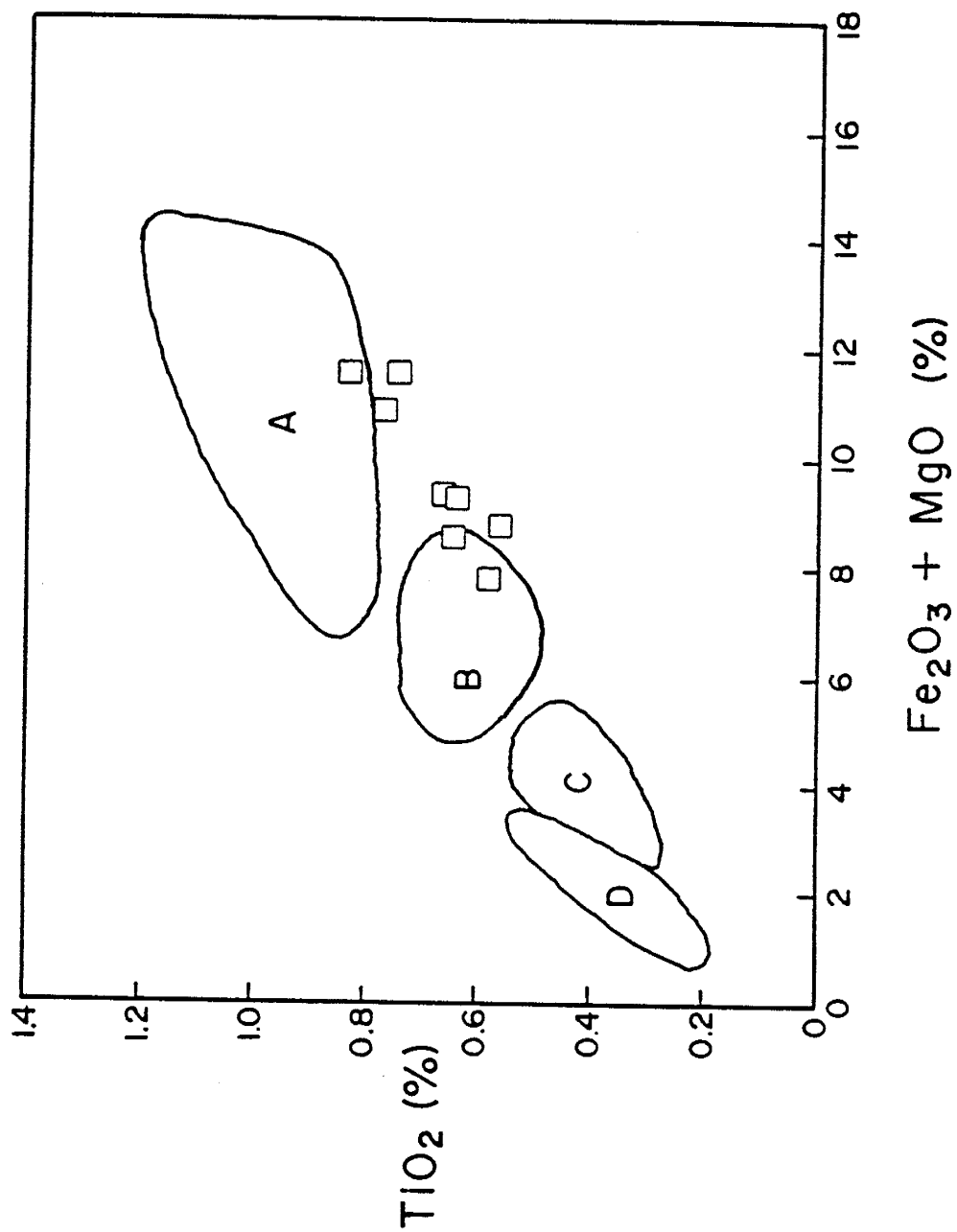


FIG. 1.7 Zr/TiO₂ versus Nb/Y plot of samples of Bukon Jedeh supracrustal rocks with volcanic protoliths (after Winchester and Floyd, 1977): (▲) pyroxene-bearing gneiss, (◆) amphibolite.

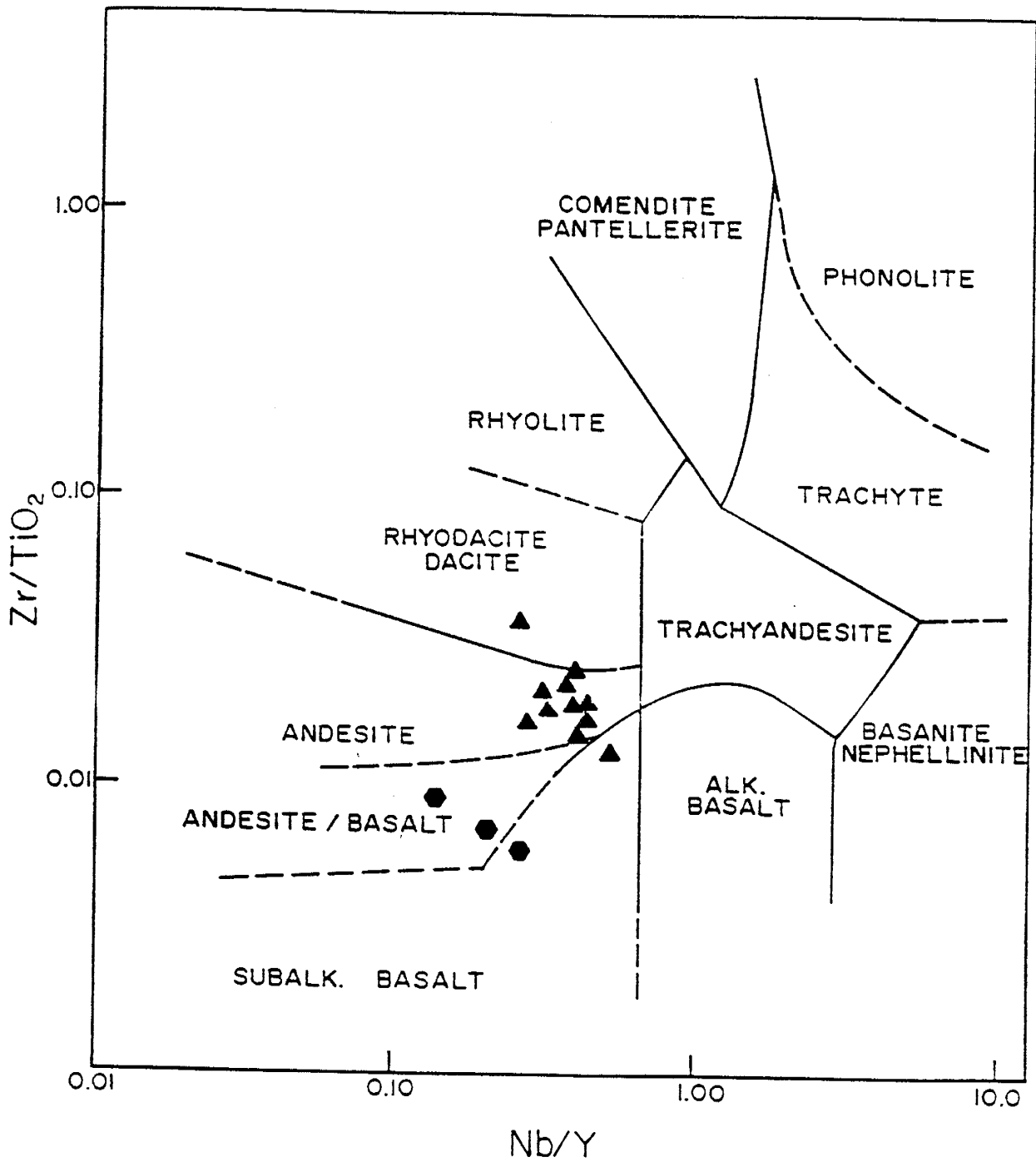


FIG. 1.8 Normative plot of granitoids on An-Ab-Or ternary diagram of Barker (1979).

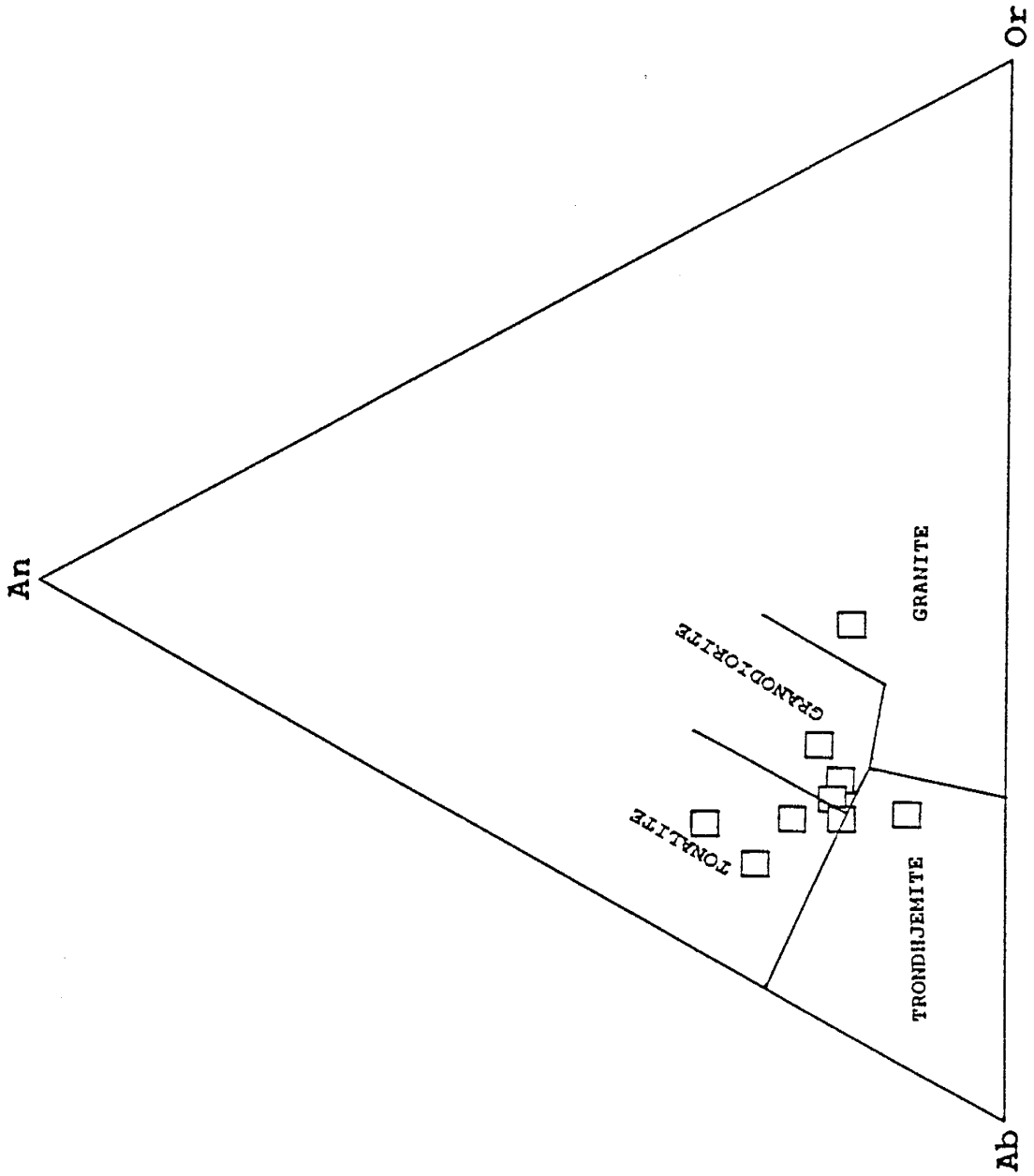


FIG. 1.9 $\text{Al}_2\text{O}_3/(\text{Na}_2\text{O}+\text{K}_2\text{O}+\text{CaO})$ versus $\text{Al}_2\text{O}_3/(\text{Na}_2\text{O}+\text{K}_2\text{O})$ plot of granitoid samples from Bukon Jedeh (after Chappell and White, 1974; Shand, 1947).

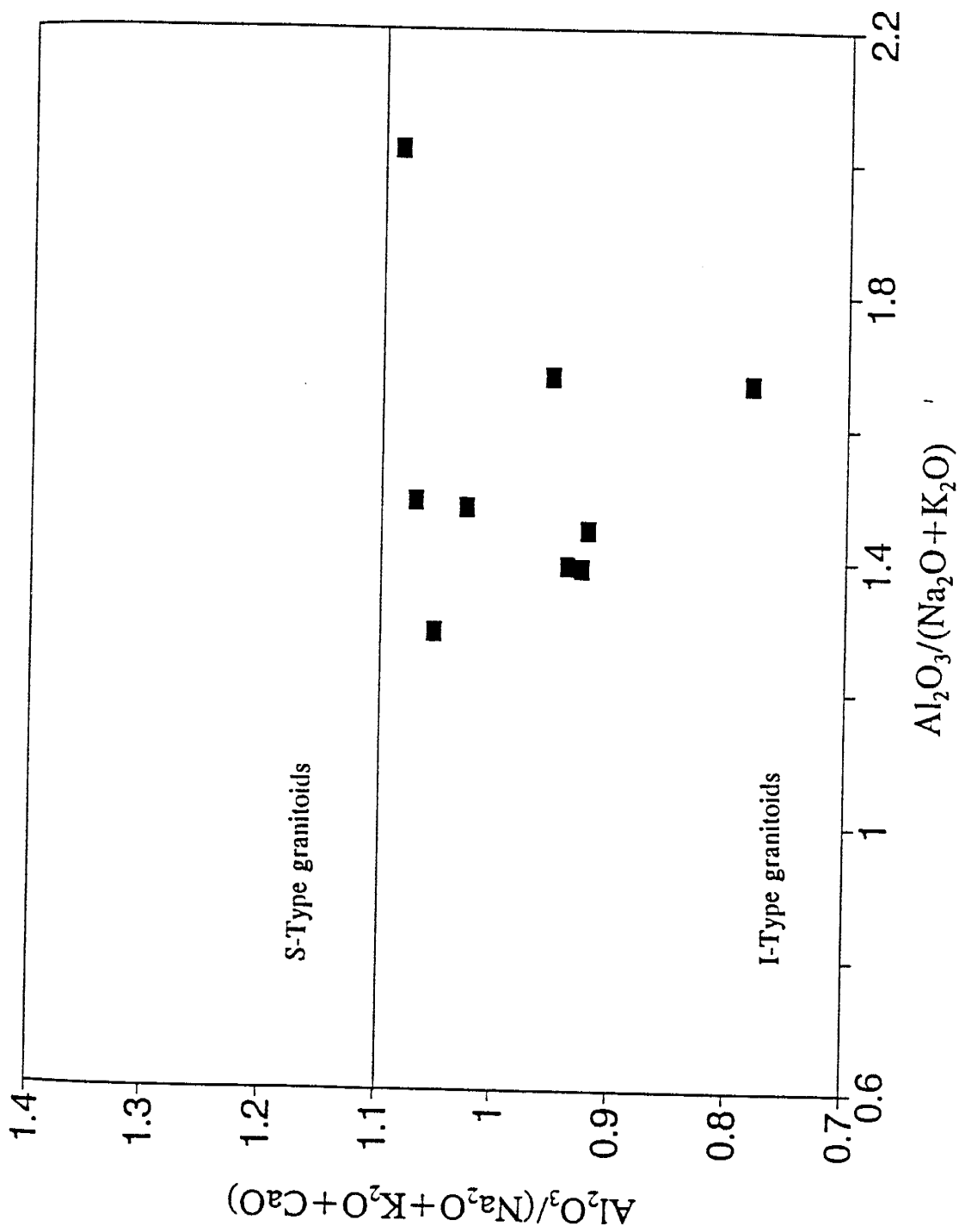


FIG. 1.10 Rb versus (Y+Nb) tectonic setting discrimination plot of Bukon Jeded granitoids (after Pearce et al., 1984). Fields shown on the figure are: SYN-COL: syn-collision granites; VAG: volcanic arc granites; WP: within plate granites; and ORG: ocean ridge granites.

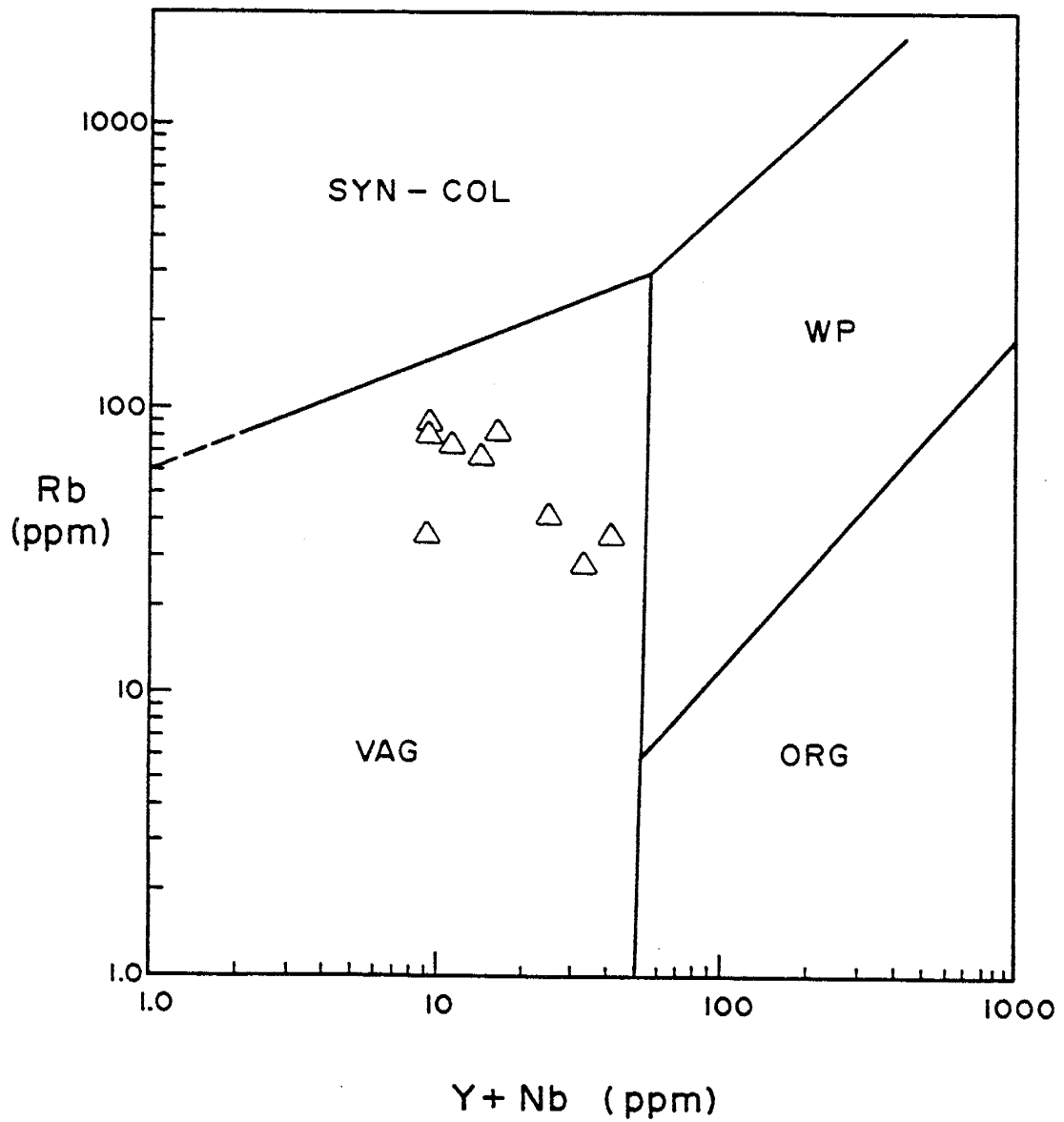


FIG. 1.11 $(\text{CaO}+\text{MgO})-(\text{SiO}_2/10)-(\text{Na}_2\text{O}+\text{K}_2\text{O})$ ternary plot of
Bukon Jedeh rocks (after Taylor and McLennan, 1985).

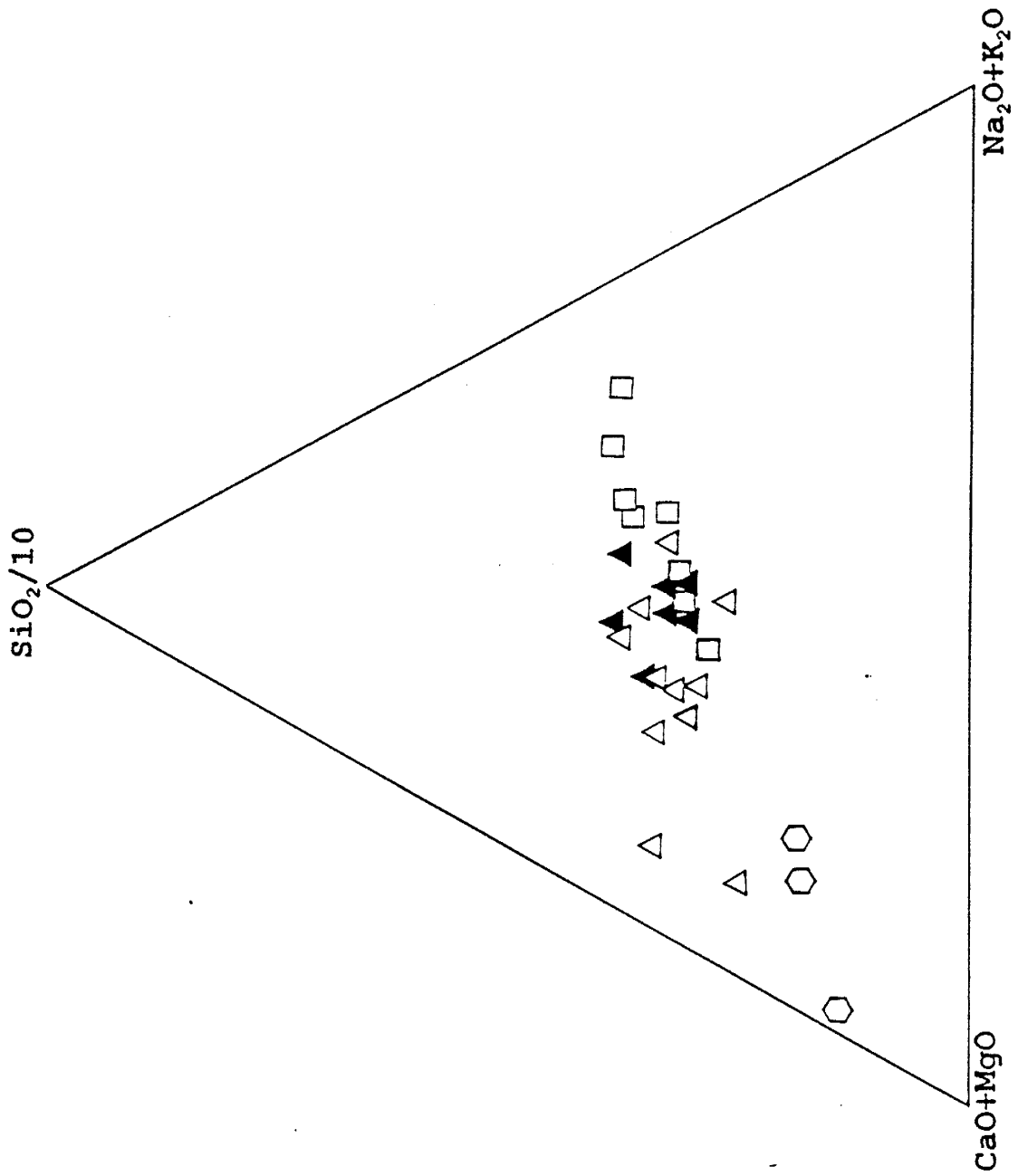


FIG. 1.12 Bukon Jedeh gold, scale bars in background are 1 mm apart: (a) Alluvial gold grains. (b) Lateritic gold with crystalline and concretionary morphologies. (c) Gold nugget from laterite ore. (d) Small dodecahedral crystal of gold. (e) Gold nuggets "g" encased by iron oxide concretion "i". (f) Gold nugget with graphite "c" on faces (field of view is 6 mm approx.). (g) Graphite along relict cleavages in gold nugget. (h) Gold grains from the saprolite (generally $\ll 1$ mm in diameter).

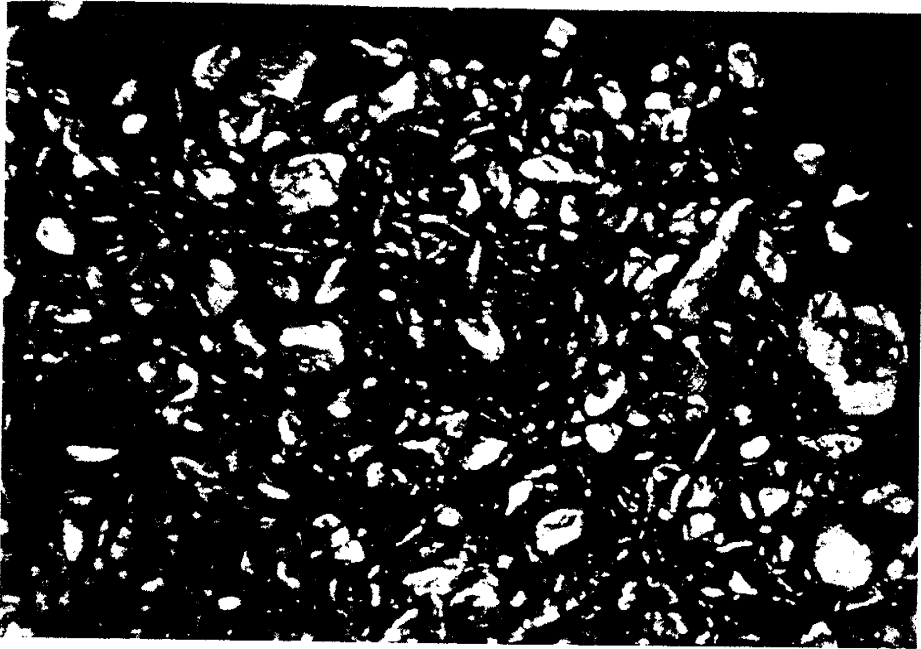
GOLD MINERALIZATION

Alluvial, lateritic and primary bedrock gold mineralizations are present in the Bukon Jedeh area. Alluvial gold is hosted principally by loose, gravel deposits, 0.2 to 1 m thick, contained within the alluvial flats on a network of streams draining the area. These gold-bearing gravels are generally buried by 2 to 3 meters of sand and silty clay overburden. Gravel bars within active stream channels also carry small amounts of alluvial gold. Gold grades in the alluvial deposits average 1.5 - 2.0 gm/m³. meter with the largest proportion of gold occurring in the lowermost 15 cm of the gravel and the top 10 cm of thoroughly weathered bedrock that underlies the gravel bed. Higher gold grades are associated with gravels containing a large proportion of pebble-cobble fraction, and having a matrix consisting of coarse sand with abundant black sand component comprising hematite, ilmenite, magnetite, garnet, corundum and zircon. Gold in alluvial deposits is generally fine grained, almost powdery in the lower courses of the streams where narrow stream valleys open up into wide alluvial plains. Coarse gold is common near the headwaters of many drainage systems in Bukon Jedeh. A diagnostic feature of this gold is its roundness and smooth abraded exteriors (Fig. 1.12a).

Lateritic deposits

Gold-bearing lateritic soils, locally referred to as koomasin, contain the most important gold deposits. Examples of this type of deposit occur within a 130 sq. km concession held by Bentley Mines, Inc., Liberia. Here, mineralization is associated with a set of low hills occupying an area 3 km wide and approximately 15 km long, and with an orientation which parallels the fabric in the predominantly gneissic bedrock. Lateritic mineralization is broadly distributed within this general area as indicated by the proliferation of local mining activities throughout this concession. Lateritic deposits are also worked by local miners outside of Bentley's concession along an eastward extension of the same chain of hills with which lateritic mineralization is associated. These continue over a total strike length of approximately 50 km. This form of mineralization is open ended east of the area of this study. Westwards, however, it disappears against the Dugbe shear system. The nature, sizes and grades of lateritic deposits and other characteristics of gold in the laterite profile were determined for the area of this study by sampling large areas on a coarse grid of 200 * 100 meters spacing, and in specific areas, on a finer mesh of roughly 50 * 50 meters spacing. A total of 810 two-tonne samples were collected from 450 test pits and processed for gold by a combination of sluicing and panning methods.

FIG. 1.12 Bukon Jedeh gold, scale bars in background are 1 mm apart: (a) Alluvial gold grains. (b) Lateritic gold with crystalline and concretionary morphologies. (c) Gold nugget from laterite ore. (d) Small dodecahedral crystal of gold. (e) Gold nuggets "g" encased by iron oxide concretion "i". (f) Gold nugget with graphite "c" on faces (field of view is 6 mm approx.). (g) Graphite along relict cleavages in gold nugget. (h) Gold grains from the saprolite (generally <<i mm in diameter).



(a)



(b)



c

(c)



d

(d)



(e)

e

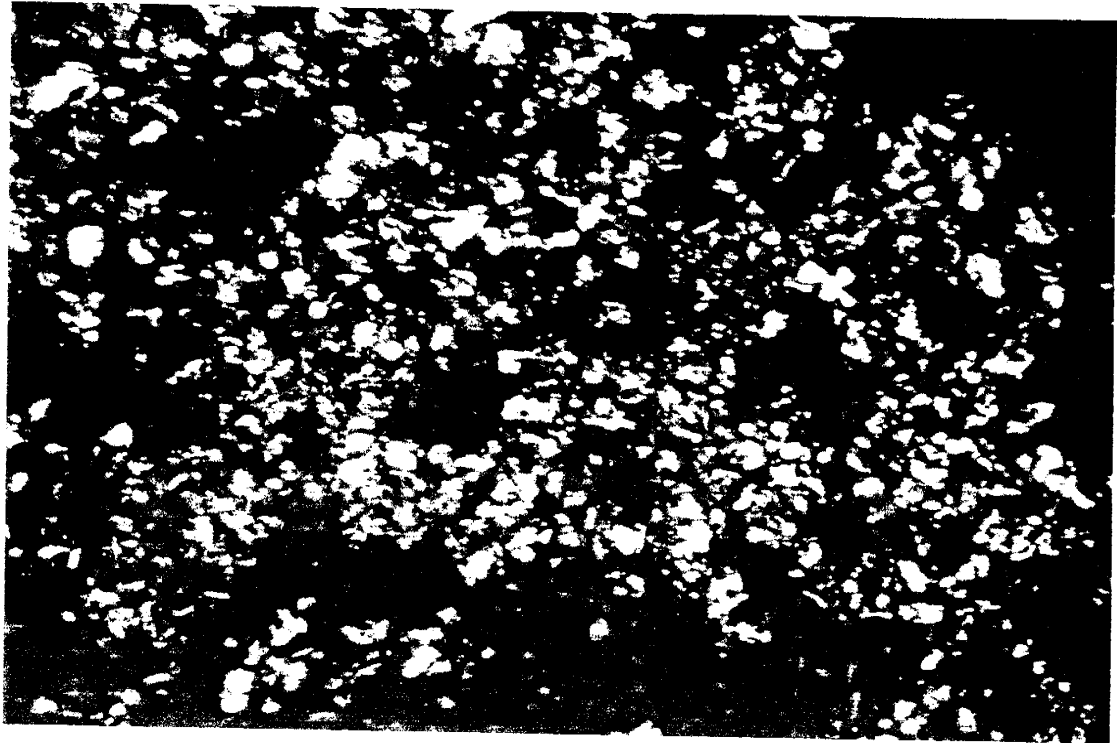


(f)

f



(g)



(h)

pit profiles indicate lateritic deposits consist of thinly developed soils, 0.2 to 2 meters thick, and underlying deeply weathered bedrock. At the top of laterite profile is a thin dark brown to black zone 8 to 12 cm thick, with a high humus content and overlying a dark red zone that contains abundant ferruginous concretions, angular quartz pebbles and lithic fragments impregnated with hydrated iron oxides. A bright red mottled zone with a high clay content underlies the top soil and grades imperceptibly into saprolite. Partially weathered to unweathered bedrock is encountered along stream valleys and beneath laterite at variable depths (Fig. 1.13a).

Measured grades from the sampling indicate anomalous to ore grade concentrations of gold in lateritic soils and underlying saprolite over the entire 18 sq. km study area (Fig. 1.14a, Appendix 1-D). Gold grades range from 0.04 to 6 ppm with an average of 0.26 ppm for the 810 samples processed. Average gold grades over large areas are generally uniform; isolated high grade areas, however, are not uncommon and their distribution roughly parallels the main fabric in bedrock. Average grades within the economic deposits commonly range from 0.25 to 0.75 ppm (Fig. 1.13b). No distinct vertical variation in gold values is noticeable in the laterite profile. Ore grade samples occur over all rock types. Within a total of 5 sq. km area where closely spaced

sampling was conducted, ore reserves totalling 18.5 million metric tons with an average grade of 0.42 ppm were proven (Fig. 1.15); cut off grade used based on estimates of production cost is 0.10 ppm (0.2 gm/m³). Seventy five kilograms of gold has been recovered from a total of 150,000 metric tons of laterite ore processed during pilot mining operations conducted in two production blocks east of Government Camp (Fig. 1.3).

Overall grain size of gold in the laterite decreases down the profile (Fig. 1.13a). In the soils, most gold grains exceed 1 mm in diameter; nuggets up to 20 mm in diameter are common and occur mainly in the ferruginous zone at the top of the profile. Downward into the saprolite, the diameter of gold grains typically ranges from 100 microns to 1 mm (Fig. 1.12h) and nuggets are rare. Gold nuggets and grains in the laterite are angular (Fig. 1.12c), and have crystalline octahedral, dodecahedral and concretionary or botryoidal shapes (Fig. 1.12b-h). Their exteriors are irregular and show no indications of abrasion. Variably corroded gold grains were observed in a number of samples collected from the top soil.

FIG. 1.13 a) Composite soil profile in Bukon Jedeh showing the variation in grain size of gold with depth; b) Representative soil profiles in areas with economic mineralization; gold grades in ppm are indicated.

(b)

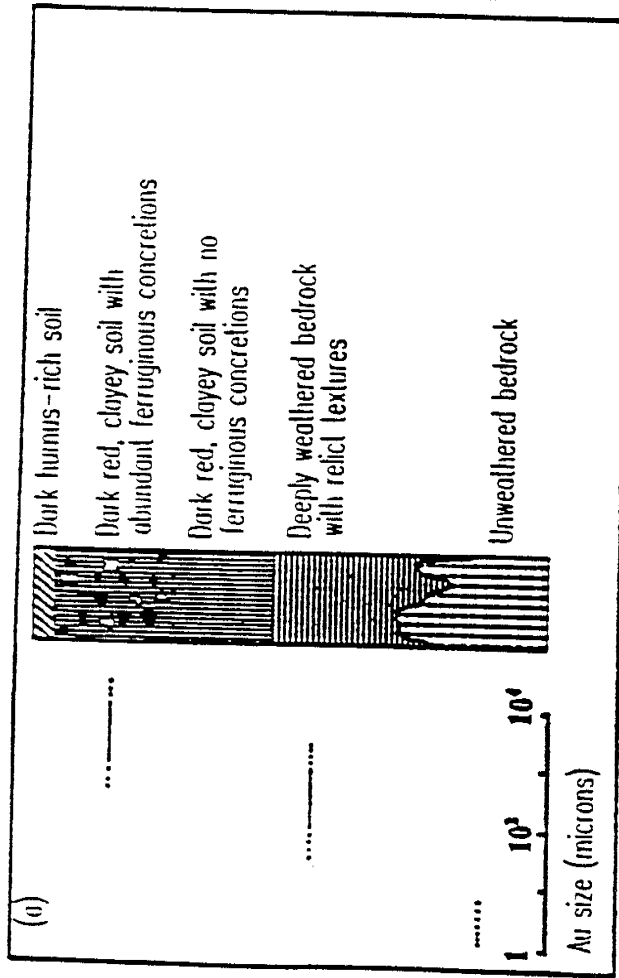
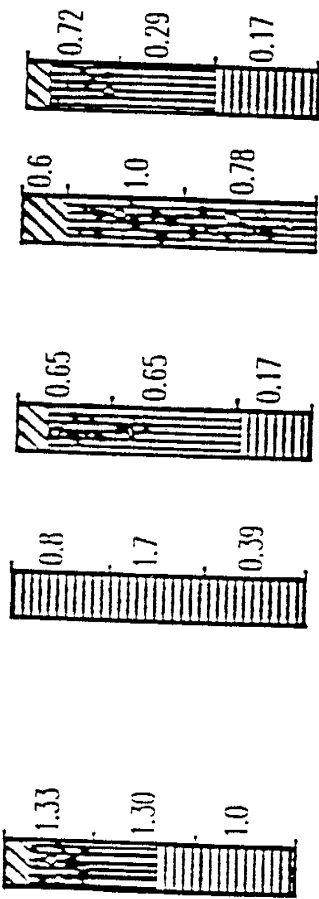
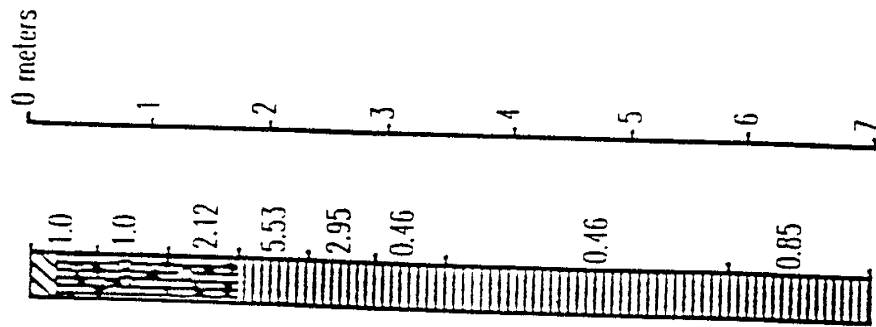
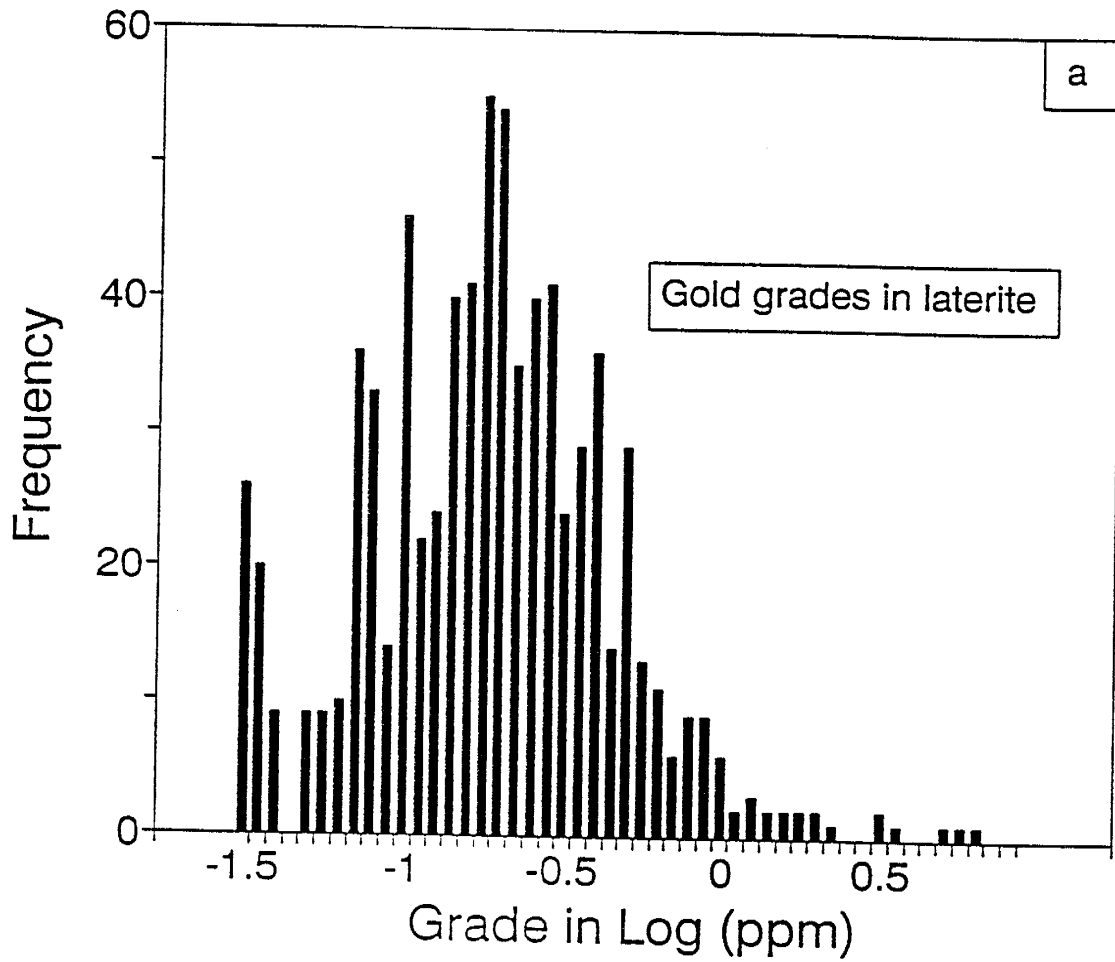


FIG. 1.14 Histogram of gold grades in (a) laterite and (b) bedrock samples from Bukon Jedeh.



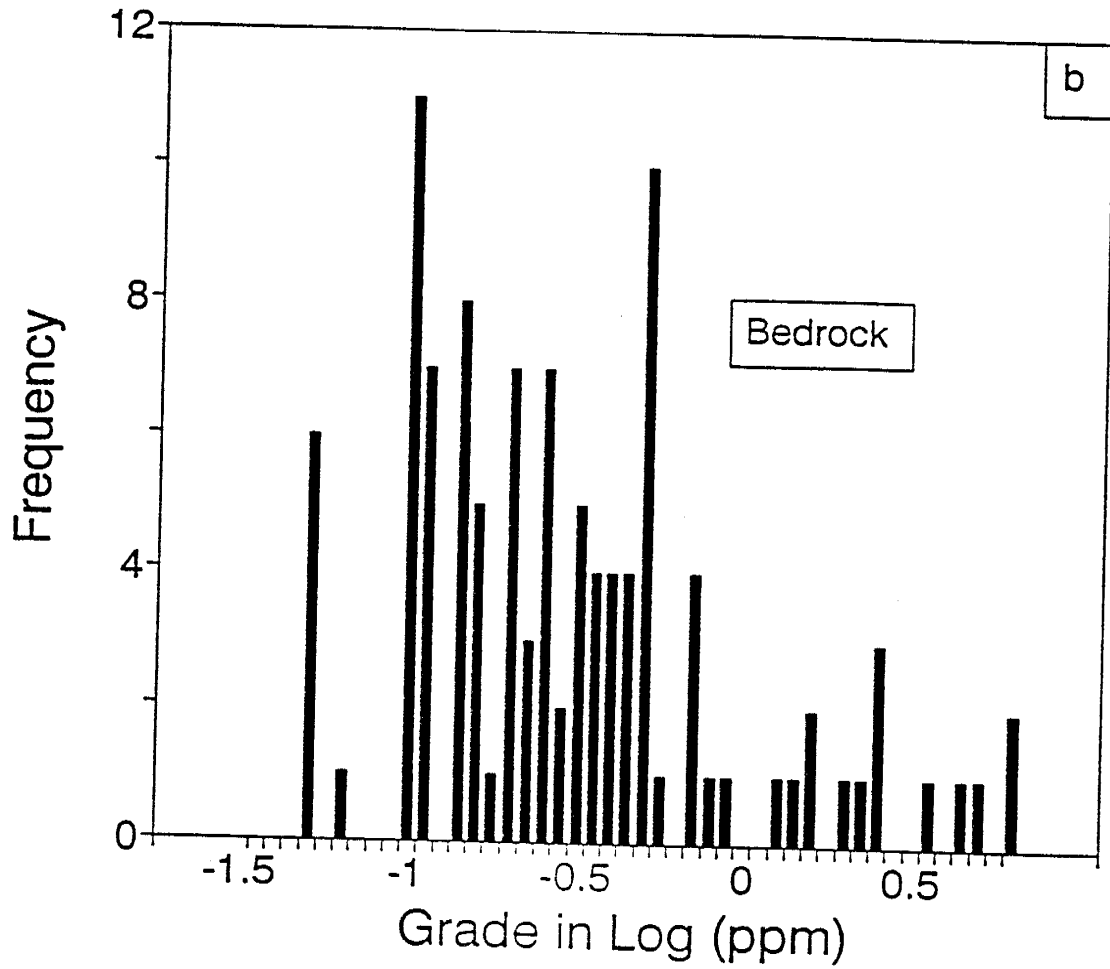
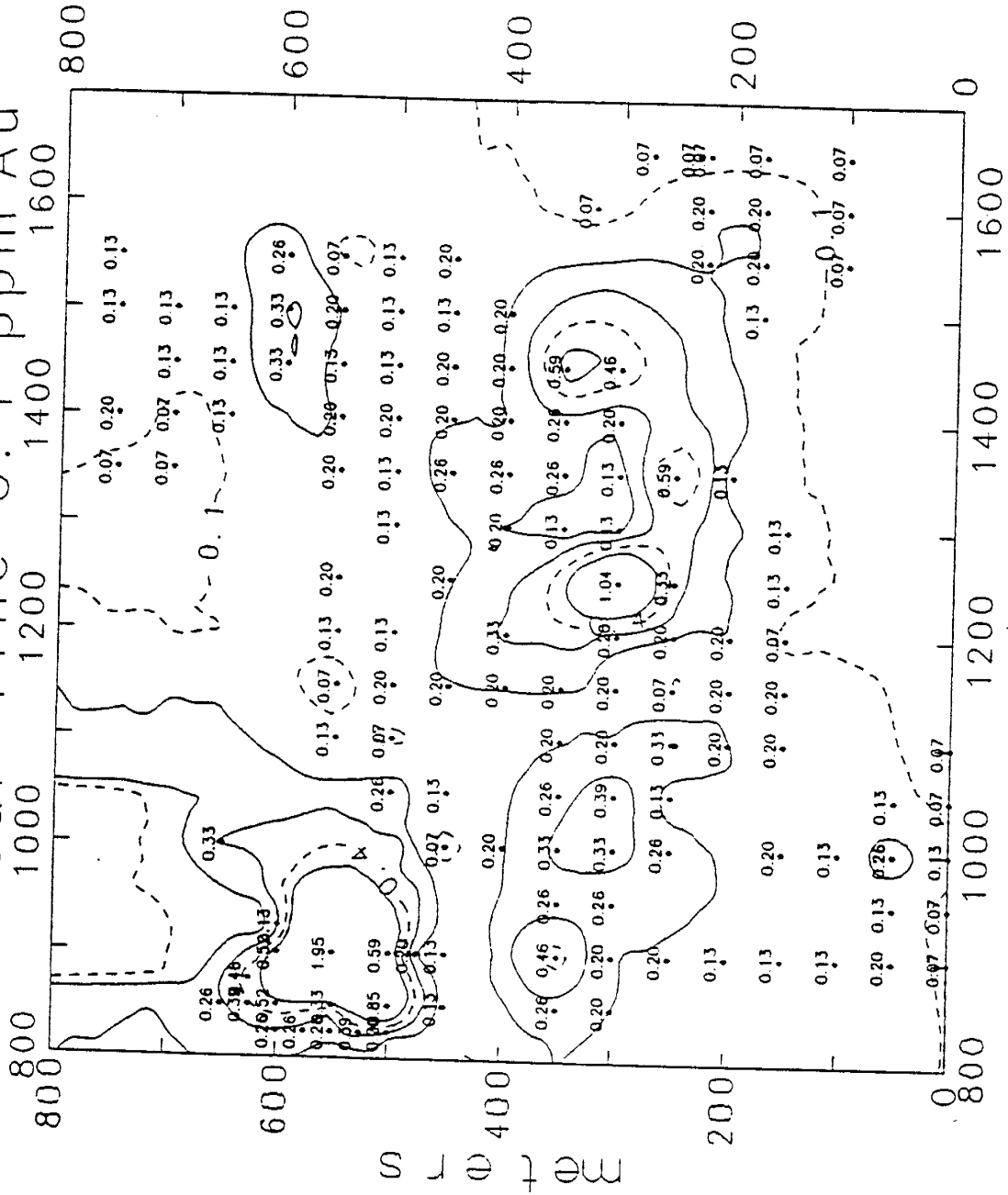


FIG. 1.15 Computer generated contours of gold values (ppm)
in a lateritic deposit east of Government Camp.

contour line 0.1 ppm Au



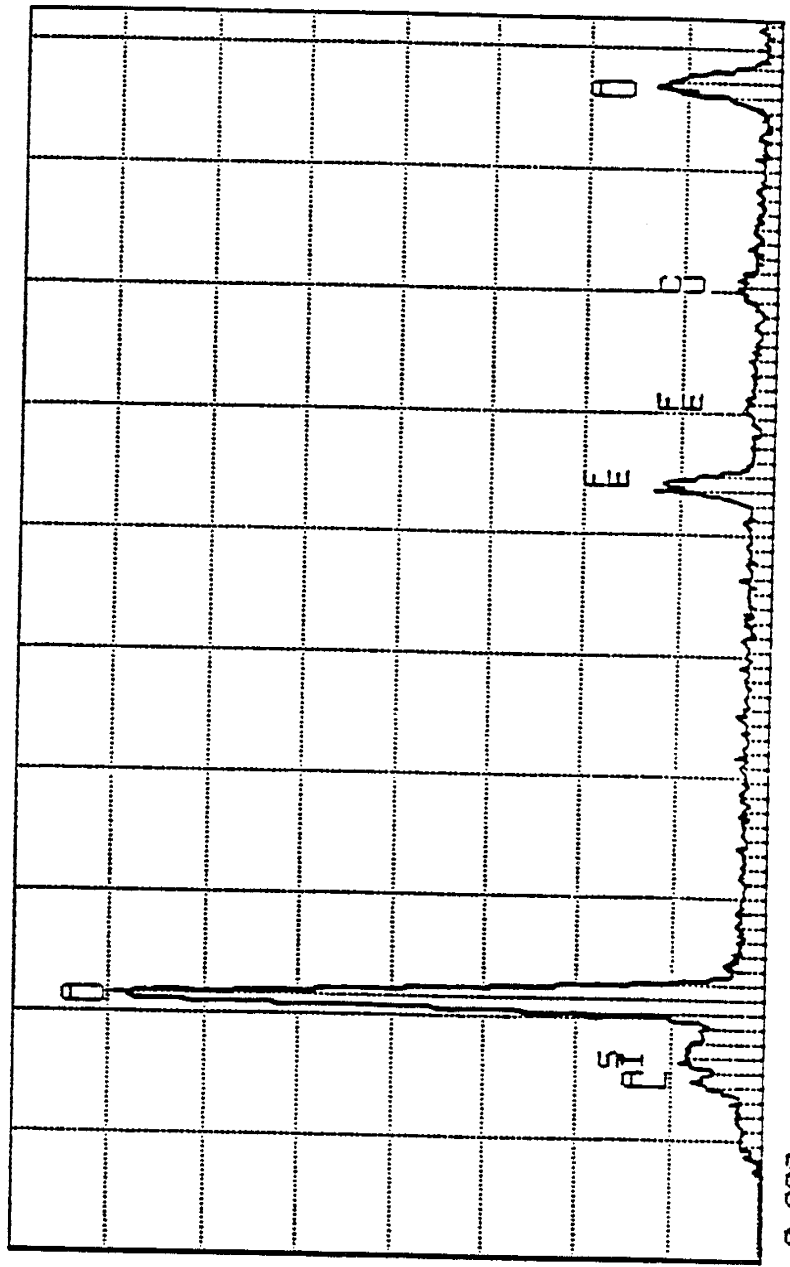
The angular and concretionary morphologies of lateritic gold grains and their crystalline shapes suggest they have not been physically transported but represent an in situ accumulation of residual and authigenic gold resulting from chemical weathering of underlying bedrock.

Gold nuggets and grains in the laterite ore are intimately associated with iron oxides and carbon. Hematite and goethite commonly encapsulate gold nuggets (Fig. 1.12e) and are responsible for most gold lost during sluicing. Scanning electron microscope spectra of iron oxide concretions show moderate gold peaks (Fig. 1.16). In the Government Camp area (Fig. 1.3), crushed samples of iron oxide concretions were panned and found to contain 6 to 12 mg of gold per pan (approximately 75 pan loads in a tonne of ore). Laterite here contains an average of 0.3 ppm gold, and iron oxide concretions form 10 to 20% of the top ferruginous zone. About 10 to 30% of gold from this zone, where iron oxide concretions are most abundant, is lost during sluicing as a result of this association. Polished sections of gold nuggets with iron oxide association indicate inclusions and minute disseminations of gold in iron oxides, particularly in goethite, and vice versa. Textural relationships between the gold and iron oxides suggest their precipitation was simultaneous.

Graphite flakes coat surfaces of gold grains and are intergrown with gold nuggets forming thin partings along relict cleavages within the nuggets (Fig. 1.12f-g). The shapes of some gold nuggets mimic the sheeted structure of graphite, and the association of these with graphite suggests they have probably been formed by replacing pre-existing graphite flakes. Graphite flakes associated with gold nuggets are detrital remnants of recrystallized graphite from the gneissic bedrock (Fig. 1.16c). Quartz also occurs as minute euhedral crystals attached to gold nuggets. Scanning electron microscope (SEM) images of some nuggets reveal quartz crystals in vugs within the nuggets.

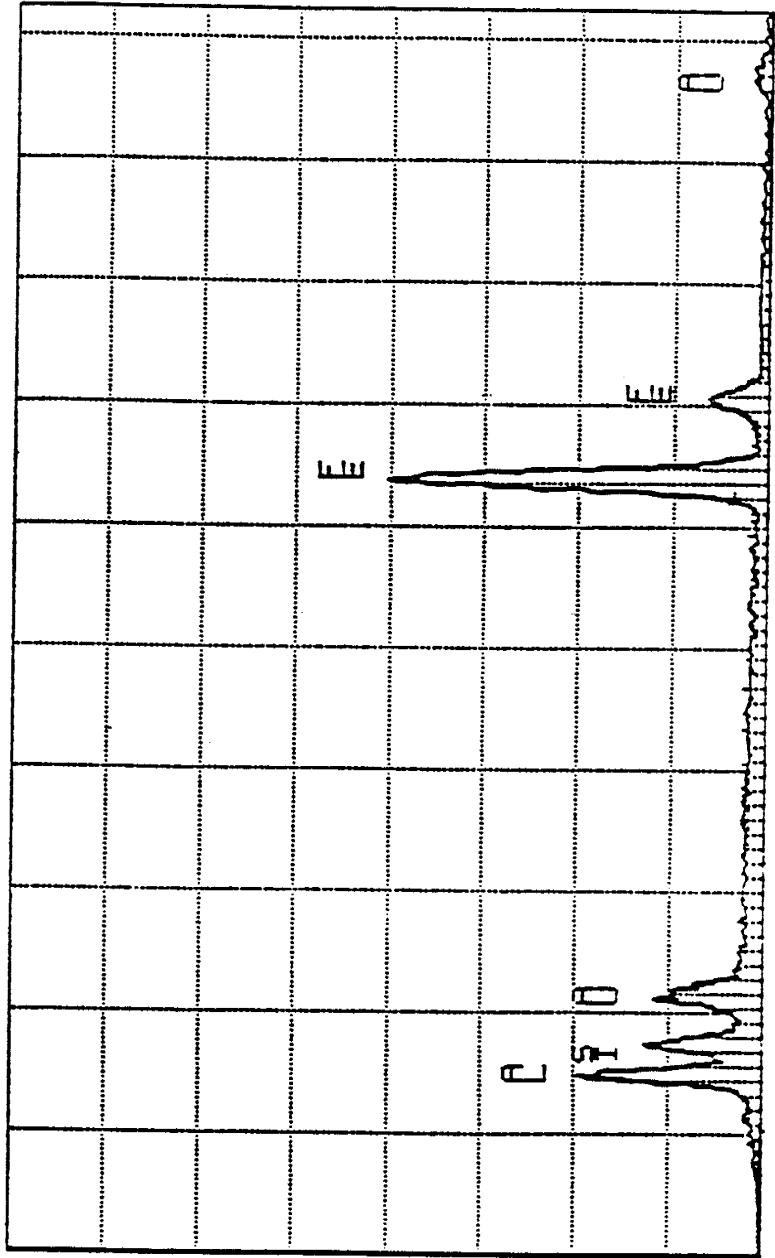
FIG. 1.16 Scanning electron microscope (SEM) spectra of (a) lateritic gold and (b) iron oxide concretion. (c) X-ray diffraction spectra of graphite associated with lateritic gold.

TN-5400 NIMT METALLURGY DEPT. FRI 28-SEP-90 07143
Cursor: 0.000KeV = 0 ROI (2) 0.000: 0.000



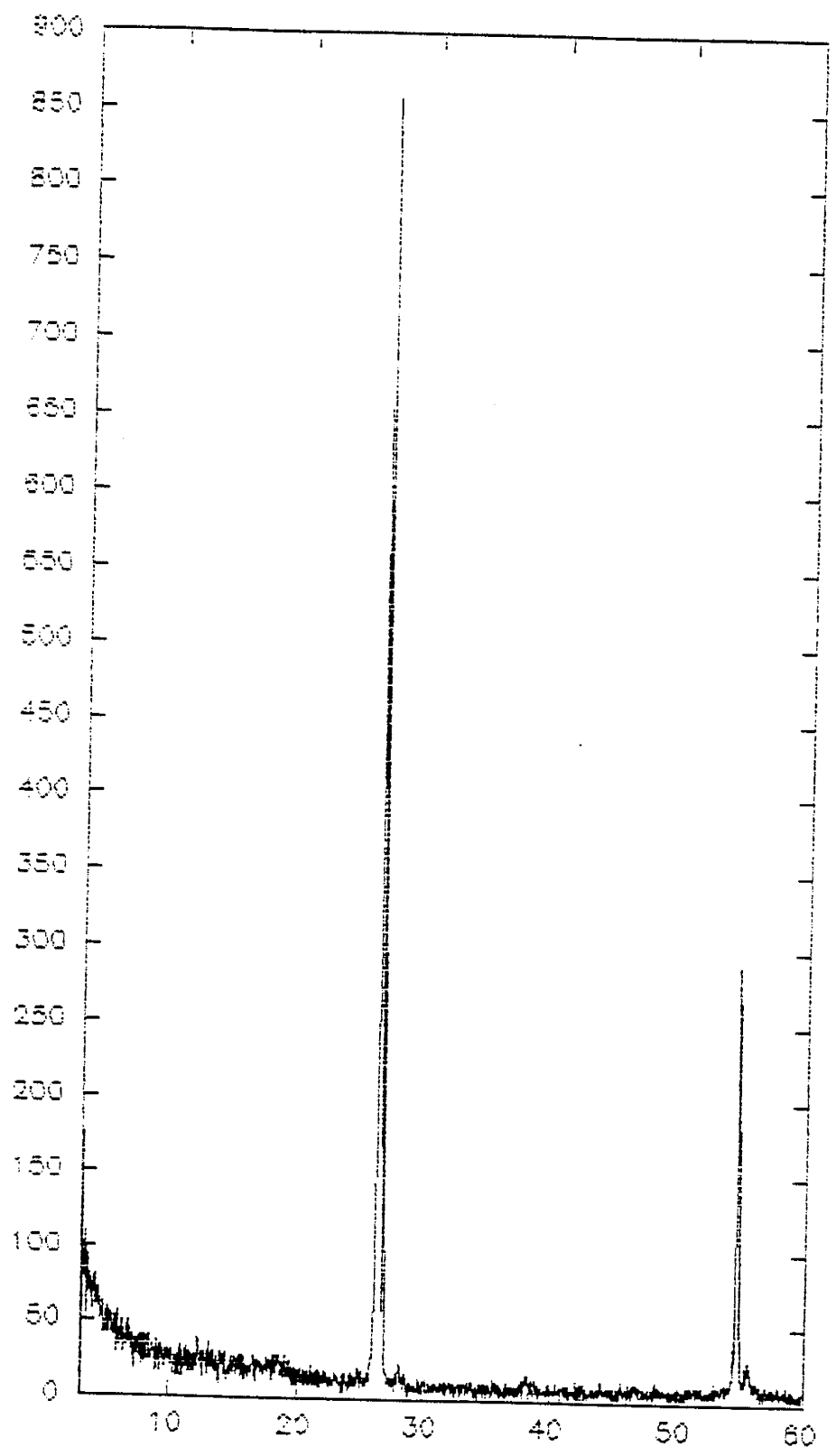
0.000 25 3 VFS = 512 10.240

TN-5400 NIMT METALLURGY DEPT. FRI 28-SEP-90 07:35
Cursor: 0.000keV = 0 ROI (2) 0.000: 0.000



0.000 25 2 VFS = 1024 10.240

Counts

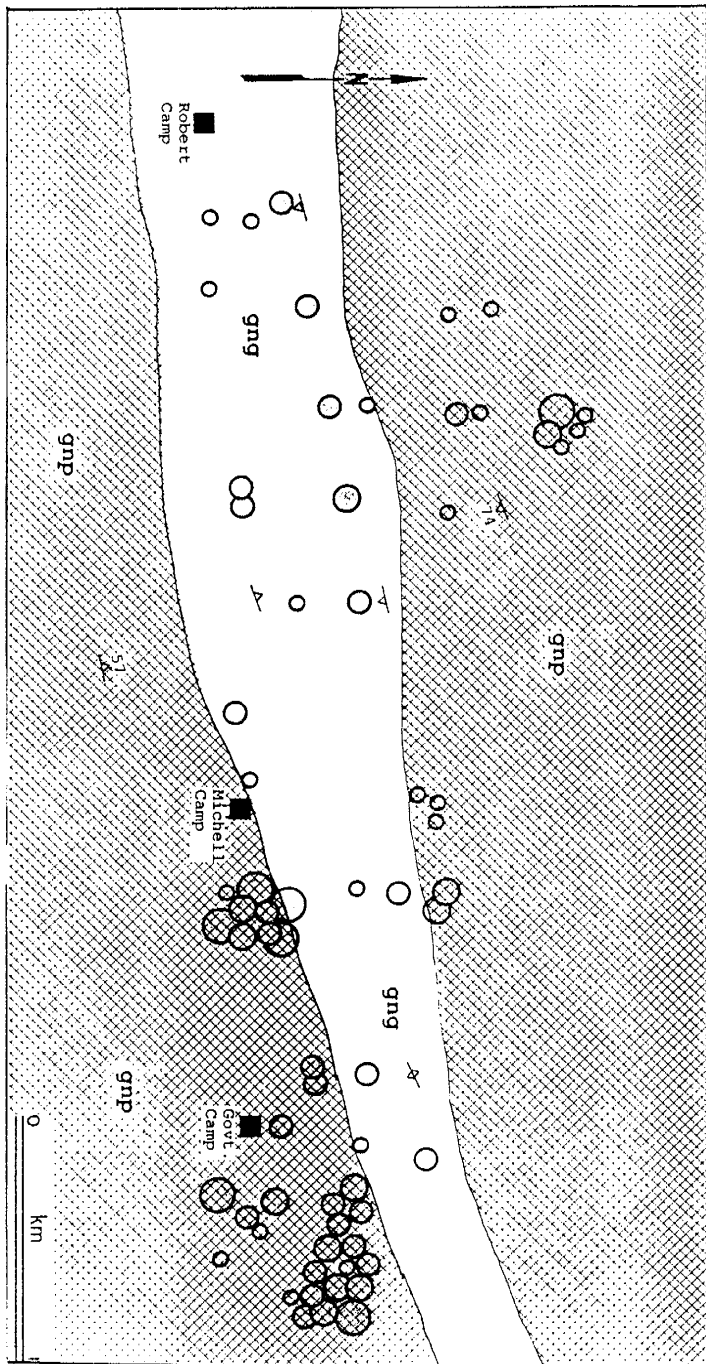


2θ

Bedrock mineralization

One hundred and ten chip samples of bedrock were analysed for gold by a combination of fire assay, organic solvent extraction using DIBK (Di-methyl isobutyl ketone), and atomic absorption methods (Appendix 1-E). Assay results indicate anomalous amounts (0.05 to 8 ppm) (Fig. 1.14b) of disseminated gold mineralization with an average grade of 0.63 ppm for the area covered. Primary gold mineralization is present in all of the different rock types represented in the area. Grades exceeding 1 ppm, however, are associated only with graphite- and pyroxene-bearing gneiss (Fig. 1.17). For any given locale, gold values in bedrock are similar to those in overlying laterite. Grades, however, tend to be more homogeneously distributed in the laterite than in bedrock. Distribution of gold in bedrock indicates mineralization is pervasive and not limited to veins or local structures, such as foliation, within the bedrock. However, if the distribution of localized high grade areas in the laterite is a reflection of inhomogeneities in the bedrock mineralization, then subsidiary structures that may be concealed by the laterite cover could be controlling centres of mineralization in bedrock.

FIG. 1.17 Simplified geologic map of Bukon Jedeh with location of bedrock samples and their gold content.



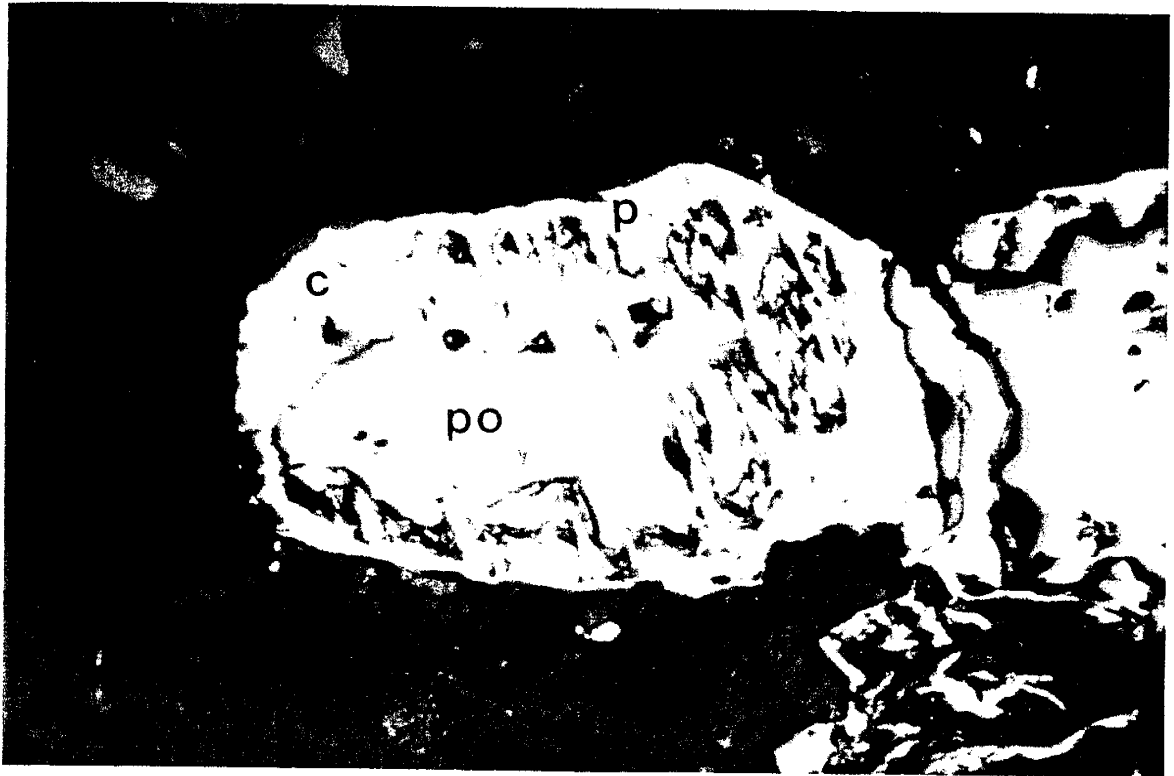
ppm Au: 0.05-0.24; ○ 0.25-0.99; ○ 1.00-3.00; ○ >3.00;

A petrographic study of 12 polished sections of bedrock samples shows an assemblage of sulphide minerals that include pyrite, pyrrhotite, chalcopyrite and minor arsenopyrite (Fig. 1.18a). No visible gold was observed in any of the polished sections studied although splits of these same samples were determined by geochemical analysis to contain between 1 and 8 ppm gold. This suggests that primary gold is fine grained and is perhaps associated with the sulphide minerals. Sulphide minerals are abundant in the more graphitic units where they commonly occur along partings within graphite (Fig. 1.18b).

Gold composition

The compositions of a total of 68 gold samples were determined by Instrumental Neutron Activation Analysis (INAA), X-ray fluorescence (XRF), and Scanning Electron Microscopy (SEM) in order to compare the chemistry of alluvial and lateritic gold in Bukon Jedeh to hypogene mineralization. Primary gold was obtained from a mesothermal quartz veins from a deposit about 120 km north of Bukon Jedeh because no visible gold was observed in bedrock within the area covered by this study. Also included in the analysis were primary gold samples from mesothermal veins in Ghana, from similar age rocks as occur in Liberia.

FIG. 1.18 (a) Photomicrograph of mineralized bedrock sample with the assemblage pyrite "p", pyrrhotite "po", and chalcopyrite "c". (b) Photomicrograph of bedrock sample showing sulphide minerals "sm" along selvages within graphite.



(a)



(b)

Preparation of gold samples for INAA analysis involved separation of primary gold in crushed ore from quartz gangue by heavy mineral separation using methylene iodide. All gold samples were cleaned in a ultrasonic bath to get rid of foreign particles. Clean, dry gold grains and small nuggets weighing between 2 and 15 mg were packed in ultra-pure quartz vials and irradiated for 4 hours at a flux of 3×10^{13} n.cm².sec⁻¹. Gold activates very well because of its large cross section (98.8 barns); all of the samples thus had substantial activity following irradiation and were allowed to decay for several weeks before being counted on two germanium detectors using NBS fly ash standard (FA-1) for calibration of Sc, Cr, Fe, Co, Sr, Sb, Ce, Nd, Eu, Tb, Yb, Hf and Th, and GXR1 as standard for calibrating Hg. Silver content in the gold samples was determined using a lead ingot with 2% silver.

Results of INAA analysis show considerable differences in composition of gold from the different deposit types. Most alluvial and lateritic gold contain less than 4 wt. % silver, minor amounts of mercury and traces of scandium. Elements typically occurring in zircon and monazite such as Zr, Th, Hf and rare earth elements occur in variable amounts in alluvial and lateritic gold. Samples of primary gold have more than 20 wt. % silver, minor to trace amounts of mercury and antimony (Table 1.3, Fig. 1.19a-b). XRF and SEM analyses

of gold nuggets indicate they contain minor iron, silicon and aluminum peaks.

The similar trace elements in lateritic and alluvial gold indicate a common origin. Bukon Jedeh alluvial gold is thus interpreted to be derived from auriferous laterite. Distinctly different minor and trace element chemistries of lateritic and primary gold indicate that lateritic gold is not a simple accumulation of primary gold liberated from its source rock. The suite of lithophile elements present in samples of lateritic gold suggests the growth of small gold nuggets and grains in surficial environments to include soil constituents such as clay, detrital zircon, monazite, sphene and iron oxides. Low amounts of silver in lateritic and alluvial gold compared with that of primary gold indicate an increase of fineness from processes operating in surficial environments.

Table 1.3. Instrumental neutron activation analysis of lateritic and alluvial gold samples from Bukon Jedeh, and primary gold from a vein deposit in Zwedru, Liberia. p, a and l are respectively primary, alluvial and lateritic gold

(ppm)	1p	2p	3p	4a	5a	6a	7l	8l
Sc				0.22		0.7	0.17	0.25
Cr								
Co				1.9				
Zr								
Sb	94	105	71					
Ce				92		140		
Nd								
Eu								
Tb								
Yb								
Hf						53		
Th				13		35		
Fe*							0.06	
Hg*	0.04			0.02	0.02	0.02	0.06	0.03
Ag*	20.92	21.96	20.59	1.22	1.31	3.97	0.52	0.52

* values given in wt. %

(ppm)	9l	10l	11l	12l	13l	14l	15l	16l
Sc		0.84	0.28	0.89	0.34	0.21	6.4	
Cr								
Co						3.8	5.9	
Zr		1779					14439	
Sb								
Ce		63			2275		13398	
Nd					0		0	
Eu					1.5		10.6	
Tb					8.8		45	
Yb							23	
Hf		31	30				303	
Th		13.5			309		2325	
Fe*		0.06	0.00	0.11				
Hg*	0.02	0.05	0.04	0.05	0.03	0.07	0.02	0.01
Ag*	2.35	0.61	0.73	0.90	3.19	1.80	6.38	3.19

(ppm)	171	181	191	201	211	221	231	241
Sc		8.61	1.04	0.43	0.23	0.11	0.26	
Cr		102	0					
Co		0	0					
Zr		20897	2500					
Sb								
Ce	148	13339	1919					
Nd		5193	580					
Eu		12.4	2.06					
Tb		46.1	6					
Yb		24	0					
Hf	7.2	53.9	45	5.3				
Th	18.5	2671	369					
Fe*			0.19					
Hg*	0.01	0.03	0.03	0.02	0.01	0.03	0.03	0.15
Ag*	4.96	3.83	3.05	0.55	3.48	0.93	2.18	1.28

(ppm)	251	261	271	281	291	301	311	321
Sc			0.18	0.43	0.14	0.68		0.29
Cr								
Co						2.1		1.3
Zr						2245		
Sb								4.3
Ce				239		286		243
Nd								
Eu								0.39
Tb								1
Yb								
Hf				14.2		28.6		8.5
Th			9	39		49		46
Fe*					0.12			
Hg*	0.06	0.03	0.02	0.04	0.06	0.05	0.05	0.05
Ag*	1.28	0.52	0.90	1.28	1.25	1.62	0.90	1.86

(ppm)	331	341	351	361	371	381	391	401
Sc	1.34			0.26	0.62	0.21	0.35	
Cr								
Co								
Zr	1972						1430	
Sb								
Ce	516			326	332		579	
Nd								
Eu								
Tb	17.4							
Yb								
Hf	65			16.2	21		21	
Th	80			85	48		74	
Fe*								
Hg*	0.03	0.02	0.01	0.07	0.04	0.04	0.04	0.03
Ag*	1.31	2.20	0.55	1.60	2.32	2.06	2.35	0.87

(ppm)	41a	42a	43a
Sc	1.14	0.57	0.63
Cr			
Co			
Zr			
Sb			
Ce	2373	754	4272
Nd	607		1145
Eu	3.7	1.1	6.2
Tb	8.3	2.9	14.9
Yb			
Hf	62	52	21.7
Th	382	102	608
Fe*			
Hg*	0.04	0.04	0.02
Ag*	4.03	1.71	1.68

FIG. 1.19a Silver-Scandium plot for alluvial, lateritic and primary gold samples from Bukon Jedeh. Silver and scandium levels in gold obtained by instrumental neutron activation analysis.

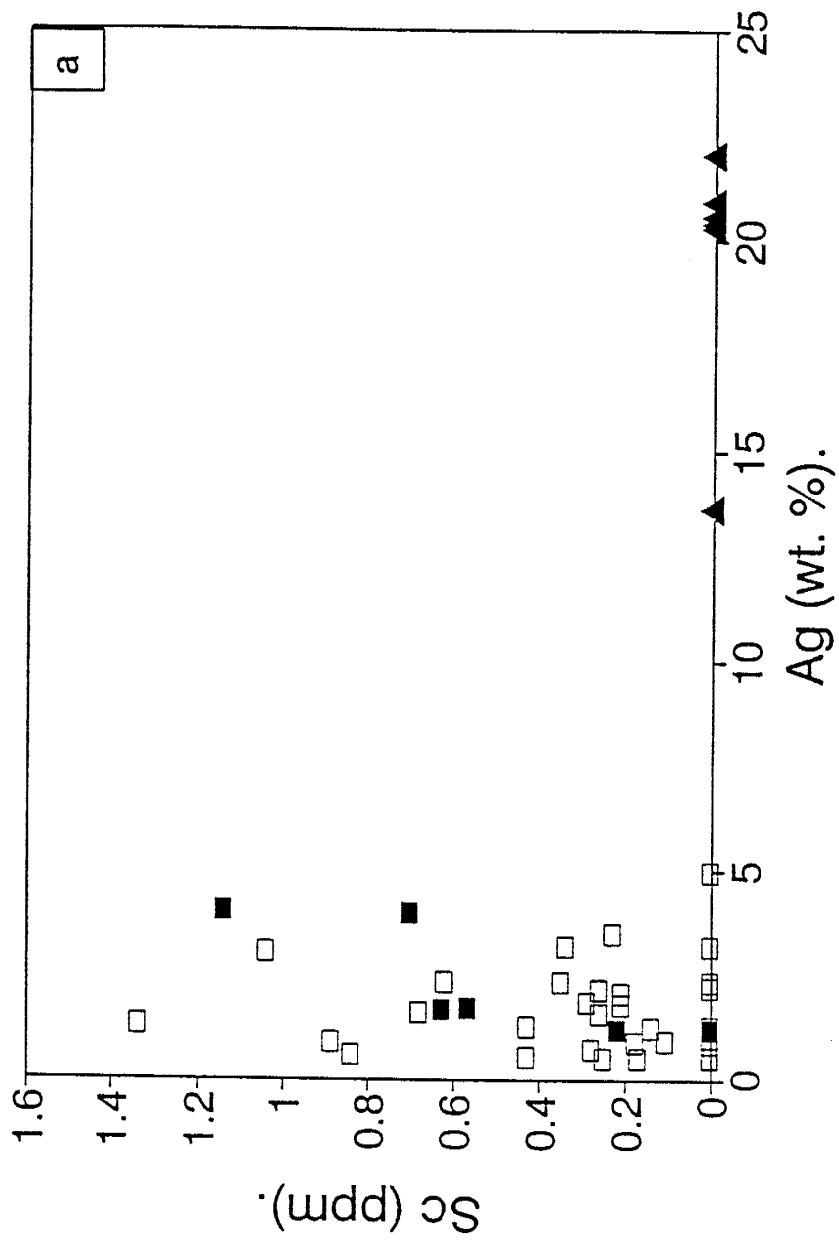
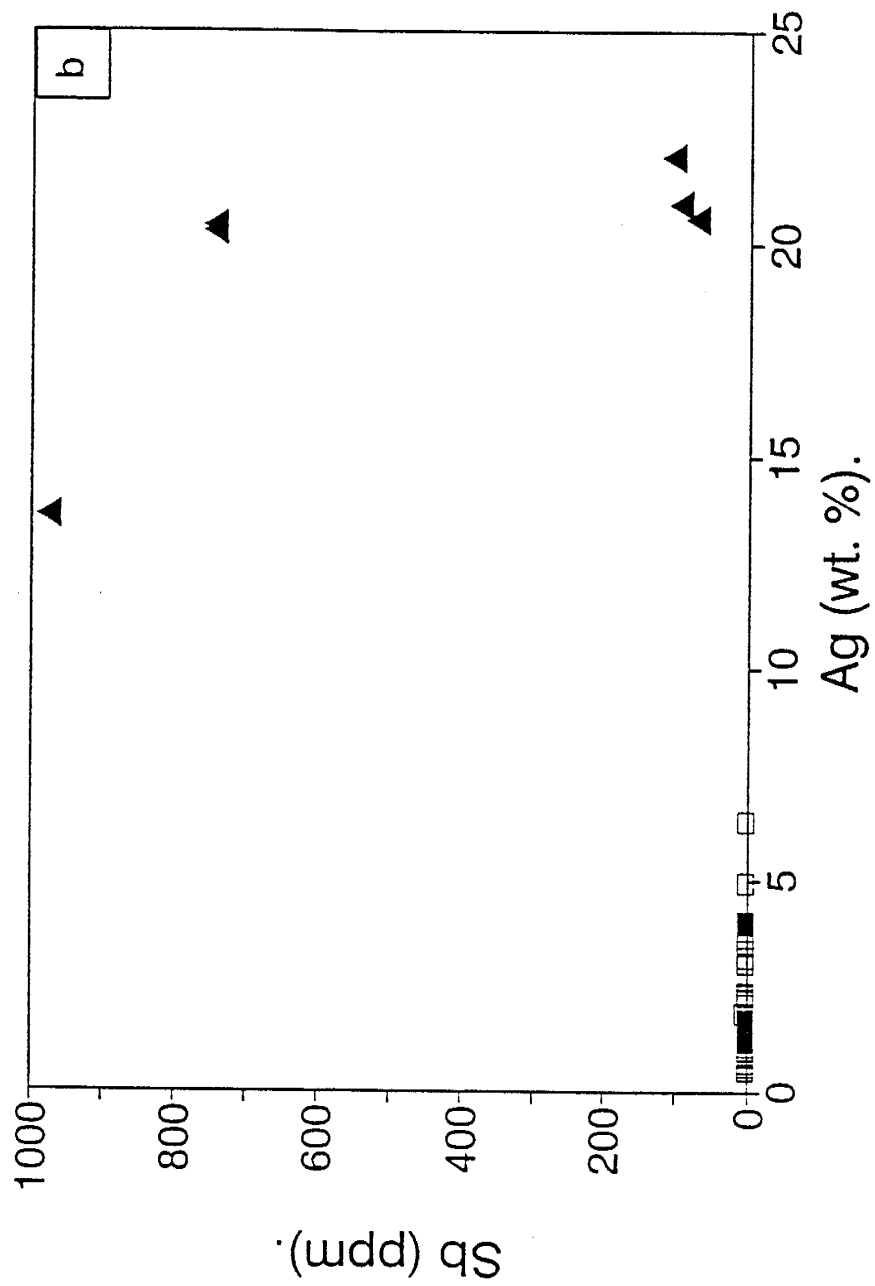


FIG. 1.19b Silver-Antimony plot for alluvial, lateritic and primary gold from Bukon Jedeh. Silver and antimony content in gold samples were obtained by INAA.



■ ALLUVIAL □ LATERITE ▲ PRIMARY

DISCUSSION

Tectonic setting of supracrustal and intrusive rocks

The mineralogical and chemical compositions of supracrustal rocks in Bukon Jedeh are similar in broad aspects to Archean greenstone successions and to Phanerozoic supracrustal rocks formed in basins associated with convergent plate boundaries (Condie, 1982). Bukon Jedeh rocks are interpreted to have formed in an arc setting based on rock association and on trace element chemistry of intrusive granitoids that indicate their emplacement in a volcanic arc setting. This is consistent with Wright et al. (1985) hypothesis that Proterozoic rocks in the West African region were formed by accretion of island arcs whose boundaries are marked by regional mylonitic zones.

Timing of primary mineralization

Constraints on the timing of primary mineralization in Bukon Jedeh are rather limited. The association of sulphide minerals with graphitic rocks suggests primary mineralization either preceded regional metamorphism or is synchronous with it. The crystallinity of graphite indicates it was produced by high metamorphic temperatures and pressures (Boyle, 1979) hence carbon must have preceded metamorphism. The absence of gold mineralization along major through-going structures

such as the Dugbe shear zone suggests mineralization in Bukon Jedeh occurred early in the geologic history of the area as these deep seated regional structures should have served as major pathways for later epigenetic mineralization. The simple Ca-Mg silicate mineral assemblage in the Bukon Jedeh rocks, in spite of the pervasive sulphide mineralization and anomalous levels of gold in the rocks, is consistent with primary mineralization occurring prior to or during high grade regional metamorphism (Barnicoat et al., 1991).

Nature of primary mineralization

Gold and associated sulphide minerals in Bukon Jedeh rocks either formed epigenetically before the peak of regional metamorphism, or syngenetically. Features of primary gold mineralization in Bukon Jedeh such as the abundance of Ca-Mg silicates and pyrrhotite, and the generally high grade of metamorphism in host rocks, are akin to those of metamorphic deposits described in high grade Archean terranes and interpreted to have formed by deep crustal fluids that were generated during regional metamorphism (Barnicoat et al., 1991; Mueller, 1988). The occurrence of gold in all rock types could best be explained by epigenetic processes.

Syngenetic mineralization could have occurred by submarine exhalation, by bacterial action during carbon deposition, or

as detrital grains in volcanoclastic and epiclastic components of the bedrock. Volcanogenic exhalative deposits have been identified in tectonic domains such as that described for Bukon Jedeh where submarine volcanic rocks are predominant (Franklin et al., 1981). In the Birimian greenstone succession in southwestern Ghana, exhalative lode gold deposits are hosted by lower Proterozoic metavolcanic and volcanoclastic rocks (Hirdes and Leube, 1989). The Birimian deposits are similar to primary mineralization in Bukon Jedeh in that both deposits are hosted by volcano-sedimentary packages of rocks that contain Mn-formation and cherts, and have trace element chemistries indicating protoliths of similar chemical compositions. The mineralogy of the Birimian lode gold deposits is similar to primary gold mineralization in Bukon Jedeh in having a few percent maximum base metal sulphides. The quartz-sericite-carbonate-chlorite alteration assemblage that characterizes the Birimian and other greenschist-hosted deposits is, however, absent in Bukon Jedeh. Such an assemblage would be unstable in the higher metamorphic temperature and pressure regimes that the Bukon Jedeh rocks have been subjected to.

A detrital syngenetic origin, such as that proposed for turbidite hosted gold deposits (Boyle, 1986), could explain the widespread occurrence of gold in Bukon Jedeh rocks. Such detrital origin is, however, considered least probable for

Bukon Jedeh because it would require the most mineralization to occur in volcanoclastic and epiclastic rocks. Most primary gold mineralization in Bukon Jedeh is, on the contrary, hosted by metavolcanic units.

The reason for the association of sulphide minerals and graphite in Bukon Jedeh is not clear. An association of graphite with sulphide minerals has been noted in volcanogenic exhalative deposits (Sangster, 1972; Simmons, 1973). Graphitic units may mark contacts between successive volcanic units, or represent contacts between volcanic and volcanoclastic rocks where most organic matter could have been incorporated into the rocks. These stratigraphic breaks would be zones with enhanced permeability where thermal waters could have migrated and deposited sulphides and gold.

The sulphide mineral-graphite association could also be the result of mineralization involving uptake and retention of metal ions by anoxic micro organisms. Bacteriogenic sulphides formed by reduction of marine sulphates would readily combine with organometallic complexes, transferring metal ions into sulphide phases. Such mechanism of bio-mineralization is well documented in modern and ancient anaerobic basins where metals are nucleated around organic sites and concentrated before reacting with bacteriogenic sulphides (Ferris et al., 1989; Beveridge et al., 1985; Krumbein,

1986).

The distribution of primary gold mineralization as indicated by bedrock assays could be the result of remobilization. Elevated background levels of gold in all of the different rocks, with isolated, bull's-eyes of ore grade mineralization within the pyroxene-bearing gneiss (Fig. 1.17) may be an indication of such remobilization which could very likely have occurred during regional metamorphism (Dostal and Dupuy, 1987; Henley, 1973; Seward, 1973). Such distribution could further reflect high grade centers such as veins and associated alteration haloes within the Bukon Jedeh bedrock. However, either syngenetic or epigenetic gold could well have been remobilized obscuring the details of the mineralization process. There is no compelling evidence for any particular mode of origin for the primary mineralization. However, the scale of mineralization, association with graphite, and the higher gold content in specific lithologic units would suggest syngenetic origin with later distribution during high grade regional metamorphism.

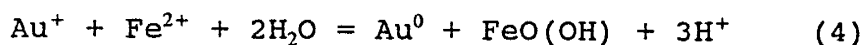
Origin of lateritic deposits

Gold-bearing laterite at Bukon Jedeh is indicated by its composition and gradual downward transition to unweathered bedrock to have formed in situ by chemical weathering of underlying bedrock. The anomalous gold content in the bedrock and its broad lateral distribution which is closely mimicked by the distribution of gold in the laterite, show that lateritic gold formed from refractory and sub-economic primary gold mineralization. Details on specific processes that occurred during weathering to form the ores must explain the following features observed in the Bukon Jedeh deposits: a) the crystalline and concretionary nature of gold and its high purity, b) common occurrence of gold nuggets in the laterite ore and their association with iron oxides and graphite, c) progressive upward increase in the overall grain size of gold, and d) the lateral and vertical variation (or lack of such) of gold grades in the laterite profile.

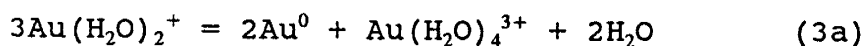
Chemical weathering would result in the liberation of gold and other resistates from mineral phases, such as sulphides, that are unstable in the weathering zone (Guibert and Park, 1985). INAA data on gold from primary, lateritic and alluvial deposits suggest a cleansing mechanism operates in the weathering zone leading to a refined lateritic gold. Gold from primary deposits typically contain 5 to 35 wt. % silver

(Morrison et al., 1991); exact values varies with factors such as geographic location and deposit type. Compositions of primary gold samples from mesothermal veins in Liberia and Ghana show that silver content in vein-type gold from Proterozoic rocks in West Africa range from 13 to 22 wt. %. The high purity of gold in the laterite and its crystalline morphology thus indicate that lateritic gold did not form by a simple accumulation of gold liberated from bedrock during chemical weathering. Rather, the gold is mostly of authigenic origin. In surficial environments gold can be mobilized by forming chloride (Cl^-) (Mann, 1984; Webster and Mann, 1984), thiosulphate ($\text{S}_2\text{O}_3^{3-}$) (Benedetti and Boulegue, 1991; Stoffregen, 1986; Webster, 1986) and organic complexes (Clove and Kelley, 1964; Machesky, 1990; Baker, 1978). Analysis of soil waters in laterites from a similar terrane in neighbouring Ghana show chloride concentrations too low to make chloride complex an effective vehicle for gold mobility (Bowell et al, 1991). In Western Australia (Mann, 1984) and India (Santosh and Omana, 1991) where chloride complexes have been determined to be responsible for gold mobility, the purity of secondary gold is exceedingly high owing to marked differences in the relative stabilities of gold-chloride and silver-chloride complexes. Silver contents in secondary gold from these areas ranges from 0.07 to 0.9 wt %, compared with an average of 2 wt. % (approx). for Bukon Jedeh gold samples.

species formed during oxidation of sulphide minerals in the weathering profile may explain the observed gold mobility. In weakly acidic to moderately alkaline soil waters, gold can be dissolved and mobilized by thiosulphate complex (Benedetti and Boulegue, 1991) (Fig. 1.20). Dissolved gold and other aqueous species generated at the weathering front will migrate upwards down a concentration gradient. The aurothiosulphate complex is metastable and breaks down by oxidation of $(S_2O_3)^{3-}$ to $(SO_4)^{2-}$ as more oxidizing environment is encountered (equation 1b), or by interaction with thio-bacteria, to give Au^+ species (Goldhaber, 1983; Orr, 1974). Au^+ ions may be reduced to Au^0 by reactions such as

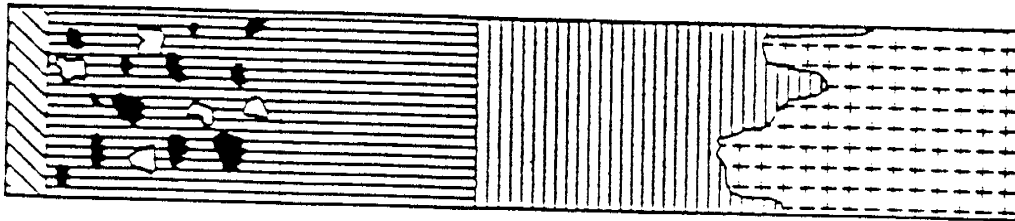


(Mann, 1984; Stoffregen, 1986), form hydroxyl complex, $AuOH(H_2O)^0$ (Vlassopoulos and Wood, 1990) which is adsorbed onto clays, hydrous Fe and Mn oxides, or exist as hydrated species and disproportionate by the reaction

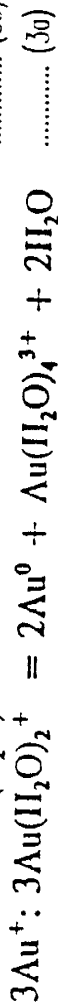
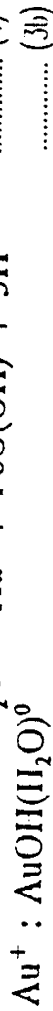
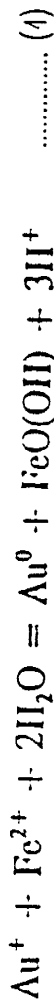
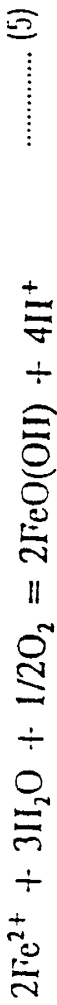


Colloidal gold formed by equation 3a, and by subsequent reduction of Au(III) is similarly taken up by adsorption (Benedetti and Boulegue, 1991). The association of gold with

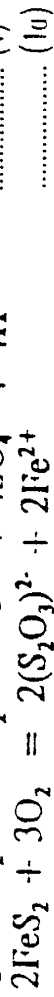
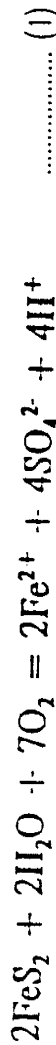
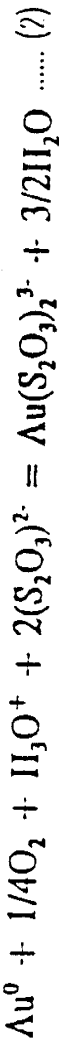
FIG. 1.20 Sulphide speciation and gold mobility in a weathering zone.



water table



weathering front



goethite and/or hematite may be explained as resulting from the coprecipitation of gold and the iron oxide phases (equation 4), or the adsorption of dissolved and colloidal gold by hydrous iron oxides. Migration of Fe^{2+} upward from the weathering front to the water table is indicated by the accumulation of iron oxide concretions in the ferruginous zone near the top of the laterite profile. A corresponding upward migration of gold cannot be documented as gold grades in the laterite profile show no distinct vertical variations; there are no zones in the saprolite or mottled zone with marked depletion in gold values. This would suggest that other mechanisms beside a redox reaction involving iron were involved in the precipitation of gold out of solution.

Gold - graphite association could be the result of adsorption. Solid organic matter is a good adsorbent for dissolved and particulate metals and can lead to their effective removal from solution (Drever et al., 1977; Drever, 1988). Large surface areas provided by micaceous graphite flakes in the weathering environment would facilitate adsorption of gold onto graphite promoting the growth of nuggets commonly found in association with graphite. Chemical replacement of graphite by Au^+ is also a possibility and may explain the occurrence of gold nuggets that take after the shape of graphite.

The coarsening in gold grain size from the weathering front upwards and the nearly exclusive occurrence of nuggets in the top ferruginous zone suggest dissolution and reprecipitation of gold at favourable sites was more effective in the upper portions of the laterite profile. Lack of vertical variation in grades in spite of increasing grain size upward, and the high purity of gold through the laterite profile suggest nuggets formed at the expense of smaller gold grains. Dissolution and mobility of gold by humic and other organic acids (Baker, 1978) generated from the decay of organic matter may explain some of the variations observed in the profile. The amount of organic matter decaying to furnish organic acids decreases downward in the laterite profile; this would result in a corresponding decrease in dissolution of gold by organic action. The growth of gold nuggets which is indicated to be promoted by repeated solution and reprecipitation of smaller gold grains, would be inhibited down the profile as less amounts of organic acids would be available to facilitate gold dissolution. If organic acids were the only agents controlling gold mobility, a downward migration of gold would be expected due to a downward migration of ground waters. The fact that observed grades in the laterite at Bukon Jedeh do not indicate such migration suggest that gold-organic acid complexes were short-lived and were rapidly immobilized, or that other processes, such as discussed above, operated concurrently.

The minuteness of primary gold in Bukon Jedeh is suggested to be an important factor in the development of nuggets in laterite. Studies of gold mineralization undergoing weathering reveal disaggregation of coarse gold (Stoffregen, 1986; Freyssinet et al., 1989a) and thin overgrowth of low-silver gold on primary gold grains (Grimm and Friedrich, 1991; Michel, 1987; Groen et al., 1990; Narayanaswamy and Krishnakumar, 1991). In the Boddington deposit in western Australia (Davy and El-Ansary, 1986) and in laterite deposits in southern Mali (Freyssinet et al., 1989a), secondary gold in the weathering profile is generally less than 5 microns in size. In both of these deposits, visible gold is common in the primary mineralization. Auriferous laterite at the Ashanti gold fields in Ghana also formed by chemical weathering of disseminated lode gold mineralization in which coarse gold is common (Bowell et al., 1991). Here also nuggets are uncommon and lateritic gold is of micron size. Thus a common characteristic of lateritic gold in which nuggets are absent or uncommon is the coarse grain size of gold in their primary sources. On the other hand, nuggets at Bukon Jedeh are associated with primary sub-microscopic gold that may occur dispersed in the lattice of pyrite, pyrrhotite, chalcopyrite and arsenopyrite (Marion et al, 1991). Gold nuggets of similar purity and shape as those at Bukon Jedeh are reported in alluvial and lateritic deposits in Coolgardie, Western Australia, and here also primary gold in

auriferous hypogene pyrite and arsenopyrite is sub-microscopic (Wilson, 1984). A logical explanation for the observed association of nuggets with primary mineralization containing sub-microscopic gold is the high surface area to volume ratio offered by the minute gold grains. Release of the molecular to micron size gold grains from sulphide minerals would facilitate their solubility in ground waters, hence promote the growth of nuggets. Even in an environment where chloride or suitable sulphur species are not available to dissolve gold, fine grained, colloidal-size gold liberated during weathering of primary gold sources may be stabilized in the laterite profile by humic acids (Ong and Swanson, 1969) and flocculate to form large grains and nuggets.

Lateral and vertical variation of gold values in the laterite may in part be attributed to inhomogeneities inherited from the primary source. Relatively uniform gold grades in the laterite, compared to grades in bedrock appears to be due to dispersion by chemical (Freyssinet et al., 1989b) and biogenic (Rose et al., 1990) processes in the weathering zone. Machesky (1990) reports up to 400 ppb gold in plants from deeply weathered terranes overlying gold deposits in Brazil. Gold taken up in soil waters by such biological means is returned to the top soil as organic litter decays. An enrichment of gold in the top soil by this mechanism is unlikely to be significant as some gold may be returned down

the profile in ground waters due to complexation of gold by organic acids.

Assuming that the lateritic deposit has formed in situ, an enrichment in its gold values over gold levels in the unweathered bedrock is to be expected. In humid tropical environments, deep chemical weathering results in chemical denudation and mass solutional loss of up to 40 % of bedrock (Thomas, 1974), producing an enrichment in resistate minerals that is unmatched in any other morphogenetic zone (Sutherland, 1985). Such enrichment is not apparent from the data collected. The inconsistency is, however, not unique to Bukon Jedeh. In the Boddington gold deposit, Western Australia, gold shows similar inconsistent surface enrichment (Davy and El-Ansary, 1986). There is no clear upward or downward increase in gold concentration at Bukon Jedeh; any such trend may have been disturbed by mechanical and biogenic processes in soils. For examples termites alone can move large amounts of soils and their metal content (Rose et al., 1990) obscuring variations that may be directly related to processes that formed the deposit. However, if enrichment in laterite did occur, it should still be evident by comparing average gold grades in laterite to average gold content in bedrock.

Average concentration of gold in lateritic deposits at Bukon Jedeh may be higher than the reported value of 0.26 ppm which only represents average of measured recoverable gold in a sluicing process and not total gold content. Inferred total gold content in laterite from the ferruginous zone, where an estimated 10-30% of gold is not recovered in a simple sluicing process, could represent up to 30% enrichment over reported concentrations of gold in laterite. Furthermore, a majority of the bedrock samples analysed for gold were obtained from areas where surface mining had exposed underlying bedrock. The reported average grade of primary mineralization 0.63 ppm must thus be viewed with some caution as it may not truly reflect average grade over the entire area.

If the lack of surficial enrichment is real, then possible explanations would include loss of gold to ground water and streams (Benedetti and Boulegue, 1991), and the shallow nature of the Bukon Jedeh laterite. Surface enrichment in a weathering profile is a slow process. The shallow soils in Bukon Jedeh would suggest that the lateritic profile there is young, and soils may not have lost a large proportion of their constituents and hence have no significant concentration of resistate minerals.

Source of alluvial gold

The location of auriferous gravel deposits on streams that originate from elevated terranes with known lateritic mineralization, similar minor and trace element chemistries of alluvial and lateritic gold, and association of graphite and iron oxides with gold from the two deposit types indicate that alluvial gold was derived from laterite.

CONCLUSION

Bukon Jedeh gneisses are subdivided into pyroxene- and garnet-bearing units with volcanic and volcanoclastic protoliths respectively. Protoliths of the gneisses and other supracrustal rocks have compositions that range from basalts to dacite and are compared with Phanerozoic volcanic rocks extruded in an island arc settings. Intrusive rocks in Bukon Jedeh are indicated to have been emplaced in a volcanic arc setting. Mineral assemblages observed in the different rocks of the area indicate metamorphism to the upper amphibolite to granulite facies.

Primary gold mineralization in Bukon Jedeh is associated with fine sulphide disseminations in bedrock and has grades locally up to 8 ppm. Gold is sub-microscopic in size and occurs in association with chalcopyrite, pyrite, pyrrhotite and minor arsenopyrite. Primary mineralization formed prior to or during regional metamorphism. Ore minerals have since been remobilized by metamorphic fluids obscuring details on the genesis of primary mineralization. Indicated lithotectonic features of Bukon Jedeh rocks are similar to those of the Birimian greenstone succession in Ghana where large volcanogenic exhalative deposits are present. The extensive nature of primary mineralization at Bukon Jedeh and the overall distribution of gold in the different rock types can

best be explained by syngenetic processes and subsequent distribution of ore minerals by metamorphic fluids. Graphitic units with which primary mineralization is commonly associated probably represent stratigraphic breaks where organic matter was incorporated into various volcanic flow units.

Lateritic gold formed in situ from primary mineralization during weathering of underlying bedrock. Micron size gold particles liberated from the sulphide minerals were dissolved in ground water by action of thiosulphate and/or organic acid complexes, and re-precipitated in the laterite profile with a resultant increase in its size and purity, and a more regular distribution than in bedrock. The high content of organic matter in soil waters percolating through the humus rich soil at the top of the laterite profile, and the minuteness of primary gold are considered important factors facilitating the dissolution of primary gold and promoting nugget growth. Distribution of auriferous laterite reflect areas of primary mineralization in bedrock.

Textural relationship between the mineral pairs: gold-graphite and gold-iron oxides, resulted from a) the adsorption of dissolved and colloidal gold onto iron oxides and onto graphite, and b) the reduction and coprecipitation of dissolved gold by ferrous ions in the weathering profile. Gold

not associated with iron oxides or graphite were deposited by adsorption of colloidal gold and $\text{AuOH}(\text{H}_2\text{O})^0$ onto clays.

REFERENCES CITED

- Baker, W. E., 1978, The role of humic acid in the transport of gold. *Geochim. Cosmochim. Acta* 42, 645-649.
- Barker, F., 1979, Trondhjemites: Definition, environment and hypothesis of origin; in *Trondhjemites, dacites and related rocks*, Barker, F., ed.
- Barnicoat, A. C., Fare, R. J., Groves, D. I. and McNaughton, N. J., 1991, Synmetamorphic lode-gold deposits in high-grade Archean settings. *Geology*, v. 19, p. 921-924.
- Benedetti, M. and Boulegue, J., 1991, Mechanism of gold transfer and deposition in a supergene environment, *Geochim. Cosmochim. Acta* 55, 1539-1547.
- Best, G. M., 1982, *Igneous and metamorphic petrology*. Publishers: W. H. Freeman and Co. 630 p.
- Beveridge, T. J. and Fyfe, W. S., 1985, Metal fixation by bacterial cell walls: *Can. Jour. Earth Sci.* 22, 1893-1898
- Bhatia, M. R., 1983, Plate tectonics and geochemical composition of sandstones: *Jour. Geol.*, v. 91 No.6, p 611-627
- Boadi, I. O. and Norman, D. I, 1990, Formation of gold nuggets in laterite soils, Bukon Jedeh, Liberia, West Africa, in *Geological Society of America abstracts with programs*, vol. 22, No. 7, p. A43.
- Boadi, I. O., Norman, D. I. and Kyle, P. R., in prep., Formation of gold nuggets in lateritic deposits, Bukon Jedeh, eastern Liberia.
- Bowell, R. J., Gize, A. P., Hoppis, H. A., Laffoley, N. A., and Rex, A. J., 1991, Mineralogical and chemical characteristics of a tropical weathering profile in Ghana: Implications for gold exploration, in *Brazil Gold '91*, E. A. Ladeira, ed. p. 713-719.
- Boyle, R. W., 1979, *The Geochemistry of Gold and Its Deposits: Geological Survey of Canada Bulletin* 280, 584 p.
- Boyle, R. W., 1986, Gold deposits in Turbidite sequences: Their geology, geochemistry, and history of the theories of their origin. In *GAC special paper* 32, Turbidite-hosted gold deposits, J. D. Keppie, R. W. Boyle and S. J. Haynes eds. p. 1-13.
- Brock, M. R., Chidester, A. H. and Baker, M. W. G., 1977, *Geologic map of the Harper quadrangle, Liberia: United States Geological Survey Miscellaneous Investigation Series Map* I-780-D, scale 1:250,000

- Butt, C. R. M., 1988, Genesis of Supergene Gold Deposits in the Lateritic Regolith of the Yilgarn Block, Western Australia, in Economic Geology Monograph 6, The Geology of Gold Deposits: The Perspective in 1988, p. 460-470
- Chappell, B. W. and White, A. J. R., 1974, Two contrasting granite types. Pacific Geol., 8, 173-174.
- Cloke, P. L., and Kelley, W. C., 1964, Solubility of gold under inorganic supergene conditions: Economic Geology, v. 59, p. 259-270.
- Condie, K. C., 1982, Early and Middle Proterozoic supra crustal successions and their tectonic settings. Am Jour. of Science vol. 282 pp 341 - 357
- Davy, R., and El-Ansary, M., 1986, Elemental in the saddle-back, Western Australia, laterite profile as a guide to mineralization: Journal of Geochemical Exploration, v. 26, p. 119-144.
- Dostal, J. and Dupuy, C., 1987, Gold in late Proterozoic andesites from northwestern Africa. Econ. Geol., vol. 82, p. 762-766.
- Drever, J. I., 1977, Sea Water: Cycles of the major elements. Dowden, Hutchinson & Ross, Stroudsburg, Pa., 345 pp.
- , 1988, The geochemistry of natural waters, 2nd. ed. 437 pp.
- Dymek, R. F. and Schiffries, C., 1987, Can. Min. 25 (pt 2), p. 291-319.
- Ferris, G. F., Shotyk, W. and Fyfe, W. S., 1989, Mineral formation and decomposition by microorganisms; in Metal ion and bacteria, Beveridge T. J. and Dole R. J. eds. pp 413-441
- Franklin, J. M., Lydon, J. W., and Sangster, D. F., 1981, Volcanic-associated massive sulfide deposits: Econ. Geol., 75th Anniversary Vol. p. 485-627.
- Freyssinet, P., Zeegers, H., and Tardy, Y., 1989, Morphology and geochemistry of gold grains in lateritic profiles of South Mali: Journal of Geochemical Exploration, v. 32, p. 17-31.
- , Lecomte, P. and Edimo, A., 1989, Dispersion of gold and basemetals in the Mborguene lateritic profile, east Cameroun: Journal of Geochemical Exploration, v. 32, p. 99-116.

- Goldhaber, M. B., 1983, Experimental study of metastable sulfur oxyanion formation during pyrite oxidation at pH 6-9 and 30°C. *Amer. J. Sci.* 283, 193-217.
- Griethuysen, H. V. van, 1971, Mineral exploration of Wm H. Muller and Co. in eastern Liberia: *Geol., Mining and metall. Soc. Liberia Bull.*, v.4, p. 88-95.
- Grimm, B. and Friedrich, G., 1991, Precipitation and concentration of gold in colluvial soils in the semiarid region of Gentio do Ouro, Central Bahia, Brazil, in *Brazil Gold '91*, E. A. Ladeira, ed. p. 343-351.
- Groen, J. C., Craig, J. R. and Rimstidt, J. D., 1990, Gold-rich rim formation on electrum grains in placers: *Can. Min.* 28: 207-228.
- Guilbert, J. M. and Park, C. F., Jr., 1985, *The Geology of Ore Deposits* 985 p. Freeman
- Henley, R. W., 1973, Solubility of gold in hydrothermal chloride solution: *Chem. Geology*, v. 11, p.73-87.
- Hirdes, W. and Leube, A., 1989, On gold mineralization of the Proterozoic Birimian Supergroup in Ghana, West Africa. *Rep. on Technical Cooperation Project No. 80.2040.6*, Ghana-German Mineral Prospecting Project. pp. 179.
- Kennedy, A., 1989, Southern Cross Mining: A new gold producer in Ghana. *Mining Magazine* 6/89, pp 476-482.
- Krumbein, W. E., 1986, Biotransfer of minerals by microbes and microbial mats in Biomineralization in lower plants and animals, B. S. C Leadbeter and R. Riding eds., Clarendon press, Oxford, 1986, p. 55-72.
- Machesky, M. L., 1990, Gold distribution and mobility in the Carajas region, Brazil: *Geological Society of America abstracts with Programs*, v. 22, No. 7, p. A60
- Mann, A. W., 1984, Mobility of gold and silver in lateritic weathering profiles: Some observations from Western Australia: *Economic Geology* v. 79, p. 38-49.
- Marion, P., Holliger, P., Boiron, M. C., Cathelineau, M., Wagner, F. E., 1991, New improvements in the characterization of refractory gold in pyrites: An electron microprobe, Mossbauer spectrometry and ion microprobe study, in *Brazil Gold '91*, E. A. Ladeira, ed. p. 389-395.
- Michel, D., 1987, Concentration of gold in insitu laterites from Mato Grosso: *Mineralium Deposita*, v. 22, p. 185-189.

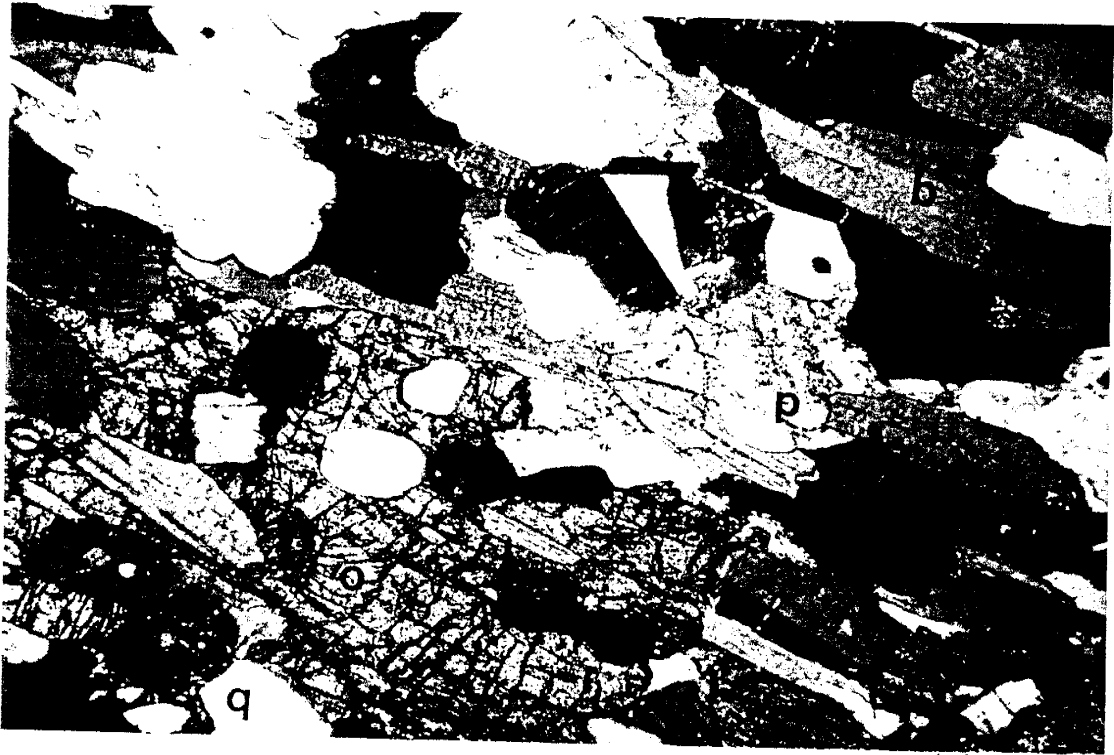
- Mueller, A. G., 1988, Archean gold-silver deposits with prominent calc-silicate alteration in the Southern Cross greenstone belt, western Australia: Analogues of Phanerozoic skarn deposits, in Ho, S. E., and Groves, D. I., eds., Recent advances in understanding Precambrian gold deposits: Perth, University of Western Australia, Dept. of Geology and University extension, v. 12. p. 141-163.
- Narayanaswamy and Krishnakumar, N., 1991, Concentration of gold in insitu laterites at Maruda, Nilambur Valley, Kerala, India, in Brazil Gold '91, E. A. Ladeira, ed. p. 743-750.
- Ong, H. L. and Swanson, V. E., 1969, Natural organic acids in the transport, deposition and concentration of gold. Q. Col. School Mines. 64: 395-407.
- Orr, W., 1974, Sulfur: Biogeochemistry. In Handbook of Geochemistry, K. H. Wedepohl, ed. pp. 16-L1 - 16-L-19.
- Pearce, J. A., Harris, N. B. W. and Tindle, A. G., 1984, Trace element discrimination diagrams for the tectonic interpretation of granitic rocks: Jour. Petrology, v. 25 part 4, pp 956-983.
- Rose, A. W., Hawkes, H. E. and Webb, J. S., 1990, Geochemistry in Mineral exploration, 657 pp. Academic Press.
- Roth, E., Groves, D., Anderson, G., Daley, L. and Staley R., 1991, Primary mineralization at the Boddington Gold Mine, Western Australia: An Archean porphyry Cu-Au-Mo deposit in Brazil Gold '91, E. A. Ladeira, ed. p. 4813-488.
- Sangster, D. F., 1972, Precambrian volcanogenic massive sulfide deposits in Canada: a review. Geol. Surv. Can. Pap. 72-22.
- Santosh, M. and Omana, P. K., 1991, Very high purity gold from lateritic weathering profiles of Nilambur, southern India: Geology, v. 19, p. 746-749.
- Seward. T. M., 1973, Thio complexes of gold and transport of gold in hydrothermal ore solutions: Geochim. et Cosmochim. Acta, v. 37, p. 379-399.
- Shand, S. J, 1947, Eruptive rocks, their genesis, composition, classification and their relation to ore deposits. 3rd Edition, 488 p. Woodbridge Ltd., Guildford.
- Simmons, B. D., 1973, Geology of the Millenbach massive sulfide deposit, Noranda, Quebec. Can. Inst. Min. Metall. Bull., Nov., 66(736):67-78.

- Stoffregen, R., 1986, Observation on the behaviour of gold during supergene oxidation at Summitville, Colorado, USA, and implications for electrum stability in the weathering environment: Applied Geochemistry, v. 1 pp 549-558.
- Streckeisen, A. L., 1976, To each plutonic rock its proper name. Earth-Science Reviews 12.
- Sutherland, D. G., 1985, Geomorphological controls on the distribution of placer deposits: Journal of geological Society of London, v. 142, p. 725-737.
- Taylor, S. R. and McLennan, S. M., 1985, The continental crust: its composition and evolution. 189 pp., Blackwell Sc. Publ.
- Thomas, M. F., 1974, Tropical geomorphology. MacMillan, London.
- Tyler, G., 1981, Heavy metals in soil biology and biochemistry, in Soil Biochemistry, E. A. Paul and J. N. Ladd, Eds., v. 5, Dekker, New York, 1981, p. 371-414.
- Tysdal, R. G., 1977, Geologic map of Juazohn quadrangle, Liberia: U.S. Geol. Surv. Miscellaneous Investigation Series Map I-779-D, scale 1:250,000.
- Tysdal, R. G., 1978, Geologic map of Juazohn quadrangle, Liberia: U.S. Geol. Surv. Bulletin 1448, 39 pp.
- Tysdal, R. G. and Thorman, C. H., 1983, Geologic Map of Liberia. United States Geological Survey Miscellaneous Investigation Series Map I-1480, scale 1:1,000,000.
- Vlassopoulos D. and Wood, S. A., 1990, Gold speciation in natural waters: I Solubility and hydrolysis reactions of gold in aqueous solutions. Geochim. Cosmochim. Acta 54, 3-12.
- Webster, J. G., 1986, The solubility of gold and silver in the system Au-Ag-S-O₂-H₂O at 25°C and 1 atm., Geochim. Cosmochim. Acta 50, 245-255.
- Webster, J. G. and Mann, A. W., 1984, The influence of climate, geomorphology and primary geology on the supergene migration of gold and silver: Jour. Geochem. Explor., v. 22, p. 21-42.
- Winchester, J. A. and Floyd, P. A., 1977, Geochemical discrimination of different magma series and their differentiation products using immobile elements: Chem. Geol., v. 20, p. 325-343.

Wright, J. B., Hastings, D. A., Jones, W. B. and Williams H.
R., 1985, Geology and mineral resources of West Africa.
pp. 187.

APPENDIX 1-A

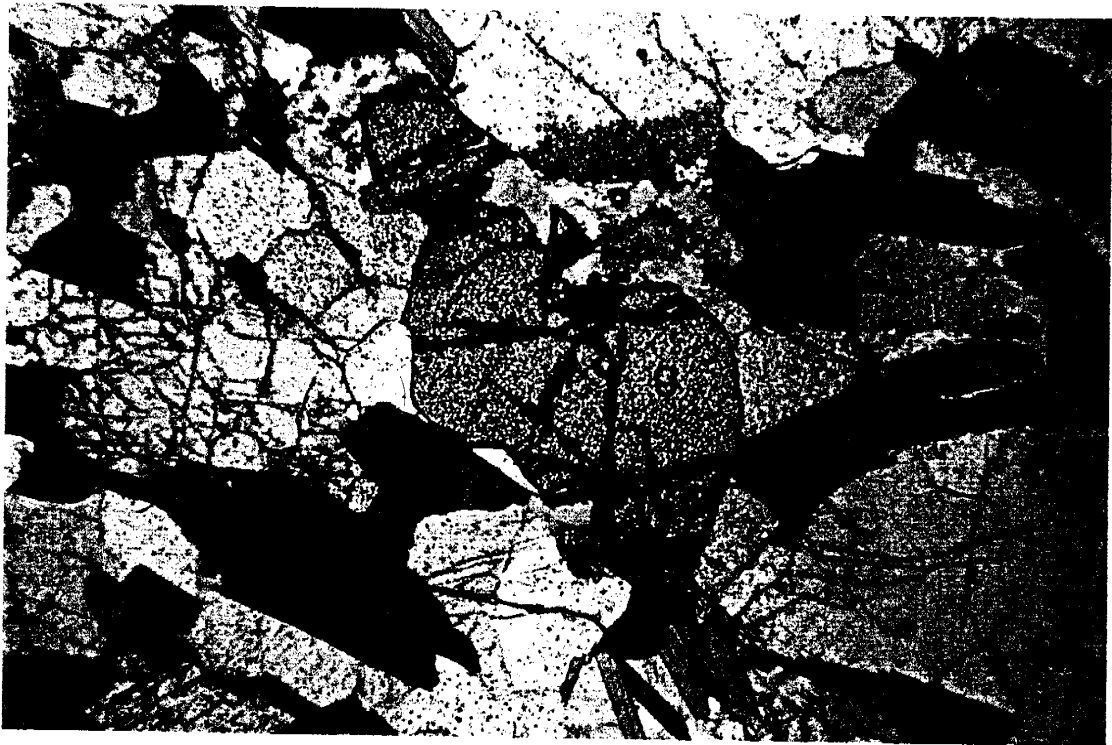
- (a) Pyroxene-bearing gneiss: show large orthopyroxene porphyroblast "o", biotite "b", plagioclase "p" and quartz "q".
- (b) Pyroxene-bearing gneiss: shows orthopyroxene "o", amphibole "a", biotite "b", plagioclase and quartz (plane light).
- (c) Garnet-bearing gneiss: shows garnet "g", biotite, plagioclase and quartz (plane light). (d) Amphibolite: shows amphibole "a", clinopyroxene "c" and plagioclase "p" (plane light). (e) Leucogranite showing large microcline crystal "m". (f) Meta-gabbro: shows orthopyroxene "o", clinopyroxene "c", amphibole "a", plagioclase "p".



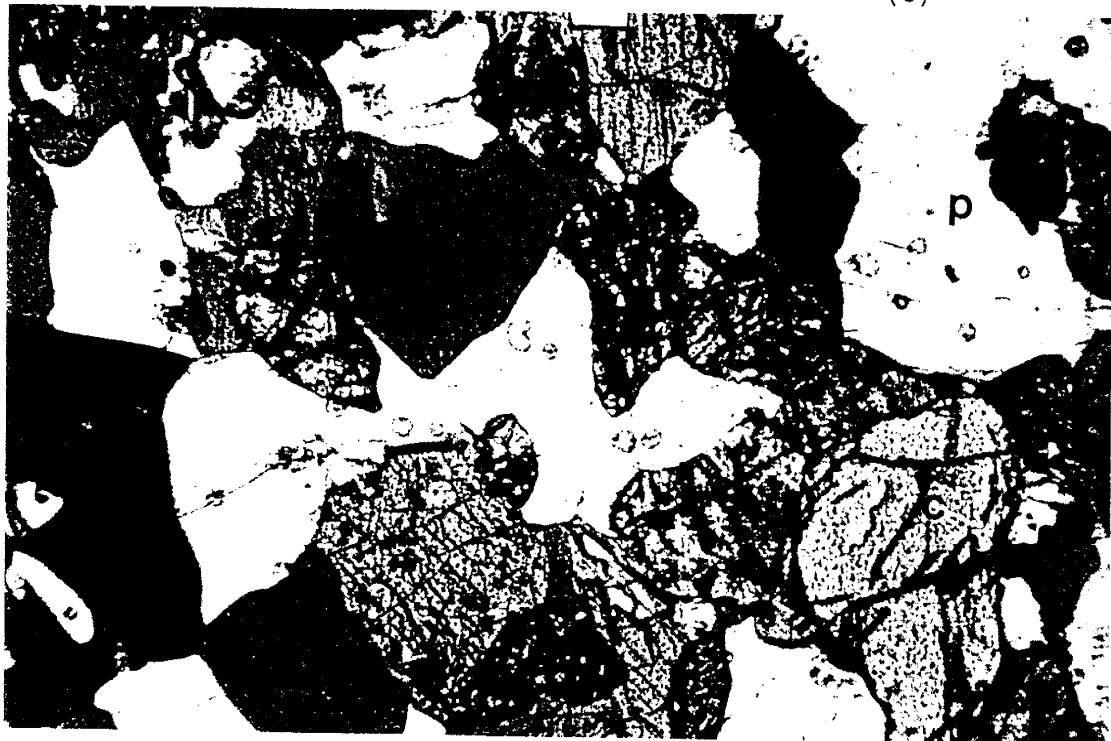
(a)



(b)



(c)



(d)



(e)



(f)

APPENDIX 1-B
MODAL ESTIMATES OF GRANITOID SAMPLES FROM BUKON JEDEH

Sample #	Absolute vol. %			Normalized vol. %			Name
	Q	AK	PLG	Q	AK	PLG	
8BR2	35	25	15	46.7	33.3	20	Granite
9BR	30	25	20	40	33.3	26.7	Granite
27BR	25	35	25	29.4	41.2	29.4	Granite
7CR	30	35	30	31.6	36.8	31.6	Granite
4BR1	30	25	30	35.3	29.4	35.3	Granite
7DR2	30	20	30	37.5	25	37.5	Granite
16CR3	20	15	40	26.7	20	53.3	Granodiorite
33FR2	30	10	50	33.3	11.1	55.6	Granodiorite
17AR1	25	5	60	27.8	5.5	66.7	Tonalite

APPENDIX 1-C

Geochemical analysis of Bukon Jedeh rocks (ggn: garnet-bearing gneiss; am: amphibolite; mg: metagabbro; pgn: pyroxene-bearing gneiss; gr: granitoid; *: garnet/pyroxene-bearing gneiss).

wt. %	IB-4BR1 gr	-45AR6 ggn	-7DR2 gr	-23BR *	-18CR am	-27BR gr	-21BR ggn	-19BR gr
SiO ₂	66.82	66.45	64.44	67.00	48.03	68.03	61.40	63.35
TiO ₂	0.43	0.56	0.47	0.05	1.15	0.17	0.66	0.63
Al ₂ O ₃	15.52	15.99	16.50	16.37	14.43	17.06	16.22	17.06
Fe ₂ O ₃	2.83	6.06	3.30	5.77	13.48	2.02	5.57	5.59
MnO	0.04	0.07	0.04	0.10	0.21	0.03	0.07	0.08
MgO	1.50	2.72	1.86	1.56	6.77	0.34	3.78	2.81
CaO	2.55	3.31	3.25	2.38	9.95	1.64	2.92	4.26
Na ₂ O	4.81	3.55	5.55	3.65	3.44	6.05	3.92	5.06
K ₂ O	2.39	1.33	2.56	1.49	0.91	3.03	2.22	1.72
P ₂ O ₅	0.15	0.20	0.16	0.09	0.09	0.04	0.14	0.22
LOI	0.37	1.37	0.67	0.23	0.48	0.48	1.63	0.81
Total	97.42	101.61	98.80	98.70	98.95	98.89	98.54	101.59

(ppm)

Pb	18	18	21	14	10		15	
Th				10				
Rb	68	78	85	28	11	85	114	42
Sr	731	476	751	355	268	1251	434	950
Y	8	14	10	29	27	6	22	16
Zr	121	106	124	29	71	59	153	130
Nb	6	7	6	3	7	3	10	8
Mo	1	1	1		1		1	1
Ga	20	17	22	15	20	20	22	23
Zn	64	63	70	19	107	30	106	80
Cu		47	16	19	80		109	26
Ni	12	37	15	17	98	10	56	37
Zr/TiO ₂	0.03	0.02	0.03	0.06	0.01	0.03	0.02	0.02
Nb/Y	0.75	0.50	0.60	0.10	0.26	0.50	0.45	0.50

CIPW MINERAL NORMS (wt. %)

Q	22.28	28.11	12.89	31.13		16.92	17.41	12.92
C	0.77	3.18		4.73		0.96	2.48	
Or	14.58	7.87	15.45	8.98	5.53	18.22	13.59	10.12
Ab	42.02	30.09	47.97	31.49	25.05	52.09	34.37	42.65
An	12.05	15.14	12.82	11.44	21.83	8.01	14.07	18.68
Ne					2.63			
Di			2.09		23.35			0.76
Hy	5.78	11.35	5.98	9.27		2.45	13.86	10.63
Ol					16.10			
Mt	1.32	2.73	1.52	2.65	3.04	0.93	2.60	2.51
Il	0.84	1.07	0.91	0.10	2.24	0.33	1.30	1.19
Ap	0.36	0.46	0.38	0.21	0.21	0.09	0.34	0.51

wt. %	IB-35ER ggn	-8BR2 gr	-11BR ggn	-27AR pgn	-52CR pgn	-29AR pgn	-28AR *	-7CR gr
SiO2	64.83	64.02	61.31	56.55	64.03	58.86	68.10	69.20
TiO2	0.64	0.52	0.64	0.64	0.58	0.69	0.17	0.36
Al2O3	16.38	15.14	16.69	17.09	15.44	17.47	16.58	15.90
Fe2O3	6.10	3.93	6.07	6.17	5.45	7.34	1.57	1.68
MnO	0.07	0.05	0.14	0.10	0.08	0.11	0.06	0.01
MgO	2.54	3.22	3.24	2.96	2.38	4.03	0.53	0.67
CaO	2.16	3.28	2.80	5.10	3.56	4.75	1.72	2.30
Na2O	3.73	4.46	3.99	5.70	3.72	3.68	3.34	3.62
K2O	2.26	2.89	2.35	1.86	1.74	1.54	5.53	4.36
P2O5	0.13	0.21	0.10	0.29	0.17	0.12	0.04	0.08
LOI	0.26	0.82	0.93	0.39	0.66	0.63	0.60	0.26
Total	99.11	98.56	98.25	96.84	97.82	99.23	98.24	98.45

(ppm)

Pb	12		15	37	14	19	27	16
Rb	124	97	83	79	73	72	95	87
U						4		
Sr	361	850	444	1155	448	456	560	611
Y	21	18	21	17	17	15	16	5
Zr	144	130	145	96	111	92	189	150
Nb	10	6	9	7	6	8	3	4
Mo	1	1	1	1		1		
Ga	22	21	21	22	20	23	14	15
Zn	93	101	96	223	69	130	17	24
Cu	23	28	63	56	16	66	12	0
Ni	38	71	52	23	33	60	11	10
Zr/TiO2	0.02	0.03	0.02	0.02	0.02	0.01	0.11	0.04
Nb/Y	0.48	0.33	0.43	0.41	0.35	0.53	0.19	0.80

CIPW MINERAL NORMS (wt. %)

Q	24.80	15.41	17.01	1.43	23.99	13.45	23.17	25.85
C	4.25		2.82		1.42	1.43	2.12	1.26
Or	13.57	17.52	14.33	11.45	10.63	9.28	33.50	26.27
Ab	32.07	38.72	34.84	50.22	32.53	31.75	28.98	31.23
An	10.03	13.09	13.66	16.20	17.10	23.23	8.48	11.10
Di		1.76		6.66				
Hy	10.96	10.16	13.04	9.20	10.26	15.89	2.60	2.63
Mt	2.79	1.82	2.82	2.89	2.53	3.37	0.72	0.77
Il	1.24	1.01	1.25	1.27	1.14	1.34	0.33	0.70
Ap	0.31	0.50	0.24	0.70	0.41	0.28	0.10	0.19

wt. %	-14BR ggn	-3AR1 pgn	-26BR mg	-14CR2 gr	-10CR ggn	-9DR1 pgn	IB-X ggn	-29B pgn
SiO2	62.29	64.50	50.69	64.00	57.69	61.97	61.51	60.51
TiO2	0.74	0.67	0.36	0.53	0.77	0.75	0.83	0.82
Al2O3	14.40	14.55	6.50	15.18	16.93	15.02	17.22	14.19
Fe2O3	7.83	7.59	9.95	4.95	7.06	7.90	7.83	8.02
MnO	0.11	0.09	0.17	0.11	0.12	0.10	0.08	0.12
MgO	3.80	2.30	16.89	1.60	3.87	3.09	3.79	3.99
CaO	3.71	3.65	13.55	3.92	2.19	5.28	3.42	5.26
Na2O	2.89	3.02	0.81	4.95	3.08	3.34	4.21	2.79
K2O	1.73	1.62	0.37	2.58	3.52	1.42	2.26	1.73
P2O5	0.17	0.18	0.04	0.14	0.11	0.22	0.23	0.18
LOI	0.64	1.01	0.70	0.47	1.79	0.14	0.57	0.71
Total	98.31	99.19	100.03	98.44	97.12	99.24	101.96	98.33

(ppm)

Pb					15		11	13
Rb	73	70	6	74	119	42	132	68
Sr	342	582	78	868	440	479	387	425
Y	23	14	21	20	21	21	18	21
Zr	135	121	32	131	144	153	132	148
Nb	9	6	3	8	10	7	9	9
Mo	1	1	1		1	1	1	1
Ga	19	18	9	19	22	18	22	19
Zn	77	70	53	70	86	77	187	89
Cu		67	112	21	75	21	36	18
Ni	50	47	183	30	61	49	60	50
Zr/TiO2	0.02	0.02	0.01	0.02	0.02	0.02	0.02	0.02
Nb/Y	0.39	0.43	0.14	0.40	0.48	0.33	0.50	0.43

CIPW MINERAL NORMS (wt. %)

Q	23.72	28.03		15.12	14.54	20.04	13.34	19.65
C	1.48	1.66			4.57		2.16	
Or	10.53	9.80	2.22	15.62	21.93	8.52	13.24	10.53
Ab	25.18	26.17	6.96	42.90	27.47	28.68	35.33	24.32
An	17.81	17.34	13.21	11.86	10.70	22.12	15.34	21.73
Di			43.78	5.88		2.46		3.22
Hy	15.82	11.77	21.74	4.97	15.63	12.61	15.01	14.81
Ol			9.08					
Mt	3.63	3.50	2.24	2.28	3.35	3.61	3.49	3.72
Il	1.45	1.30	0.69	1.03	1.54	1.45	1.56	1.61
Ap	0.41	0.43	0.09	0.33	0.27	0.52	0.53	0.43

wt. %	IB-9BR gr	-23ER pgn	-15AR1- am	-16CR3- gr	-11DR pgn	-33FR2 gr	-29AR2 pgn
SiO2	67.02	65.69	44.70	59.13	64.72	67.61	54.82
TiO2	0.49	0.57	1.07	1.09	0.47	0.31	0.57
Al2O3	14.84	15.31	12.76	16.57	13.41	16.69	15.25
Fe2O3	3.29	5.55	13.68	6.31	6.08	3.63	9.27
MnO	0.05	0.08	0.22	0.09	0.17	0.04	0.18
MgO	1.68	3.74	6.90	2.56	2.14	1.55	3.72
CaO	2.83	5.17	10.91	6.19	8.64	3.92	10.41
Na2O	4.77	2.88	2.81	5.23	1.34	4.19	1.68
K2O	2.61	0.90	0.59	1.25	0.22	1.27	0.24
P2O5	0.16	0.24	0.09	0.25	0.10	0.03	0.15
LOI	0.70	0.88	0.77	0.52	1.62	1.01	1.94
Total	98.45	101.02	94.51	99.18	98.91	100.26	98.24

(ppm)

Pb	12	13	15				12
Rb	75	33	8	33	5	36	7
Sr	700	399	142	740	678	530	461
Y	6	25	29	23	23	4	21
Zr	120	129	75	183	175	123	97
Nb	5	10	6	17	6	5	6
Mo	1	1	1	1	1	1	1
Ga	19	19	19	19	16	16	22
Zn	64	43	124	73	65	32	92
Cu	20	39	130	69	27	13	111
Ni	15	47	76	61	40	15	81
Zr/TiO2	0.02	0.02	0.01	0.02	0.04	0.04	0.02
Nb/Y	0.83	0.40	0.21	0.74	0.26	1.25	0.29

CIPW MINERAL NORMS (wt. %)

Q	21.05	27.72		8.29	36.21	26.77	17.76
C		0.78				1.38	
Or	15.82	5.33	3.77	7.52	1.34	7.58	1.48
Ab	41.39	24.43	20.37	45.05	11.70	35.81	14.86
An	11.66	24.14	22.10	18.37	30.89	19.45	34.88
Ne			2.88				
Di	1.35		29.50	9.15	10.46		14.87
Hy	5.88	13.46		6.04	5.40	6.70	10.30
Ol			15.70				
Mt	1.52	2.50	3.27	2.89	2.82	1.65	4.36
Il	0.95	1.09	2.20	2.11	0.92	0.60	1.13
Ap	0.38	0.56	0.23	0.59	0.24	0.07	0.36

APPENDIX 1-D

Gold values recovered from Bukon Jedeh laterite by sluicing.

#	ppm	#	ppm	#	ppm	#	ppm
1.	0.33	39.	0.65	77.	0.07	115.	0.38
2.	0.07	40.	0.16	78.	0.65	116.	0.38
3.	0.28	41.	0.03	79.	0.53	117.	0.28
4.	0.21	42.	0.49	80.	0.09	118.	0.20
5.	0.36	43.	0.37	81.	0.21	119.	0.26
6.	0.15	44.	0.07	82.	0.47	120.	0.12
7.	0.16	45.	0.34	83.	0.36	121.	0.15
8.	0.16	46.	0.55	84.	0.07	122.	0.18
9.	0.13	47.	0.10	85.	0.13	123.	0.12
10.	0.15	48.	0.18	86.	0.61	124.	0.09
11.	0.22	49.	0.29	87.	0.43	125.	0.28
12.	0.03	50.	0.18	88.	0.03	126.	0.16
13.	0.05	51.	0.13	89.	0.46	127.	0.08
14.	0.01	52.	0.26	90.	0.01	128.	0.16
15.	0.35	53.	0.21	91.	0.22	129.	0.16
16.	0.07	54.	0.04	92.	0.07	130.	0.15
17.	0.03	55.	0.54	93.	0.03	131.	0.13
18.	0.07	56.	0.23	94.	0.42	132.	0.20
19.	0.07	57.	0.26	95.	0.38	133.	0.10
20.	0.03	58.	0.33	96.	0.47	134.	0.18
21.	0.03	59.	0.29	97.	0.78	135.	0.39
22.	0.03	60.	0.36	98.	0.22	136.	0.40
23.	0.90	61.	0.08	99.	0.26	137.	0.29
24.	0.26	62.	0.09	100.	0.18	138.	0.26
25.	1.68	63.	0.07	101.	0.59	139.	0.49
26.	0.08	64.	0.26	102.	0.36	140.	0.16
27.	0.07	65.	0.10	103.	0.48	141.	0.46
28.	0.14	66.	0.03	104.	0.15	142.	0.16
29.	0.14	67.	0.31	105.	0.03	143.	0.07
30.	0.08	68.	0.25	106.	0.07	144.	0.81
31.	0.03	69.	0.34	107.	0.59	145.	0.78
32.	0.02	70.	0.03	108.	0.18	146.	0.18
33.	0.20	71.	0.21	109.	0.29	147.	0.47
34.	0.14	72.	0.26	110.	0.26	148.	0.65
35.	0.39	73.	0.02	111.	0.36	149.	0.08
36.	0.85	74.	0.03	112.	0.29	150.	0.33
37.	0.02	75.	0.12	113.	0.29	151.	0.14
38.	0.28	76.	0.80	114.	0.26	152.	0.33

#	ppm	#	ppm	#	ppm	#	ppm
153.	0.13	191.	0.23	229.	0.18	267.	0.03
154.	1.43	192.	0.28	230.	0.04	268.	0.05
155.	0.86	193.	1.30	231.	0.21	269.	0.44
156.	0.20	194.	0.39	232.	0.04	270.	0.47
157.	0.37	195.	0.34	233.	0.20	271.	0.07
158.	0.39	196.	0.59	234.	0.30	272.	0.24
159.	0.78	197.	0.46	235.	0.14	273.	0.88
160.	0.10	198.	0.27	236.	0.12	274.	0.03
161.	1.03	199.	0.23	237.	0.07	275.	0.56
162.	1.95	200.	0.65	238.	0.06	276.	0.07
163.	0.98	201.	0.11	239.	0.08	277.	0.10
164.	0.20	202.	0.26	240.	0.54	278.	0.64
165.	0.42	203.	0.43	241.	0.07	279.	0.04
166.	0.25	204.	0.33	242.	0.46	280.	0.23
167.	0.33	205.	0.16	243.	0.14	281.	0.10
168.	5.53	206.	0.20	244.	0.07	282.	0.20
169.	2.93	207.	0.16	245.	0.17	283.	0.12
170.	0.33	208.	0.36	246.	0.01	284.	0.16
171.	0.55	209.	0.08	247.	0.10	285.	0.33
172.	0.23	210.	0.07	248.	0.03	286.	0.16
173.	0.46	211.	0.39	249.	0.16	287.	0.10
174.	0.21	212.	0.02	250.	0.19	288.	0.07
175.	0.46	213.	0.31	251.	0.06	289.	0.10
176.	0.20	214.	0.13	252.	0.14	290.	0.05
177.	0.23	215.	0.09	253.	0.15	291.	0.05
178.	0.26	216.	0.14	254.	0.15	292.	0.10
179.	0.79	217.	0.28	255.	0.35	293.	0.05
180.	0.18	218.	0.18	256.	0.05	294.	0.20
181.	0.85	219.	0.23	257.	0.03	295.	0.10
182.	0.72	220.	0.12	258.	0.28	296.	0.12
183.	0.23	221.	0.20	259.	0.16	297.	0.10
184.	0.18	222.	0.20	260.	0.10	298.	0.08
185.	0.72	223.	0.30	261.	0.07	299.	0.10
186.	0.29	224.	0.08	262.	0.06	300.	0.15
187.	0.25	225.	0.21	263.	0.10	301.	0.23
188.	0.23	226.	0.10	264.	0.39	302.	0.16
189.	0.28	227.	0.08	265.	0.34	303.	0.16
190.	1.30	228.	0.23	266.	0.12	304.	0.12

#	ppm	#	ppm	#	ppm	#	ppm
305.	0.13	343.	0.32	381.	0.06	419.	0.07
306.	0.01	344.	0.50	382.	0.30	420.	0.11
307.	0.05	345.	0.21	383.	0.16	421.	0.14
308.	0.03	346.	0.20	384.	0.09	422.	0.04
309.	0.07	347.	0.47	385.	0.02	423.	0.03
310.	0.08	348.	0.39	386.	0.44	424.	0.07
311.	0.20	349.	0.07	387.	0.36	425.	0.10
312.	0.46	350.	0.26	388.	0.08	426.	0.07
313.	0.51	351.	0.10	389.	0.06	427.	0.08
314.	0.38	352.	0.10	390.	0.23	428.	0.03
315.	0.20	353.	0.18	391.	0.33	429.	0.20
316.	0.20	354.	0.12	392.	0.23	430.	0.07
317.	0.20	355.	0.22	393.	0.48	431.	0.01
318.	0.10	356.	0.75	394.	0.36	432.	0.22
319.	0.10	357.	0.29	395.	0.16	433.	0.23
320.	0.12	358.	0.25	396.	0.08	434.	0.28
321.	0.10	359.	0.13	397.	0.23	435.	0.33
322.	0.16	360.	0.16	398.	0.38	436.	0.46
323.	0.07	361.	0.12	399.	0.16	437.	0.14
324.	0.10	362.	0.30	400.	0.24	438.	0.13
325.	0.16	363.	0.59	401.	0.03	439.	0.04
326.	0.13	364.	0.07	402.	0.31	440.	0.14
327.	0.33	365.	0.20	403.	0.36	441.	0.16
328.	0.33	366.	0.12	404.	0.05	442.	0.16
329.	0.07	367.	0.46	405.	0.37	443.	0.12
330.	0.26	368.	0.91	406.	0.36	444.	0.10
331.	0.07	369.	0.60	407.	0.10	445.	0.05
332.	0.13	370.	0.46	408.	1.30	446.	0.13
333.	0.14	371.	0.33	409.	0.25	447.	0.07
334.	0.25	372.	0.47	410.	0.18	448.	0.14
335.	1.25	373.	0.32	411.	0.14	449.	0.07
336.	0.10	374.	0.33	412.	0.21	450.	0.20
337.	0.23	375.	0.33	413.	0.10	451.	0.16
338.	0.52	376.	0.25	414.	0.12	452.	0.13
339.	0.29	377.	0.05	415.	0.26	453.	0.20
340.	0.72	378.	0.71	416.	0.20	454.	0.16
341.	0.11	379.	0.94	417.	0.07	455.	0.09
342.	0.26	380.	0.10	418.	0.05	456.	0.22

#	ppm	#	ppm	#	ppm	#	ppm
457.	0.12	495.	0.09	533.	0.15	571.	0.16
458.	0.27	496.	0.07	534.	0.18	572.	0.14
459.	0.13	497.	0.16	535.	0.14	573.	0.18
460.	0.33	498.	0.08	536.	0.16	574.	0.12
461.	0.03	499.	0.03	537.	0.08	575.	0.21
462.	0.18	500.	0.36	538.	0.10	576.	0.20
463.	0.13	501.	0.24	539.	0.23	577.	0.20
464.	0.22	502.	0.24	540.	0.03	578.	0.17
465.	0.07	503.	0.22	541.	0.04	579.	0.36
466.	0.33	504.	0.53	542.	0.15	580.	0.18
467.	0.07	505.	0.49	543.	0.10	581.	0.14
468.	0.26	506.	0.36	544.	0.03	582.	0.42
469.	0.21	507.	0.19	545.	0.16	583.	0.44
470.	0.21	508.	0.21	546.	0.03	584.	0.53
471.	0.14	509.	0.16	547.	0.10	585.	0.42
472.	0.59	510.	0.08	548.	0.16	586.	0.18
473.	0.36	511.	0.10	549.	0.10	587.	0.20
474.	0.08	512.	0.20	550.	0.16	588.	0.23
475.	0.39	513.	0.10	551.	0.36	589.	0.30
476.	0.05	514.	0.16	552.	0.13	590.	0.18
477.	0.13	515.	0.46	553.	0.19	591.	0.07
478.	0.08	516.	0.10	554.	0.14	592.	0.15
479.	0.27	517.	0.08	555.	0.09	593.	0.14
480.	0.06	518.	0.08	556.	0.21	594.	0.16
481.	0.19	519.	0.09	557.	0.31	595.	0.23
482.	0.07	520.	0.33	558.	0.18	596.	0.19
483.	0.20	521.	0.08	559.	0.16	597.	0.13
484.	0.05	522.	0.08	560.	0.36	598.	0.26
485.	1.14	523.	0.06	561.	0.44	599.	0.13
486.	1.24	524.	0.20	562.	0.13	600.	0.42
487.	1.46	525.	0.10	563.	0.33	601.	0.10
488.	0.42	526.	0.11	564.	0.20	602.	0.10
489.	0.07	527.	0.07	565.	0.17	603.	0.20
490.	0.15	528.	0.06	566.	0.20	604.	0.26
491.	0.14	529.	0.04	567.	0.20	605.	0.20
492.	0.22	530.	0.14	568.	0.07	606.	0.10
493.	0.21	531.	0.08	569.	0.14	607.	0.05
494.	0.07	532.	0.18	570.	0.27	608.	0.03
609.	0.07	649.	0.10	689.	1.63	729.	0.16
610.	0.08	650.	0.06	690.	0.52	730.	0.58
611.	0.23	651.	0.42	691.	0.27	731.	0.33
612.	0.03	652.	0.29	692.	0.21	732.	0.24
613.	0.15	653.	0.06	693.	0.27	733.	0.31

#	ppm	#	ppm	#	ppm	#	ppm
614.	0.13	654.	0.07	694.	0.16	734.	0.20
615.	0.18	655.	0.13	695.	0.43	735.	0.12
616.	0.01	656.	0.13	696.	0.10	736.	0.47
617.	0.29	657.	0.16	697.	0.26	737.	0.23
618.	0.21	658.	0.10	698.	0.36	738.	0.53
619.	0.05	659.	0.20	699.	0.18	739.	0.14
620.	0.02	660.	0.23	700.	0.13	740.	0.88
621.	0.13	661.	0.13	701.	0.10	741.	0.69
622.	0.07	662.	0.08	702.	0.29	742.	0.80
623.	0.16	663.	0.29	703.	0.20	743.	0.38
624.	0.21	664.	0.23	704.	0.28	744.	0.59
625.	0.05	665.	0.31	705.	0.26	745.	0.46
626.	0.13	666.	0.27	706.	0.10	746.	0.23
627.	0.12	667.	0.33	707.	0.03	747.	0.59
628.	0.03	668.	0.19	708.	0.04	748.	0.26
629.	0.12	669.	0.11	709.	0.20	749.	0.46
630.	0.07	670.	0.45	710.	0.37	750.	0.62
631.	0.08	671.	0.11	711.	0.12	751.	1.03
632.	0.07	672.	0.85	712.	0.11	752.	0.96
633.	0.10	673.	0.46	713.	0.10	753.	0.98
634.	0.08	674.	0.56	714.	0.09	754.	0.48
635.	0.08	675.	0.18	715.	0.20	755.	0.14
636.	0.23	676.	0.18	716.	0.14	756.	0.07
637.	0.21	677.	0.23	717.	0.13	757.	0.10
638.	0.16	678.	0.12	718.	0.18	758.	0.08
639.	0.25	679.	0.28	719.	0.20	759.	0.09
640.	0.18	680.	0.10	720.	0.13	760.	0.10
641.	0.13	681.	0.17	721.	0.13	761.	0.12
642.	0.23	682.	0.28	722.	0.18	762.	0.05
643.	0.16	683.	0.17	723.	0.20	763.	0.25
644.	0.07	684.	0.18	724.	0.14	764.	0.25
645.	0.07	685.	0.18	725.	0.17	765.	0.07
646.	0.10	686.	0.12	726.	0.20	766.	0.03
647.	0.02	687.	0.01	727.	0.08	767.	0.08
648.	0.02	688.	0.05	728.	0.18		

APPENDIX 1-E

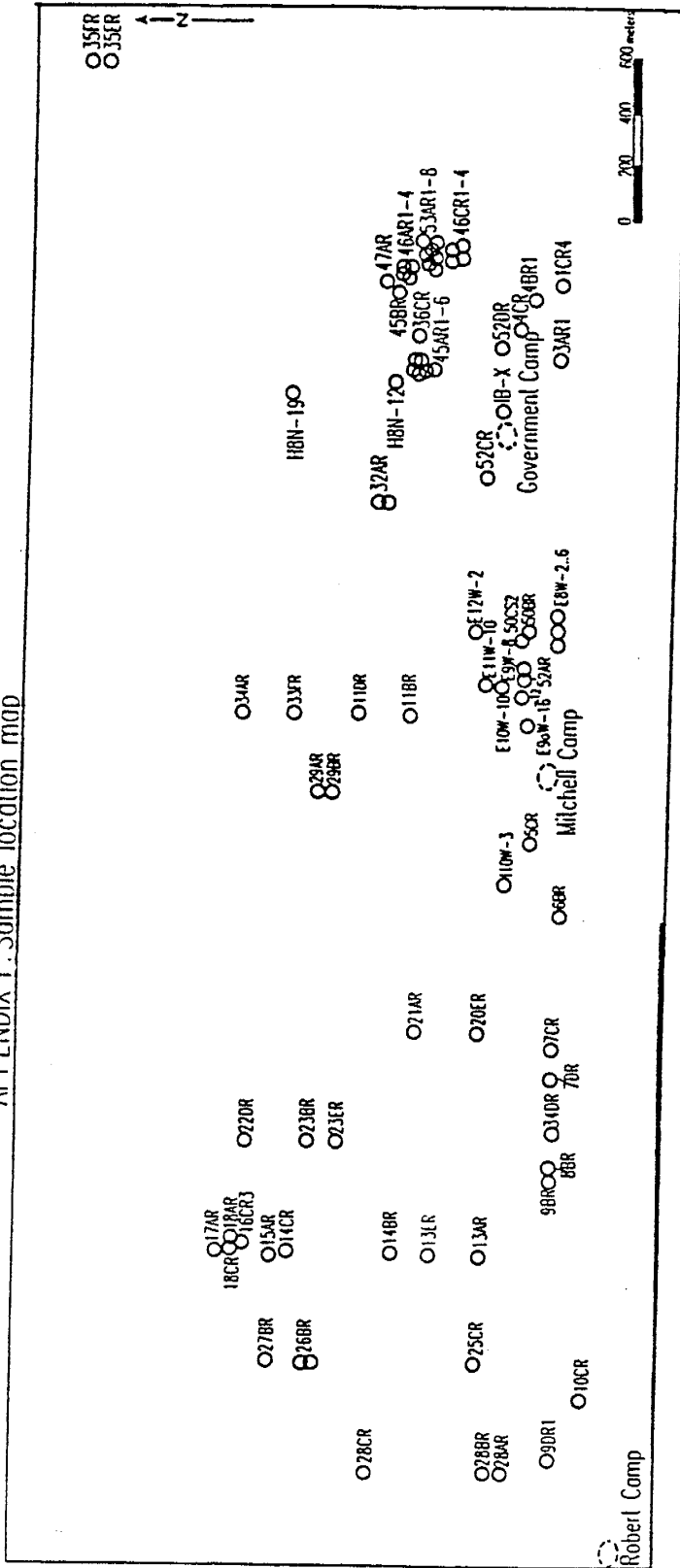
Assays of bedrock samples from Bukon Jedeh, Liberia.

Sample #	Description	ppm(g/ton)
52DR	Pegmatite	2.5
26BR	Pyroxenite	0.2
15AR1	Amphibolite	0.1
E9aW-18	Px-bearing gniess	8
45AR4	Pegmatite	0.05
#8 Blk 1 W	Px-bearing gniess	0.2
18CR	Amphibolite	0.75
3AR1	Px-bearing gniess	4
4BR1	Granite	0.1
1CR4	Iron concretion	0.1
45AR1	Pegmatite	0.5
50CS2	Px-bearing gniess	0.5
H4N-8	Px-bearing gniess	0.5
32AR3	vein qtz in gt-gneiss	0.05
52BR1	Px-bearing gniess	0.8
14CR3	vein qtz	0.7
46CR2	Px-bearing gniess	0.7
45AR3	Px-bearing gniess	0.5
35ER	Garnet-bearing gneiss	0.5
E9aW-16	Px-bearing gniess	0.7
45BR1	Px-bearing gniess	0.5
45AR6	Px-bearing gniess	0.25
I10W-3	Garnet-bearing gneiss	1.4
H8N-19B	Garnet-bearing gneiss	0.35
29AR	Px-bearing gneiss	0.05
25CR	vein qtz in gar. gneiss	0.7
46CR1	Px-bearing gniess	2
46CR	Px-bearing gniess	3.5
35FR	3' wide vein qtz	0.25
33FR1	vein quartz in gneiss	2.4
21AR3	graphitic vein qtz in gneiss	0.5
53AR6	weathered gneiss (blk. 1A)	0.5
16CR3	brecciated contact gn/granite	4.6
45AR6	Partly weathered gneiss	0.37
46CR3	Px-bearing gniess	1.49
46AR3	Px-bearing gniess	0.42
53AR5	Px-bearing gniess	1.44
45AR2	Px-bearing gniess	1.91

Sample #	Description	ppm(g/ton)
46CR4	Px-bearing gniess	0.14
H8N-12	Garnet-bearing gneiss	0.14
23BR1	vein quartz	0.11
29AR2	Px-bearing gniess	0.14
8BR1	vn quartz in foliated granite	0.42
53AR7	Px-bearing gniess	0.06
~ Blk 1B	vn quartz in gneiss	0.37
5CR	Garnet-bearing gneiss	0.24
9DR1	Amphibolite	0.11
17AR2	gn/granite contact w/py	0.1
17AR	granite	0.11
18AR2	vn quartz in gneiss	0.13
4CR	vn qtz in foliated granite w/py	0.27
32AR3*	vn qtz w/graphite	0.32
14CR2	Px-bearing gniess	0.14
33FR2	vn qtz	1.45
11DR	Px-bearing gniess	0.29
11BR3	vn qtz in gneiss	0.24
14BR	Garnet/Px-bearing gneiss	0.11
10CR	Garnet-bearing gneiss	0.19
H8N-19	Garnet-bearing gneiss	0.26
45AR3	Px-bearing gniess	0.05
45BR1	weathered gneiss	0.56
50CS2	Weathered Px-bearing gneiss	3.2
53AR8	weathered gneiss	0.19
52AR1	weathered gneiss	0.11
46AR2	Px-bearing gniess	0.34
46CR4	Px-bearing gniess	2.46
50BR	Px-bearing gniess	1.23
47AR	qtz in decomposed gneiss	0.11
E9aW-12	Px-bearing gniess	1.38
46BR2	Px-bearing gniess	0.38
6BR	Pegmatite w/graphite	0.32
13AR2	qtz w/graphite	
53AR4	Px-bearing gniess	0.49
36CR	vn qtz in gneiss	0.19
28AR	Garnet-bearing gneiss	0.41
19BR	Granitoid	
22DR	pyroxene-bearing gneiss	0.3
27BR	Granitoid	0.13
52CR	Px-bearing gniess	0.31
23ER	Px-bearing gniess	0.32
34DR	Granitoid	0.13
20ER	vn quartz in gneiss	0.19

Sample #	Description	ppm(g/ton)
29BR	Px-bearing gniess	0.18
23BR1	vn qtz in gneiss	0.21
9BR	foliated granite w/amethyst qtz	0.31
E8W-2	Px-bearing gniess	3.23
E8W-4	Px-bearing gniess	6.66
E8W-6	Px-bearing gniess	0.37
E9W-2	Px-bearing gniess	0.1
E9W-4	Px-bearing gniess	0.44
E9W-6	Px-bearing gniess	0.1
E9W-8	Px-bearing gniess	0.5
E9W-10	Px-bearing gniess	0.1
E10W-2	Px-bearing gniess	0.1
E10W-4	Px-bearing gniess	0.1
E10W-6	Px-bearing gniess	0.1
E10W-8	Px-bearing gniess	0.1
E11W-2	Px-bearing gniess	0.1
E11W-4	Px-bearing gniess	0.1
E11W-6	Px-bearing gniess	0.1
E11W-8	Px-bearing gniess	0.19
E11W-10	Px-bearing gniess	0.25
E12W-2	Px-bearing gniess	0.31
E12W-4	Px-bearing gniess	0.1
E12W-6	Px-bearing gniess	0.1
E12W-8	Px-bearing gniess	0.16
E12W-10	Px-bearing gniess	0.19
E10aW-10	Px-bearing gniess	0.25
13ER	garnet-bearing gneiss	0.45
23ER2	garnet-bearing gneiss	1.65

APPENDIX F: Sample location map



PART II

NATURE OF SOURCE TERRANE AND ORIGIN OF GOLD
IN THE TARKWA PALEOPLACER DEPOSIT,
GHANA, WEST AFRICA.

ABSTRACT

The Tarkwaian Group that hosts gold paleoplacers in Ghana was studied to determine the nature of its source terrane and mechanism for gold concentration. Tarkwaian rocks are fluvial and are postulated to have been deposited in intracratonic rift basins within Proterozoic Birimian metavolcanic belts. The Banket Formation, the unit that hosts the Tarkwa deposits, varies across the Tarkwa basin from immature to mature sedimentary units. Immature sediments are debris flows comprising polymictic, matrix supported conglomerates, breccias and grits. Clasts are angular to subrounded volcanic fragments (>80% of clast component), chert and rounded quartz pebbles. Cross-bedded quartz arenites and clast supported conglomerates with <10% lithic fragments are interbedded with the immature units. Mature sediments consist of up to three quartz-pebble conglomerate bands interbedded with cross-bedded quartz-arenites and grits. Conglomerates are either matrix or clast supported, and are essentially monolithic with clasts composed of rounded vein quartz. Matrix material in the conglomerates contain abundant hematite and magnetite, and minor amounts of tourmaline, zircon, apatite, ulvospinel and gold. Paleocurrent direction indicate that the immature and mature sedimentary units are proximal and distal facies equivalents.

Gold is dispersed through a column of immature sediments, 50 to 70 meters thick, with an average grade of 1.46 ppm. Grades vary locally from 0.1 to 6 ppm; the higher grades occur within horizons of clast supported conglomerates. In mature sedimentary units, gold is concentrated in conglomerate bands 0.5 to 2 meters thick, at average grades of 15.41 ppm in the clast-supported conglomerate and 5.6 ppm in matrix-supported conglomerates. Gold from the Tarkwa paleo-placer contains less than 4 wt. % Ag and trace amounts of Hg, Sc and Sb. Overall composition of Tarkwa gold is similar to that of gold from lateritic deposits.

Volcanic fragments from immature Banket Formation sediments have a quartz sericite assemblage and commonly contain minute quartz stringers with casts of euhedral rhombic crystals. Compared to Birimian metavolcanic rocks, the fragments have higher amounts of normative corundum and lesser Ca, Na and Mg. On a Zr/TiO₂ versus Nb/Y variation diagram, the volcanic fragments are indicated to have protoliths with dacite to rhyodacite compositions whereas samples of exposed Birimian metavolcanic and volcanoclastic rocks show protoliths with basaltic and andesitic compositions. Nine volcanic fragments and 2 chert fragments were analysed by instrumental neutron activation analysis. Ten of the 11 analysis showed anomalous levels of gold ranging from 0.05 to 5.66 ppm. The lithic fragments analysed were collected from

multiple sites within the southern Tarkwa basin which suggests that primary gold mineralization in source area was pervasive and associated with felsic volcanic rocks and chert.

A Rb-Sr isochron age of 2.15 +/- 0.11 Ga and an initial $^{87}\text{Sr}/^{86}\text{Sr}$ ratio of 0.70057 +/- 0.43 were obtained for samples of Birimian metavolcanic rocks. Isotopic data on samples of the lithic volcanic fragments scatter between the 2.15 Ga isochron and a 1.968 Ga isochron obtained by Taylor et. al. (1988) for post Tarkwaian granitoids. The isotopic data suggest that the volcanic fragments have similar isotopic systematics as the Birimian metavolcanics and support derivation of the Banket Formation and its gold content from the Birimian Supergroup.

Critical events in the formation of the Tarkwa ores were chemical weathering of extensive deposits in felsic volcanics, stripping of the soils and regolith mantle and their deposition as debris flows along margins of the Tarkwa basin. Localized reworking of these created the better grades seen in the proximal ores; reworking in distal areas resulted in mature conglomerates in which gold was concentrated to grades exceeding 8 ppm.

INTRODUCTION

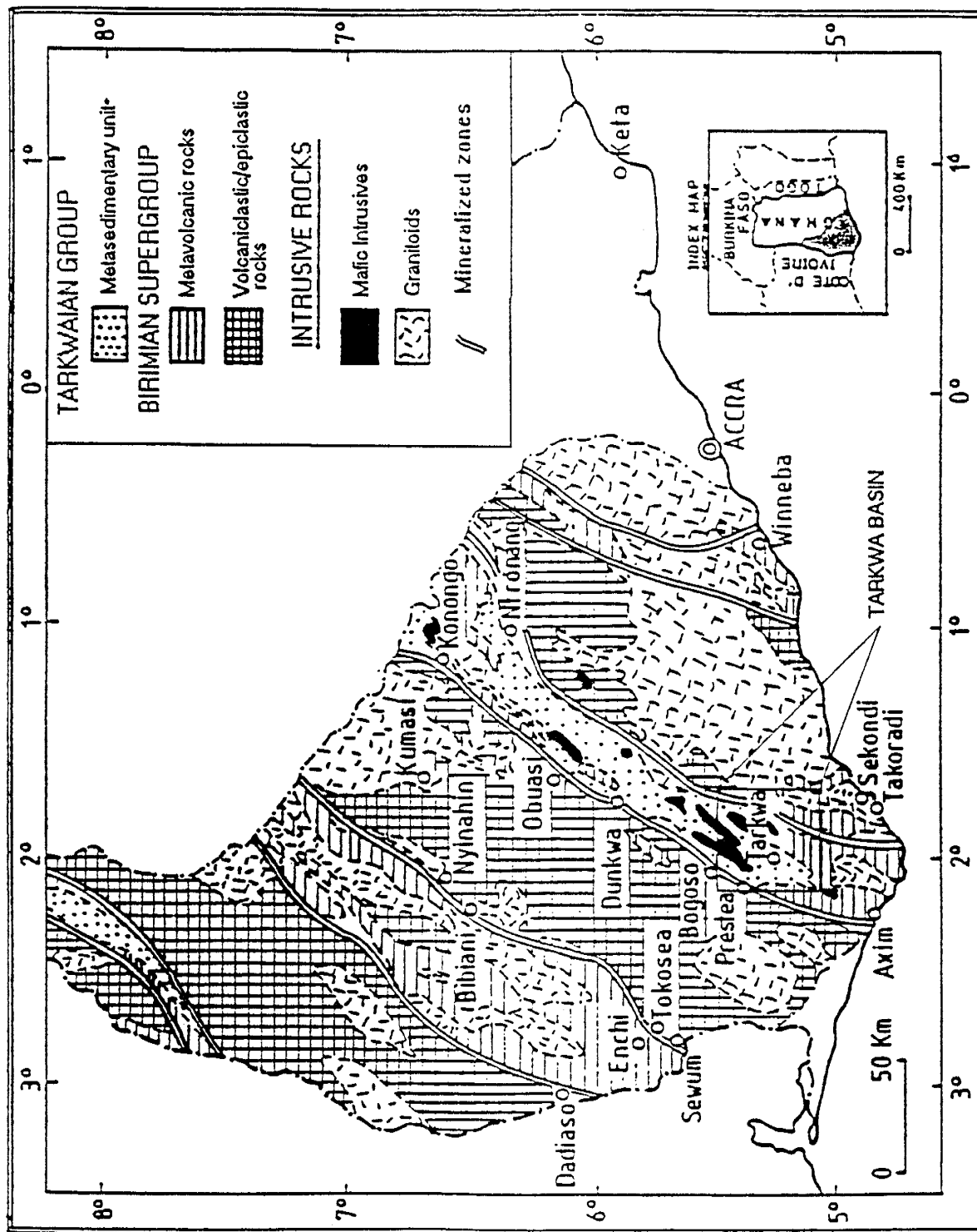
Paleoplacer deposits constitute an important class of gold deposits accounting for more than 50% of the world's total gold production (Boyle, 1979; Sutherland, 1985). They are poorly understood, in spite of their long history of extensive mining, and only a few examples are known worldwide. The Witwatersrand in South Africa, Tarkwa in Ghana and Serra de Jacobina in Brazil are the 3 auriferous paleoplacer deposits that have produced significant gold. Smaller examples are reported in Canada (Boyle, 1979), Russia (Smirnov, 1969; Levin et al., 1970), India, Gabon and Finland (Krendlev et al., 1966). Gold from these deposits is produced largely from mature quartz-pebble conglomeratic units (reefs) within successions of fluvial sediments (Robb and Meyer, 1990; Junner et al., 1942; Bateman, 1958). Since their discovery, the genesis of these deposits has stirred up considerable discussion and controversy. Opinions over the years have been divided between a placer and a hydrothermal origin for the gold. Their stratabound nature, association of the gold with abundant detrital heavy minerals in quartz-pebble conglomerates, and the presence of primary gold mineralization in neighbouring basement rocks are cited, among other features, as evidence for a modified or metamorphosed placer origin for gold in these deposits (Mellor, 1916, 1931; Reinecke, 1927, 1930; Junner et al., 1942; Pretorius, 1964, 1976; Sestini,

1971, 1973; Minter, 1978, 1979, 1988; Armstrong, 1966; Robb and Meyer, 1990, 1991). Proponents of a hydrothermal origin cite the abundance of non-detrital pyrite and uraninite in the Witwatersrand and the Jacobina deposits. Gold grains from the conglomerates also lack the abraded exteriors that generally characterize modern alluvial placers. Other evidence cited in support of a hydrothermal origin include the scattered distribution of gold in host conglomerate bands, the presence of gold and sulphide bearing quartz veins along faults and fractures, and presence of minerals commonly associated with epigenetic mineralization such as sericite, chlorite, tourmaline and base metal sulphides (Graton, 1930; Davidson, 1953, 1964; Phillips and Myers, 1989). The current consensus among most geologists favours the modified placer theory as it accomodates most of the features observed in the deposits (Boyle, 1979).

The nature of source terranes for these ancient mega-placers and an explanation on their generally higher gold contents compared with modern placers remain enigmatic. The widely accepted modified placer origin of these deposits has been in dispute because such a hypothesis necessitates source areas that can account for the large accumulations of gold in the deposits (Robb and Meyer, 1990). Data on immature and mature sediments of the Tarkwa deposit are presented herein to indicate the nature of the Tarkwa source terrane and processes

leading to the levels of gold present in that deposit.

FIG. 2.1 Generalized geologic map of southwestern Ghana showing parallel set of mineralized vein systems in the Birimian Supergroup (after Kesse, 1982).



Regional Geology

Bedrock in the southwestern portion of Ghana consists of an older greenstone succession, the Birimian Supergroup, overlain by a package of fluvial sediments that represent erosional products of basement granite-greenstone terrane into intra-cratonic rift basins that developed within the latter during the Eburnean orogeny (Kesse, 1985)

Birimian Supergroup

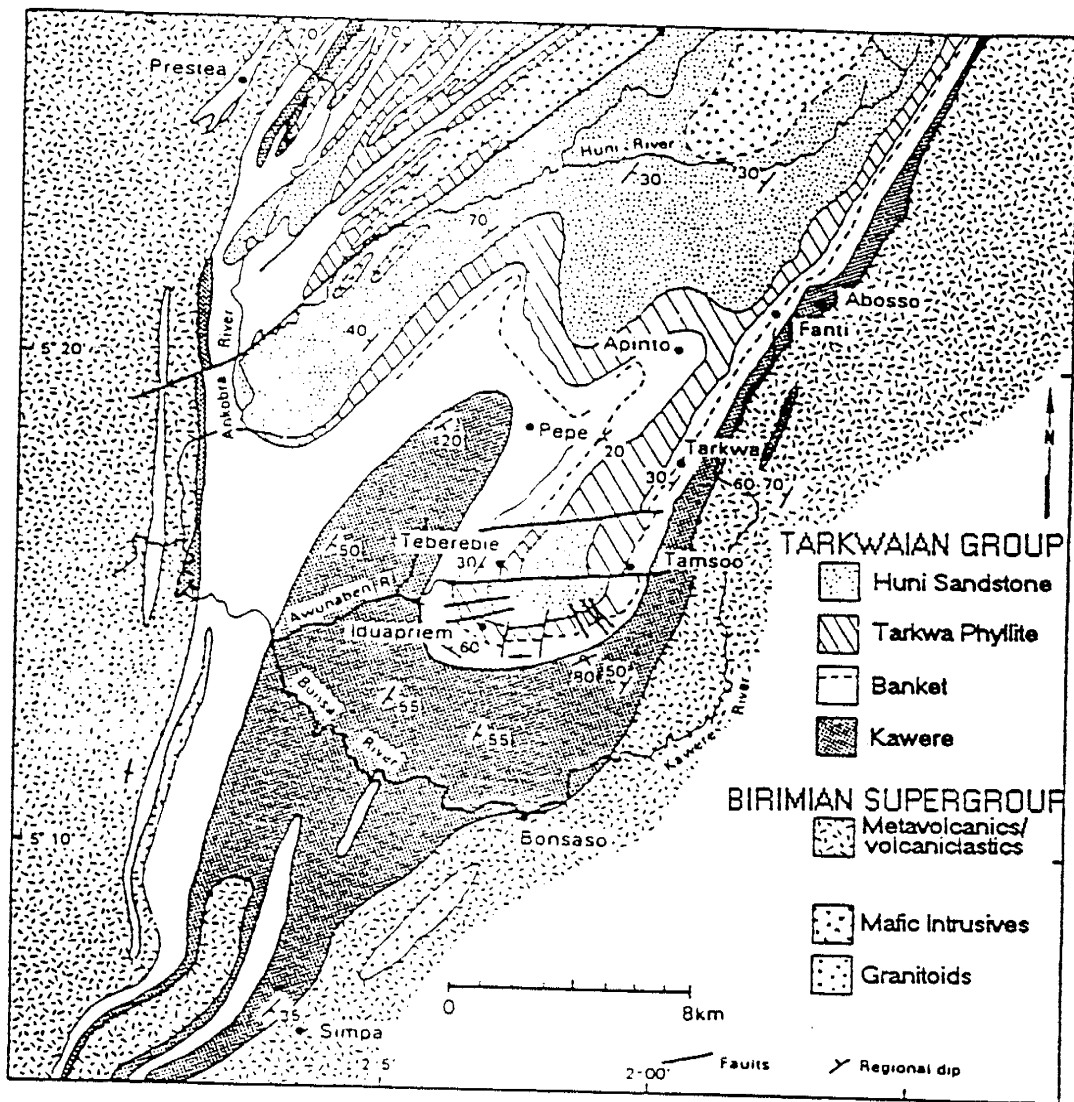
The Birimian Supergroup consists of belts of metavolcanic rocks with near parallel disposition that are separated by basins containing volcaniclastic and epiclastic rocks (Fig. 2.1). The rocks are isoclinally folded and metamorphosed to the greenschist facies. Metavolcanic rocks of the Birimian Supergroup have an Sm/Nd isochron age of 2.166 ± 0.066 Ga; the metasediments give a model Sm/Nd age of 2.195 Ga (Taylor et al., 1988; Lenz in Hirdes et al., 1987). Tonalitic and granodioritic granitoids intruded the metavolcanic and metasedimentary rocks respectively during the Eburnean event at 2.1 Ga (Leube et al., 1990; Bonhomme, 1962). Transition zones between the belt metavolcanics and the basin metasediments are gradational and are characterized by a chemical facies defined by cherts, manganiferous and carbon-rich metasediments, Fe-Ca-Mg carbonates and disseminated sulphide mineralization (Leube et al., 1990; Junner 1932).

Tarkwaian Group

Tarkwaian Group rocks are a molasse-like succession of sediments that rest upon, and are folded with the Birimian Supergroup. They occur in all five Birimian metavolcanic belts in Ghana and are most extensively studied in the Ashanti belt that stretches from Konongo past Prestea in southwesterly direction (Leube et al., 1990) (Fig. 2.1). Formation age of the Tarkwaian sediments is constrained by Rb/Sr whole-rock ages of 2.081 ± 0.025 Ga for Eburnean granitoids underlying the sediments and 1.968 ± 0.049 Ga for post-Tarkwaian granitoids (Hirdes et al., 1988; Taylor et al., 1988). Junner et al. (1942) subdivides the Tarkwaian group into four formations that include a basal Kawere unit, the Banket, Tarkwa Phyllite and the Huni Sandstone Formation at the top (Fig. 2.2). The Kawere and Banket Formations are coarse clastic sediments comprising quartz-arenites, grits, breccias and conglomerates, and with average thicknesses of 500 meters and 120 meters, respectively. The Tarkwa Phyllite and the youngest unit, Huni Sandstone, have average thicknesses of 200 meters and 1500 meters, respectively (Sestini, 1973). Sestini (1973) describes the Banket Formation as alluvial fan deposits with braided channels deposited in elongate intramontane basins. Strogon (1988) describes the entire Tarkwaian succession as an upward fining fluvial sequence; the Tarkwa phyllites represents an overbank facies and the conglomerates in the

Kawere and Banket Formations mark periods of interruption of this sequence.

FIG. 2.2 Geologic map of the Tarkwa basin (Modified from Junner et al., 1942).



Gold Deposits

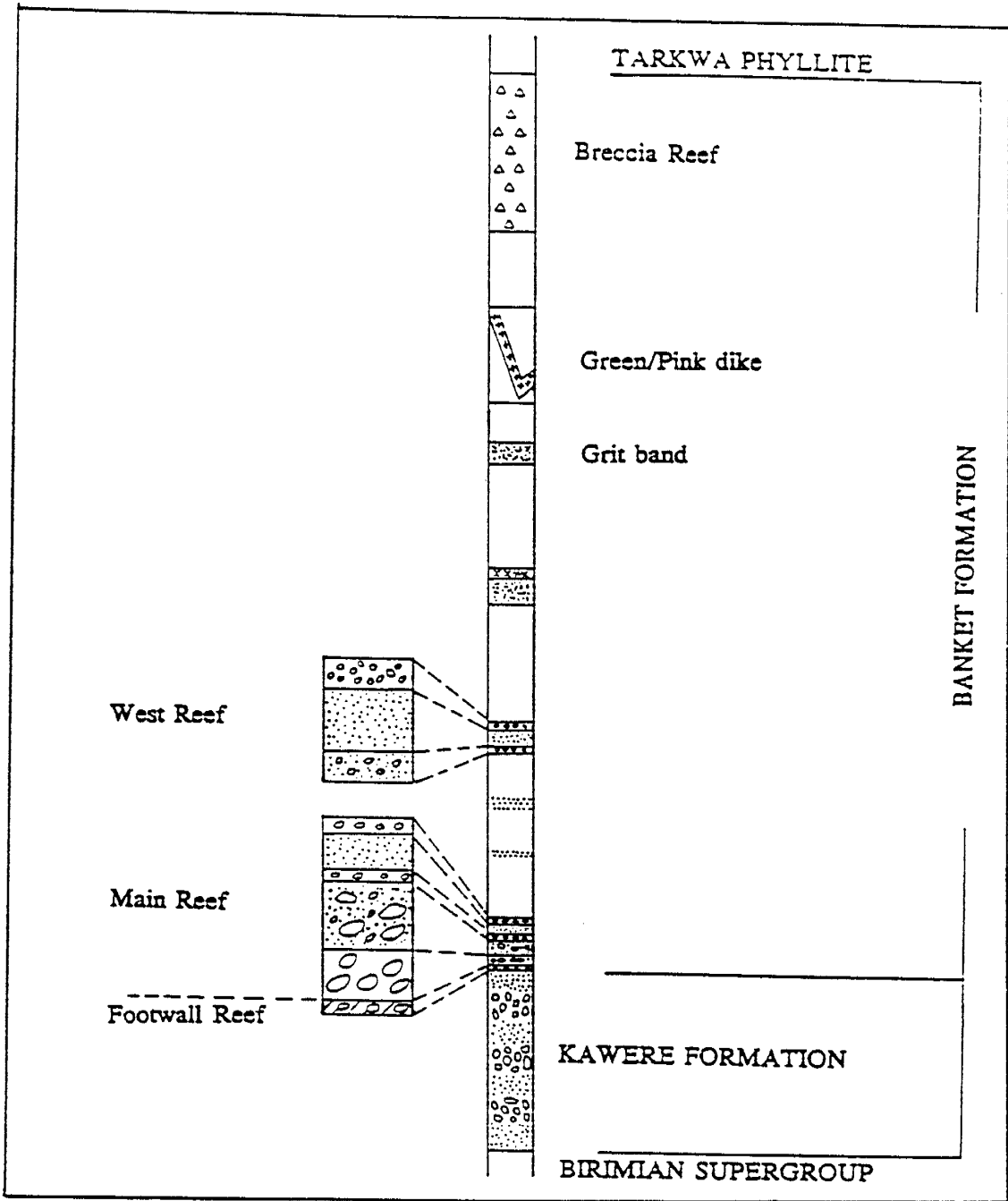
Three main types of gold mineralization are described in the Birimian rocks. The most extensively studied of these is a system of steeply dipping mineralized mesothermal veins that occur along roughly parallel linear belts trending diagonally through the country (Kesse and Barning, 1988; Amanor and Gyapong, 1988; Hirdes and Leube, 1989; Leube et al., 1990) (Fig. 2.1). Mineralized veins occurring along the western flank of the Ashanti belt are of the most economic importance as they host a majority of Ghana's lode gold deposits including the rich deposits of Ashanti Goldfields in the Obuasi area with an average grade of one ounce of Au per ton (Kitson, 1930) (Fig. 2.1). Linear belts along which the mineralized vein systems occur, represent major NE-SW trending faults and shear zones developed between competent volcanic belts and incompetent basin sediment (Hirdes and Leube, 1989; Junner, 1935; Cooper, 1934). The vein-type mineralization contains largely free milling gold with minor amounts of sphalerite, pyrite, chalcopyrite, galena, tennantite and tetrahedrite (Gyapong, 1980).

Disseminated auriferous sulphides occur at the fringes of the "shear zone" vein-type mineralization (Amanor and Gyapong, 1988; Appiah et al., 1991). They are best developed within the chemical facies in transitional zones between the meta-volcanics and metasedimentary rocks. Carbonaceous units and

interbedded cherty bands in this zone are recognized to have background gold levels an order of magnitude higher than crustal abundance of gold (Hirdes et al., 1989). The sulphide ore is composed principally of arsenopyrite, pyrite, pyrrhotite and minor amounts of chalcopyrite, galena, sphalerite, and stibnite (Gyapong, 1980; Appiah et al., 1991). In deeply weathered Birimian rocks, the disseminated sulphide mineralization is oxidized to depths that may exceed 100 meters (Gyapong, personal comm., 1989) resulting in the liberation of very minute free milling gold that is readily amenable to heap leaching.

Gold in the Tarkwaian sediments occurs principally in the Banket formation and is generally at ore grades in conglomeratic bands or reefs present near the base of that unit. Four reef horizons interbedded by grits and quartzites (or quartz-arenites) are described in the Banket formation (Junner et al., 1942) (Fig. 2.3). Each reef horizon contains two or more conglomerate bands that are separated from each other by clean cross-bedded quartzites. Most gold production has been from the more persistent Basal or Main Reef which has an average grade of 8 to 9 ppm in the Tarkwa area. Over 8 million ounces of gold have been mined from the Banket reefs in the Tarkwa basin (Nunoo and Tsiriku., 1988).

FIG. 2.3 Stratigraphic column of the Banket Formation showing reef horizons (modified from Nunoo et al., 1988).



Source Area Problem

Implicit in the widely accepted modified placer theory on the genesis of auriferous quartz-pebble conglomerates is the availability of source terranes where gold and other detritus in the sedimentary basins could have been derived. For the Witwatersrand deposit, Pretorius (1976) and Viljoen et al., (1970) favoured derivation from a typical granite-greenstone terrane, such as the Barberton to the east of the Witwatersrand basin. Utter (1978) and Meyer (1983) compare the chemistry of detrital chromites from the Witwatersrand basin with chromite grains from the adjacent Barberton greenstone belt. Their results suggest contrasting rock types in source areas of the West and Central Rand units of the Witwatersrand Group. Robb and Meyer have interpreted the same data as reflecting an evolving source terrane during sedimentation of the Witwatersrand Group. Meyer et al. (1985) place some constraints on source area of the Witwatersrand deposit by comparing Co, Ni and Au contents of detrital pyrite from the Witwatersrand with those of hypogene pyrite from neighbouring Archean granite-greenstone basement. Their data indicate that pyrites with Co/Ni ratios and Co, Ni and Au abundances similar to detrital pyrites from the Witwatersrand occur in gold deposits from a number of greenstone belts and from a variety of granites in the southwestern Transvaal. Pyrites from deposits in the Barberton granite-greenstone terrane were, however, found to be markedly different from detrital pyrite

in the Witwatersrand in their trace element chemistry. Erasmus et al. (1982) also constrains the source of Witwatersrand basin sediments by comparing Ag and Hg contents of detrital Au from the basin with hypogene Au from adjacent Archean terranes. Wronkiewicz and Condie (1987) present geochemical data on Witwatersrand shales that indicate an increase in granitic input over greenstones upward in the Witwatersrand stratigraphy.

Models on source terranes for the Witwatersrand deposit have invariably faced serious mass balance problems because neither the exposed Archean basement rocks in the Witwatersrand basin hinterland nor rocks of the Barberton granite-greenstone terrane to the east of the basin contain sufficient levels of gold to adequately account for the gold contained in the Witwatersrand basin (Pretorius, 1976; Viljoen et al., 1970; Robb and Meyer, 1990). Robb and Meyer (1990) present drill core data that indicate that granites and gneisses in the Witwatersrand basin hinterland, now largely buried under Proterozoic cover, contain a pervasive hydrothermal alteration and a significant enrichment in gold and uranium, and suggest these could have furnished the gold and uranium in the Witwatersrand.

Mineralized quartz veins in the Birimian Supergroup have long

been considered the principal sources of gold in the Tarkwa basin. Junner et al. (1942) note the similarity in grain-size between gold grains from the mineralized veins and those from the Tarkwa deposit. In a summary on that deposit, Boyle (1979) concludes that most of the gold was derived from primary quartz veins in the Birimian. Hirdes et al. (1988) suggest that gold enrichment in the Tarkwa basin has been the result of repeated reworking of immature Kawere sediments.

Methods of Investigation

The objectives of this study were addressed by field and laboratory methods. Surface exposures, adits and underground workings in the Tarkwaian basin were studied. In the Iduapriem - Teberebie areas (Fig. 2.2) where excellent sections of the Banket Formation are exposed in adits, individual units of the formation were described and their thicknesses noted to establish a detail stratigraphy of the Banket in that area. Sedimentological characteristics such as clast size and type, sorting, packing and percent lithic fragments of constituent units of the Banket and the Kawere Formations were noted in the field. Long, intermediate and short axes of quartz clasts in conglomerates and breccias of the Banket Formation were measured and are used to construct the depositional environment of Tarkwaian sediments. Continuous channel samples of various units of the Banket were obtained and analysed to determine the distribution of gold in the formation. Grab

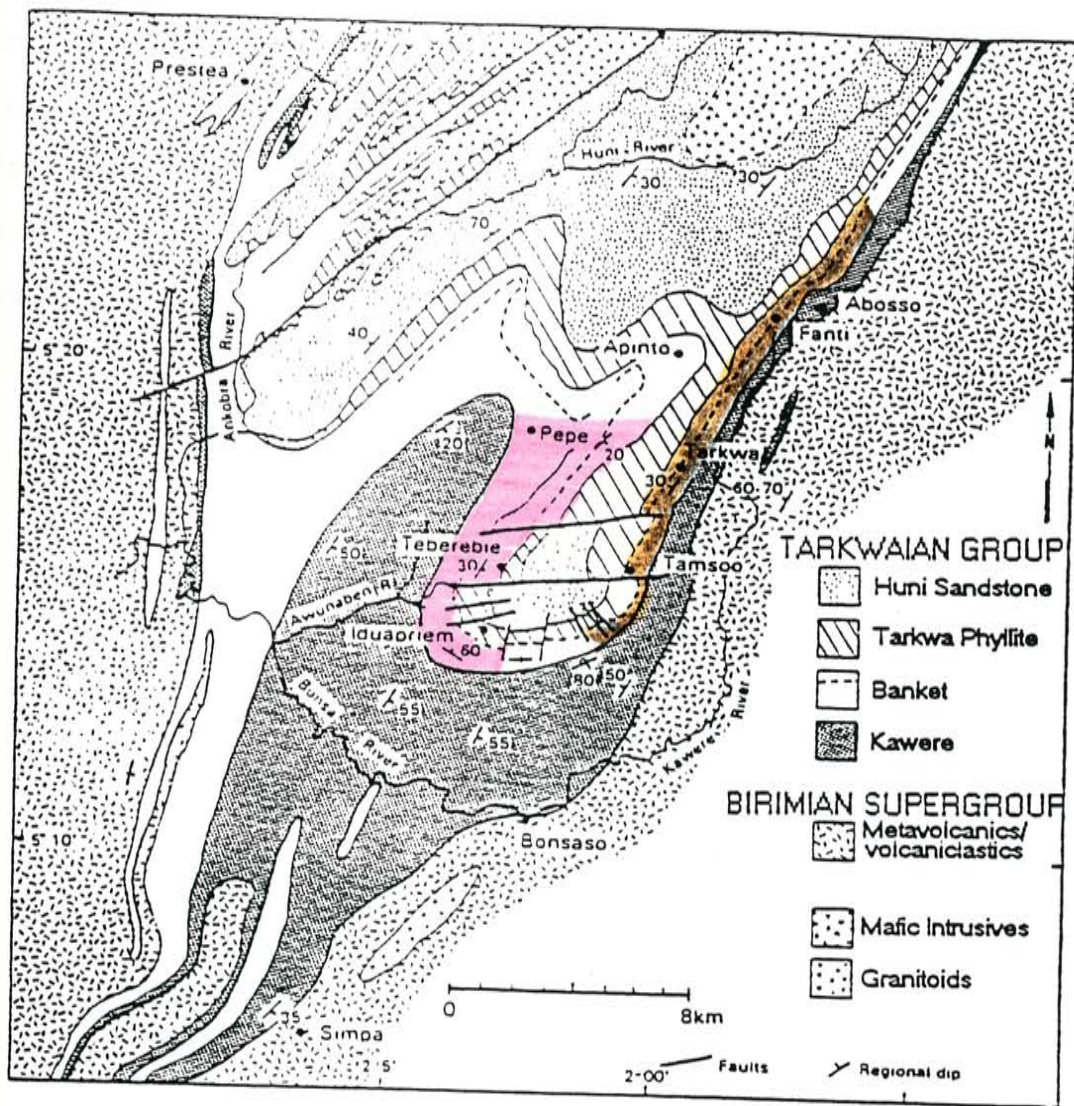
samples of Birimian rocks were also analysed for gold by a combination of fire assay and atomic absorption methods. These supplement large amount of assay data on drill core and chip samples made available by various mining companies in Ghana. The levels of gold and other trace elements in lithic fragments from the Banket and Kawere Formations were determined by Instrumental Neutron Activation Analysis (INAA). A petrographic description of thin- and polished-sections of samples of basement Birimian rocks, Banket conglomerate and lithic fragments from the conglomerate was undertaken. Data on major and trace element chemistry for a total of 53 basement Birimian Supergroup and lithic fragment samples were obtained by X-ray fluorescence spectrometry (XRF). Rb-Sr isotopic analyses were obtained for 7 Birimian samples and 6 lithic fragments from the Banket and Kawere Formations. Trace element levels in 2 gold samples from the Banket reefs and 3 from mineralized veins in the Birimian were determined by INAA.

GEOLOGY OF THE BANKET FORMATION

Stratigraphy, composition and texture

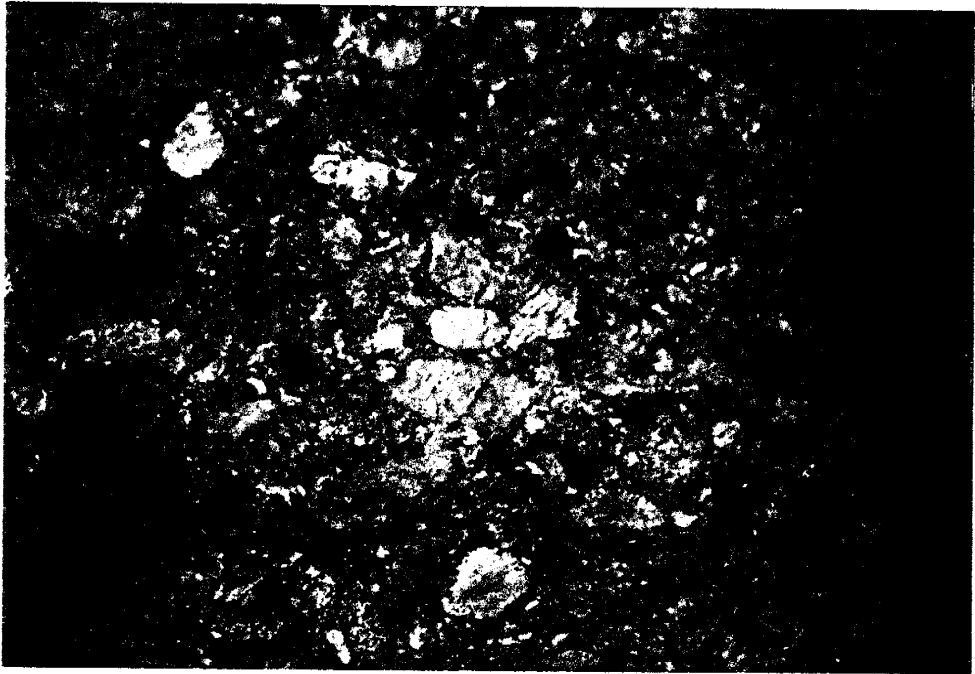
The Banket Formation varies in the Tarkwa basin from immature to mature sedimentary units (Fig. 2.4). In the west-southwestern portion of the basin, at Pepe, Iduapriem and Teberebie, the Formation consists of an interbedded series of polymictic, matrix supported conglomerates, breccias and grits (Fig. 2.5a-b). Individual units of this package of immature sediments have variable thicknesses, are discontinuous along strike and separated from each other by erosional contacts. Clasts in the sediments here are poorly sorted; in the breccias, clast diameter ranges from less than 0.5 cm to over 20 cm. Clasts are also poorly oriented and are composed of rounded vein quartz and a variety of angular to sub-angular rock fragments that include felsic volcanics, cherts, argillites and sandstones. Vein quartz and lithic fragments constitute 10-35% and 65-90%, respectively, of the clast component in the breccias. In the matrix supported conglomerates, rock fragments and more stable vein-quartz are present in roughly equal amounts. The matrix in these immature sediments contain abundant sericite and constitutes 15-25% and 40-60% of the breccias and paraconglomerates, respectively. Mature clast supported conglomerates with less than 10% lithic component, cross-bedded quartz arenite and massive argillaceous sandstones occur within the immature sediments at Iduapriem and Teberebie (Fig. 2.5c-d).

FIG. 2.4 Distribution of immature and mature sedimentary units in the Tarkwa basin.

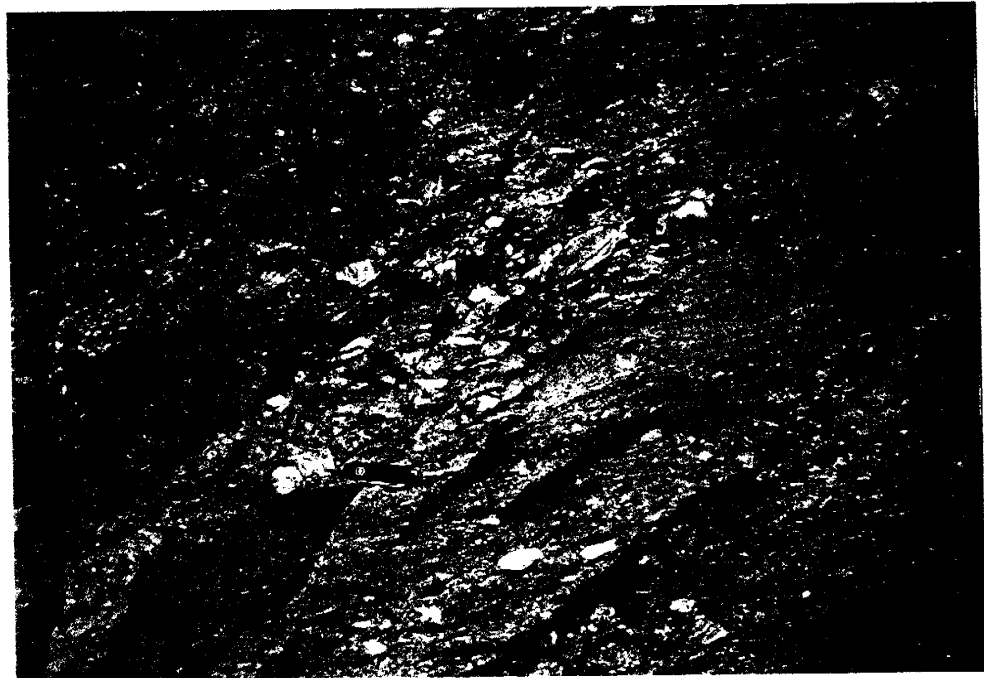


Immature sedimentary units;
 Mature sedimentary units

FIG. 2.5 Immature sedimentary rock units of the Basket Formation at Teberebie: (a) polymictic conglomerate containing sub-rounded lithic volcanic fragments "v" and small rounded quartz pebbles "q"; (b) grit with sub-angular lithic fragments; (c) clast supported conglomerate and (d) cross-bedded quartz arenite interbedded with immature Basket sediments at Iduapriem.



(a)



(b)



(c)



(d)

Thicknesses of the mature conglomerates in these areas commonly range from 0.4 to 4 meters. In an adit at Iduapriem, the mature conglomerate exceed 10 meters in thickness. The immature sediments in the southern portion of the Tarkwa basin are interpreted, based on their composition and texture, to represent debris flows deposited in proximal areas of the basin. Mature conglomerates within the debris flows are the result of localized reworking. A textural inversion in the immature sediments represented by the co-existence of large angular lithic fragments and smaller, rounded, more resistant vein-quartz suggests that previously deposited pebble horizons were incorporated in later debris flows.

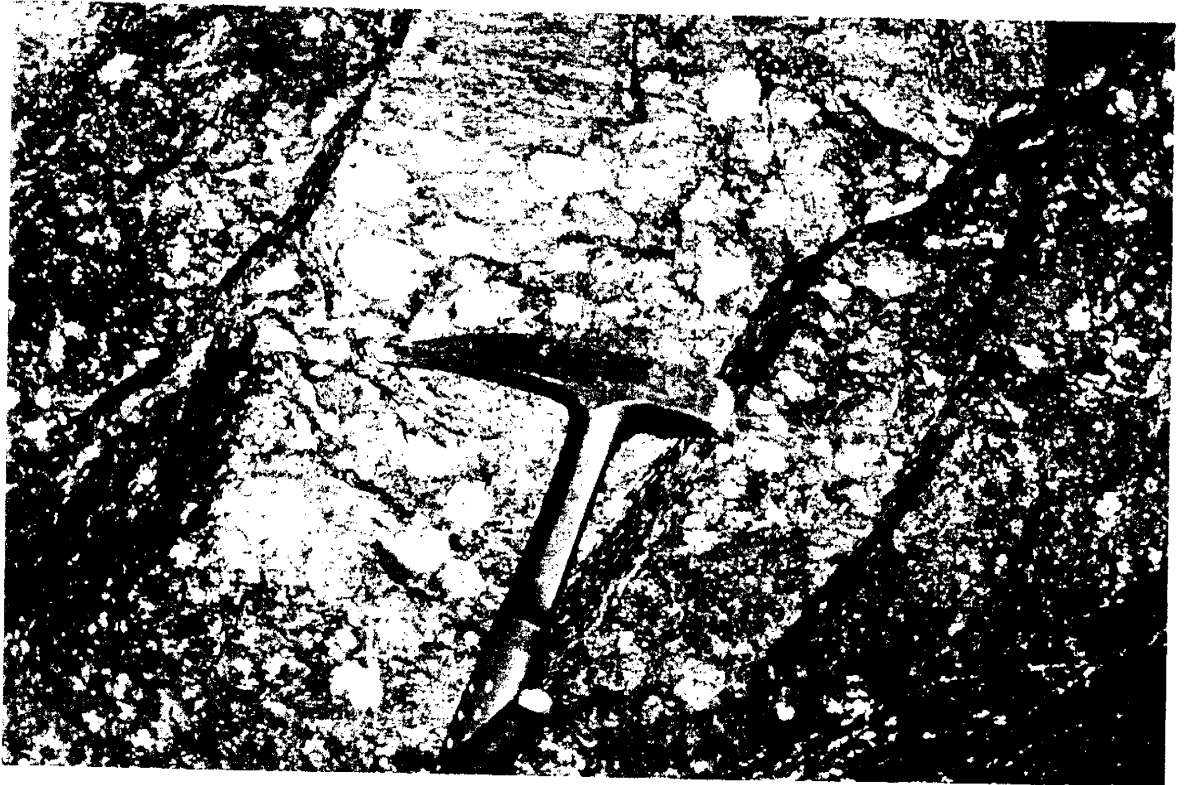
North-northeast of Iduapriem and Teberebie, a more mature succession of the Banket Formation occurs in deep underground workings and is responsible for the bulk of gold production from the Tarkwa basin. In the Akoon and Apinto mine areas, the formation consists of up to three oligomictic conglomerate reefs interbedded with cross-bedded quartz arenites and grits (Fig. 2.6a). The breccia unit is poorly developed here and occurs at the top of the formation. Further north in the Fanti area (Fig. 2.2), the number of conglomerate units is reduced and only one reef horizon may be present. Reef thickness in this part of the basin typically ranges from 0.5 to 2 meters, with individual reef horizons containing thin partings of quartz arenite. It is common to find in underground workings,

conglomerate reefs reduced to a single pebble line or completely washed out leaving thin hematitic bands (Fig. 2.6d). The auriferous horizon in such areas may be identified by the juxtaposition of pink hanging-wall quartzite on gray argillaceous footwall quartzite with a high hematite impregnation marking contact. Well packed, clast supported conglomerates are more common in this part of the basin occurring within or overlying loosely packed, matrix supported conglomerates. Matrix material constitutes between 5-15% of the clast supported conglomerates and may exceed 50% in the matrix supported conglomerates (Fig. 2.6). Clasts in both conglomerates types are essentially monolithic and are composed of rounded vein quartz (Fig. 2.6f). In the breccia reef at the top of the formation, clasts consist of vein quartz, cherts and jasperoid. The Main Reef is generally poorly sorted; clasts in this unit range from less than 1 cm to 15 cm in diameter. Sorting is better in the West Reef which lies some 5 to 15 meters stratigraphically above the Main Reef. Clast size in the West reef is commonly 1 to 2 cm in diameter. The rarity or lack of lithic fragments in mature Banket Formation sediments in the north and northeastern portion of the basin suggest they represent a reworked, distal facies of the debris flows that occur in the south.

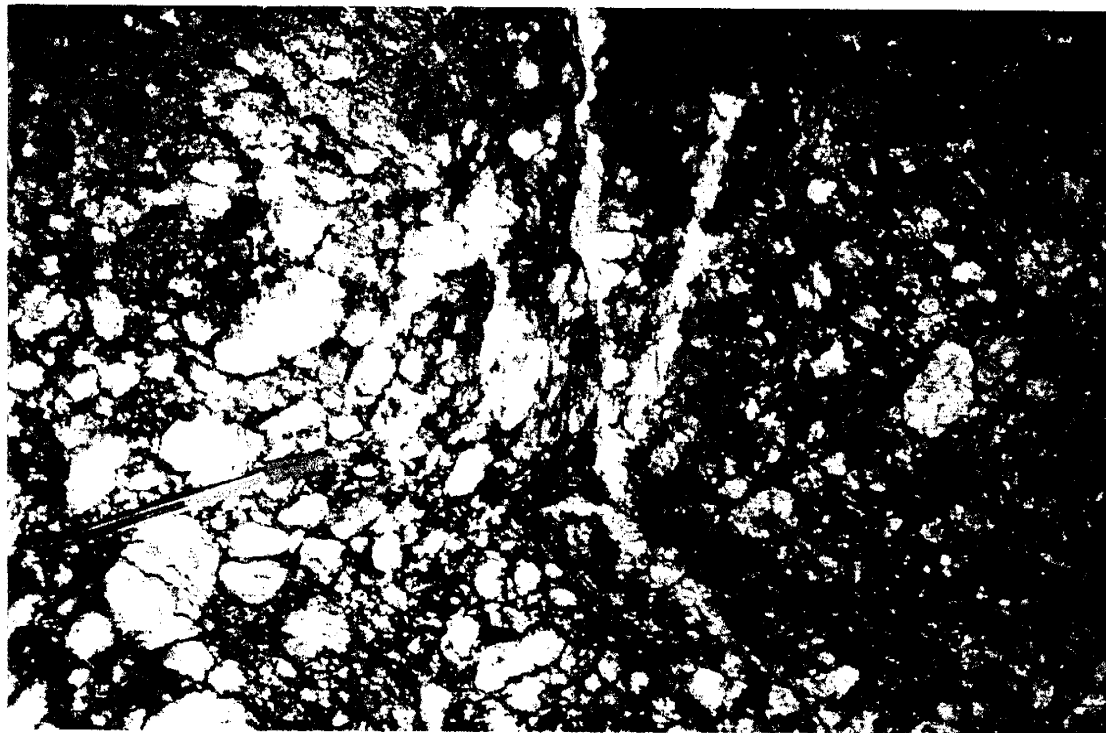
FIG. 2.6 (a) Multiple conglomeratic bands at the base of the Main Reef at the Apinto Mines. (b) Loosely packed Main Reef. (c) Compact, clast supported Main Reef. (d) Main Reef at Apinto Mines reduced to a single pebble line. (e) West Reef at the Akoon Mines (AVS): moderately packed and better sorted (marked area is 6" * 6"). (f) Polished surface of a sample of well packed and well sorted West Reef from AVS with high amount of detrital heavy mineral content in matrix.



(a)



(b)



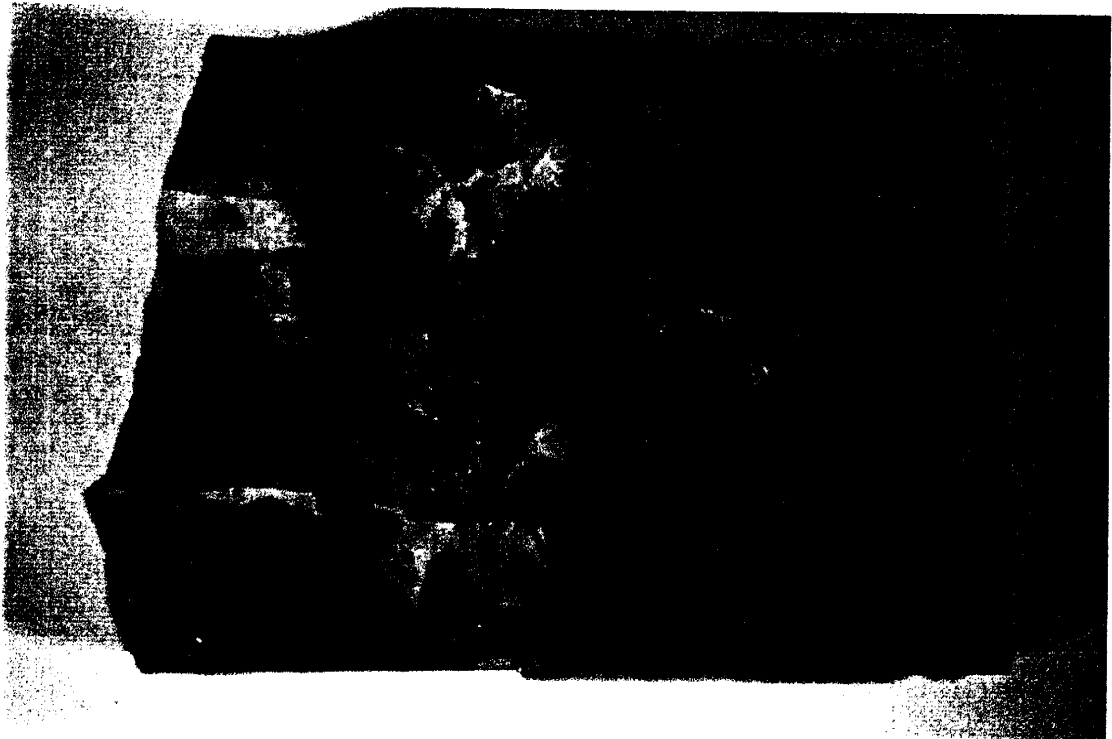
(c)



(d)



(e)



(f)

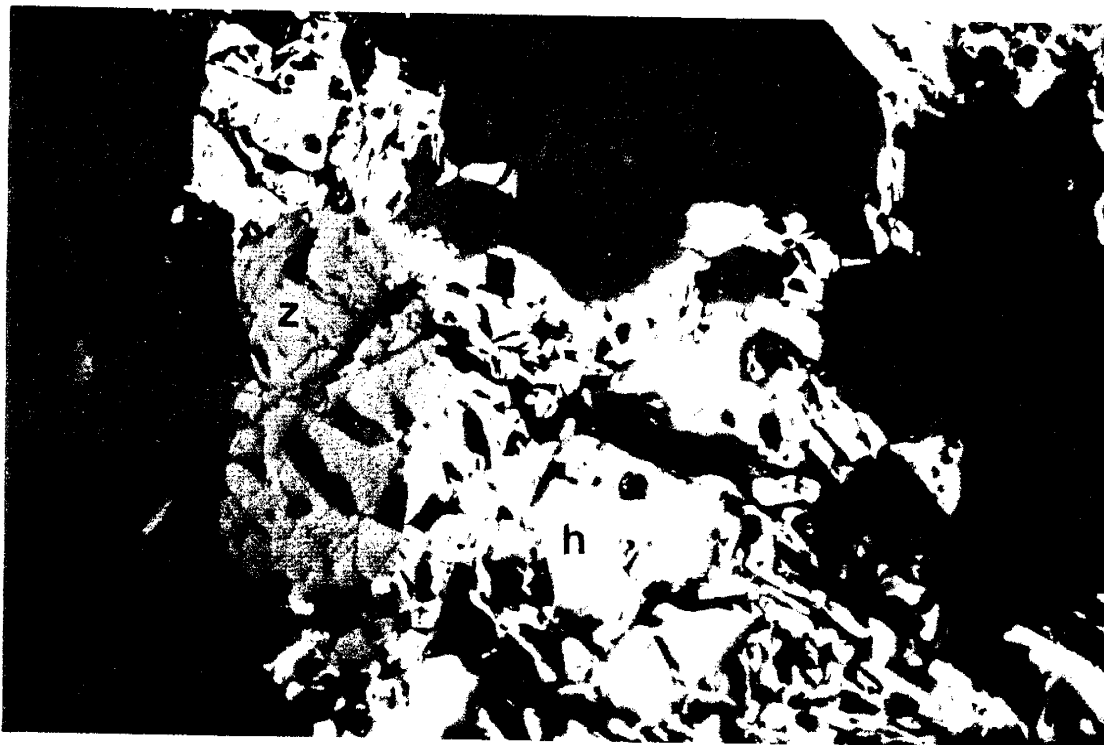
Detrital heavy minerals in Banket sediments

Detrital heavy minerals in the matrix of mature and immature conglomerates are hematite, magnetite, tourmaline, zircon, apatite and ulvospinel. Gold is also detrital and is closely associated with these minerals (Fig. 2.7). The proportion of detrital heavy minerals is considerably higher for the well packed and mature conglomerates (fig. 2.6f). Detrital heavy minerals are also abundant in the cross-bedded quartz arenites where they are concentrated along sedimentary structures. Less mature argillaceous sands and grits generally contain low amounts of heavy minerals.

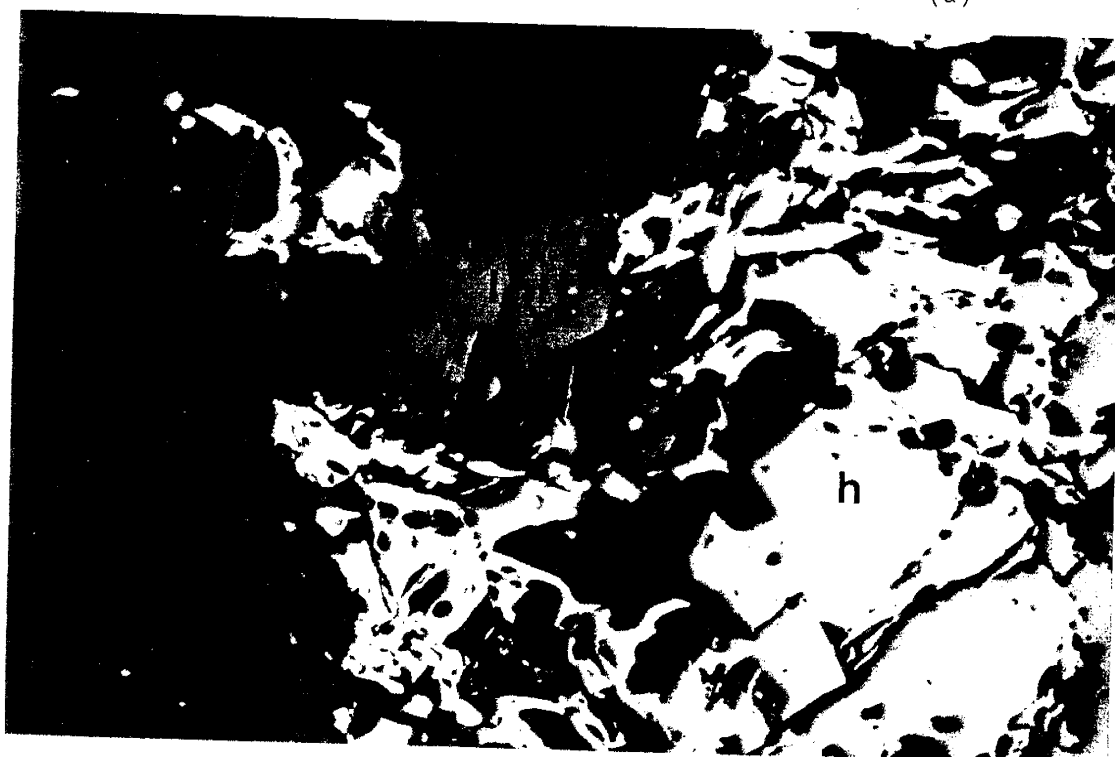
Sphericity and oblate-prolate indices

Quartz pebbles and cobbles in the Banket conglomerates are typically elongate in shape. Measurements of long, intermediate and short axes of quartz clasts chiseled out of matrix supported, polymictic conglomerates have been used to determine sphericity and oblate - prolate indices for the Banket sediments (Table 2.1). On a sphericity versus oblate-prolate index diagram (Dobkins and Folk, 1970), most pebbles from the immature sediments plot in the field defined by river-deposited pebbles. Average sphericity and oblate - prolate indices of clasts from Iduapriem, Teberebie and Pepe areas indicate fluvial depositional environment for sediments of the Banket formation (Fig. 2.8). Wentworth's sphericity indices for the pebbles are also consistent with deposition in a fluvial

FIG. 2.7 (a) Photomicrographs showing hematite "h", zircon "z" and gold "g" in West Reef. Field of view is 1.0 mm approx.



(a)



(b)

Table 2.1 Sphericity and oblate-prolate indices of quartz pebbles/cobbles in Banket sediments.

IDUAPRIEM			Sphericity		Oblate-Prolate
L ¹	I	S	W*	DF+	DF#
8	6.5	4.5	1.611	0.730	-1.270
10.5	6.5	5.5	1.545	0.762	5.727
11.5	9	5.5	1.864	0.664	-1.742
9.5	7.5	4.5	1.889	0.657	-2.111
12	9	6	1.750	0.693	0.000
5	5	4	1.250	0.862	-6.250
9.5	7	6	1.375	0.815	3.393
9	6	5.5	1.364	0.824	5.844
8	6.5	4.5	1.611	0.730	-1.270
10.5	7.5	5.5	1.636	0.727	1.909
8.5	8	4.5	1.833	0.668	-7.083
9.5	7.5	5	1.700	0.705	-1.056
12	8	7	1.429	0.799	5.143
8	6	4.5	1.556	0.750	1.270
6.5	5.5	5	1.200	0.888	2.167
8.5	7.5	5	1.600	0.732	-3.643
7.5	6	4.5	1.500	0.766	0.000
9	7	5.5	1.455	0.783	1.169
8.5	6.5	5	1.500	0.768	1.214
12	7	6	1.583	0.754	6.667
			1.563	0.754	0.504

* Wentworth's sphericity index: $(L+I)/2S$

+ Dobkins and Folk sphericity index: $(S^2/L*I)^{1/3}$

Dobkins and Folk oblate-prolate index:

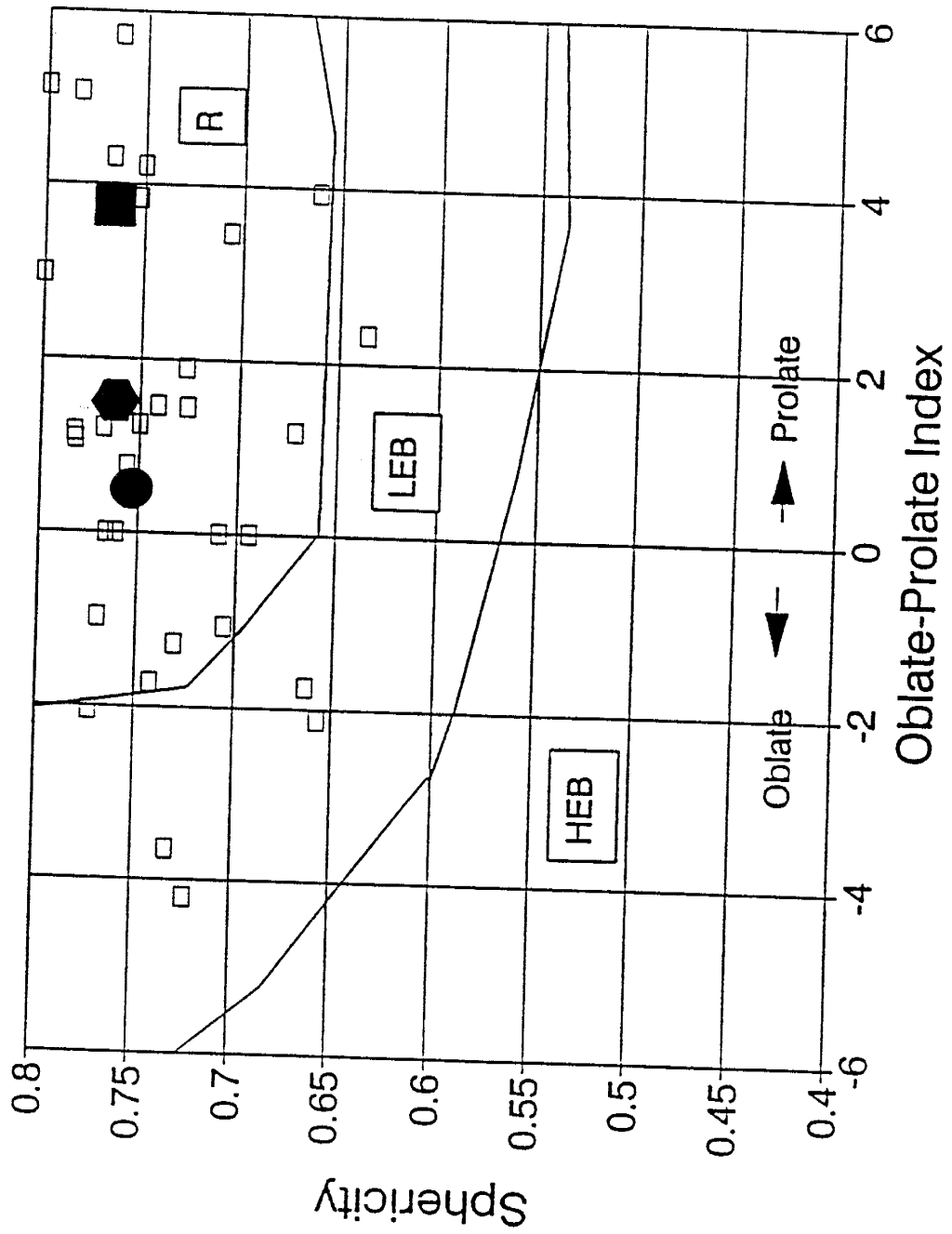
$$10*(L-I)/(I-S)-0.5)/(S/L)$$

¹L, I and S are, respectively, long, intermediate and short diameters of pebbles/cobbles in cm.

TEBEREBIE			Sphericity	Oblate-Prolate	
L	I	S	W*	DF+	DF#
9.5	7	5.2	1.587	0.741	1.487
6	5	3.5	1.571	0.742	-1.714
9.5	8.2	6	1.475	0.773	-2.036
7.8	6	4.5	1.533	0.756	0.788
7.6	5	4	1.575	0.750	4.222
6	5.5	4.4	1.307	0.837	-2.557
11	8	5.8	1.638	0.726	1.459
10	7	4.6	1.848	0.671	1.208
8.3	6.3	5.5	1.327	0.833	3.234
8.3	5.1	3.5	1.914	0.661	3.952
7.7	6	4.7	1.457	0.782	1.092
7	4.6	4.2	1.381	0.818	5.952
5.4	4.3	3.2	1.516	0.761	0.000
7.3	4.9	3.9	1.564	0.752	3.854
7.9	5.5	5.5	1.218	0.886	7.182
9.3	8.3	5.4	1.630	0.723	-4.195
			1.534	0.763	1.496

PEPE			Spherecity	Oblate-Prolate	
L	I	S	W*	DF+	DF#
12.3	6.1	5.8	1.586	0.765	9.625
10.6	7.8	6.5	1.415	0.799	2.983
6.5	5.4	4	1.488	0.770	-0.975
9.6	7.3	5	1.690	0.709	0.000
9	6.5	5.5	1.409	0.803	3.506
11.6	7.6	6.5	1.477	0.783	5.074
10	7.1	6.2	1.379	0.815	4.244
15	9.8	7.2	1.722	0.707	3.472
6.5	4.5	4.4	1.250	0.871	6.683
8.4	5.6	4.6	1.522	0.766	4.325
7.1	4.6	2.9	2.017	0.636	2.332
			1.541	0.766	3.752

FIG. 2.8 Sphericity and oblate-prolate indices of quartz clasts from Iduapriem, Teberebie and Pepe plotted on a Sphericity versus Oblate-Prolate index diagram (after Dobkins and Folk, 1970). The field R, LEB and HEB represent, respectively, river, low energy beach and high energy beach depositional environments. Filled circle, hexagon and square represent averages of data from Iduapriem, Teberebie and Pepe, respectively.

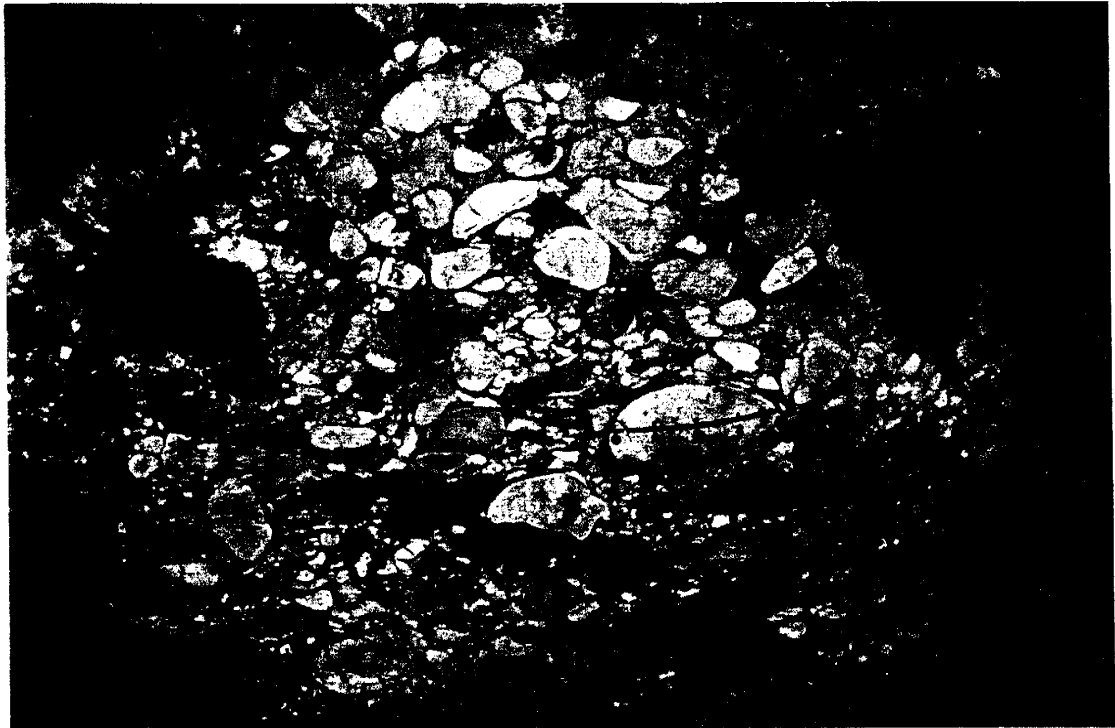


environment (Wentworth, 1922).

Geology of the Kawere Formation

The Kawere Formation is a discontinuous unit at the base of the Tarkwaian Group. Outcrops were examined at Abooso, Bonsaso, Wassa Agona and at Bogrekrom near Tarkwa (Fig. 2.2). The formation consists of polymictic, clast supported conglomerates interbedded with sandstones. Clasts of the conglomerates are well packed and comprise vein quartz (5-15%) and lithic fragments (85-95%) that include felsic volcanics, cherts, sandstones and argillites. Sorting is poor in the conglomerates; clast sizes range from less than 1 cm to about 20 cm in diameter. Quartz pebbles are at the lower end of the spectrum with diameters typically below 2.5 cm. Lithic fragments co-existing with the quartz in the conglomerates generally have elongate shapes and are well oriented with their long axes parallel to bedding (Fig. 2.9). The high content of lithic fragments in the Kawere conglomerates, and degree of roundness of the fragments are indicative of a compositionally immature sediment that has acquired a significant degree of textural maturity. These characteristics suggest that the Kawere conglomerates formed as a result of mechanical weathering and deposition in a fluvial environment.

FIG. 2.9 Photograph of the Kawere conglomerate with rounded and elongate lithic fragments.



GOLD MINERALIZATION IN BANKET SEDIMENTS

There are notable differences in the distribution and grade of gold mineralization occurring in various parts of the Tarkwa basin. In the immature proximal sediments located in the southernmost portion of the basin, gold mineralization is dispersed through a column of sediments 50 to 70 meters thick and has grades of 0.1 to 6 ppm (Fig. 2.10 and 2.11). Assays of grits, breccias polymictic matrix supported conglomerates and cross-bedded sands with abundant hematite typically show gold levels in a range of 0.2 to 2 ppm. Massive sandstone units that interbed the coarser sediments contain less than 0.2 ppm gold. Higher gold grades up to 20 ppm occur in relatively mature conglomerates in which unstable lithic fragments have been destroyed. For example, in lenses of clast supported quartz-pebble conglomerates within immature sedimentary units at Iduapriem, average gold grade is 5 ppm (Fig. 2.10). The decrease in the content of unstable lithic fragments in the mature conglomerates, and corresponding increase in their levels of gold and other detrital heavy minerals indicate that they represent zones of localized reworking where stable heavy minerals were concentrated by mechanical processes whereas unstable fragments were destroyed by the same processes.

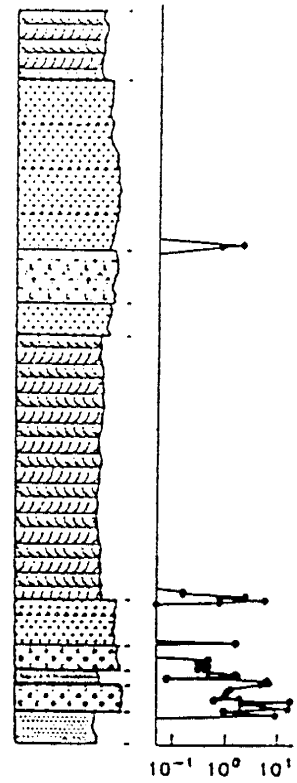
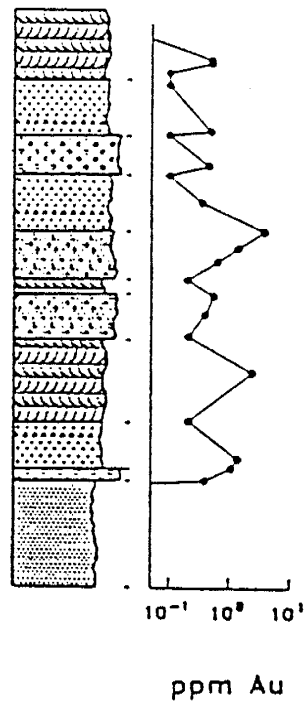
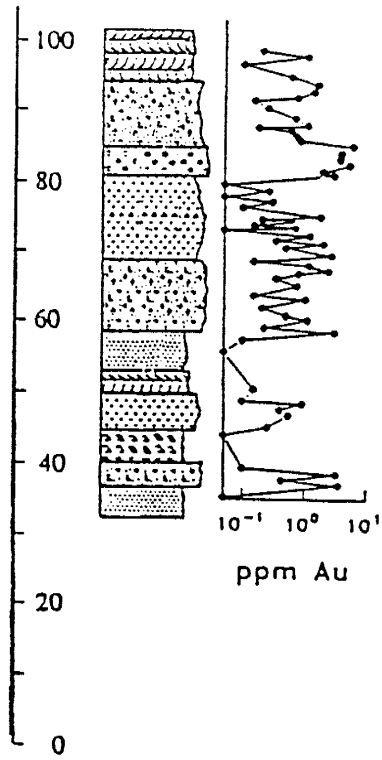
FIG. 2.10 Stratigraphy and gold content of the Basket Formation at Iduapriem, Teberebie and Akoon.


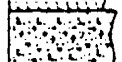




Meters

IDUAPRIEM

TEBEREBIE

AKOON

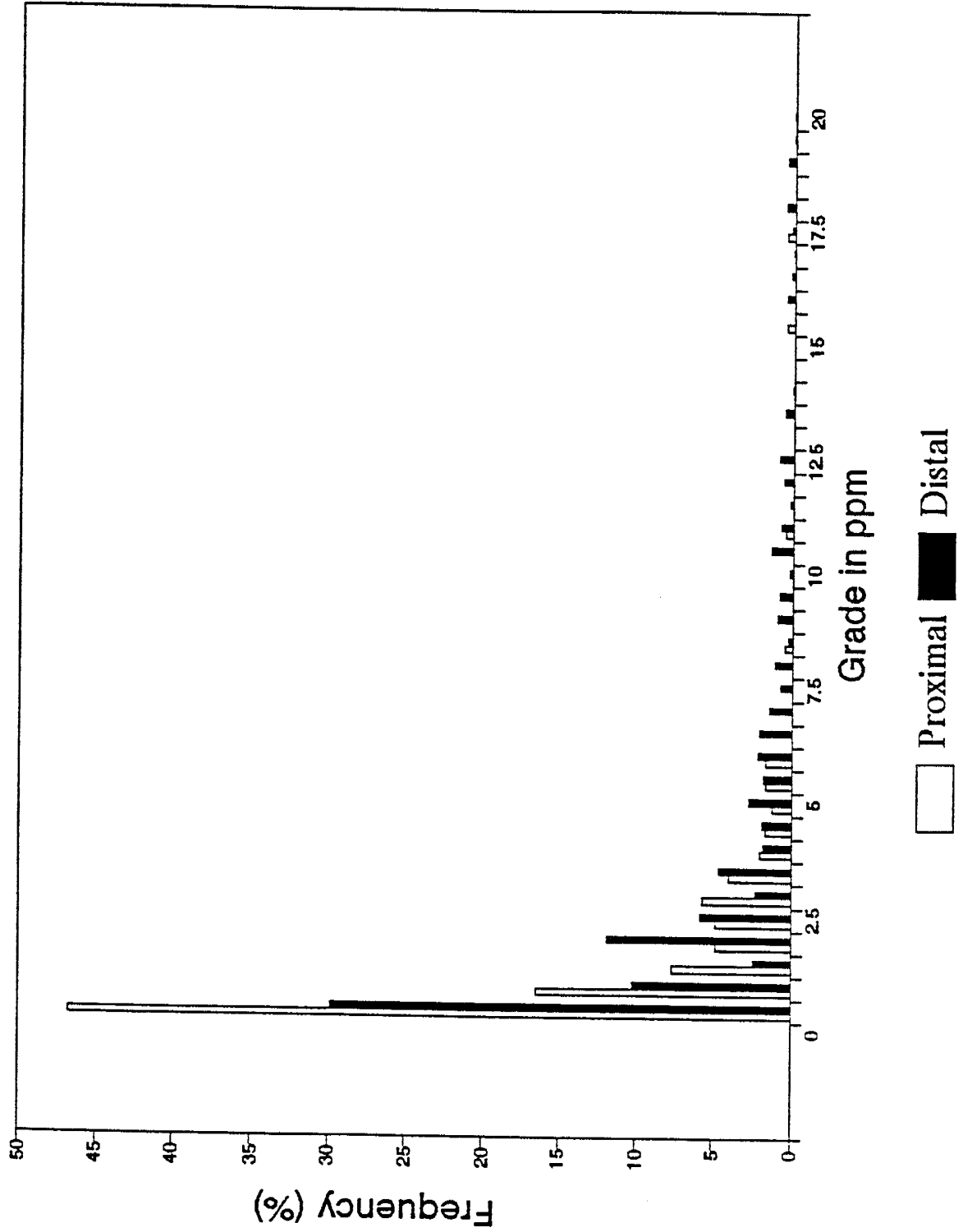


-  Crossbedded quartz arenite
-  Matrix supported conglomerate / breccias
-  Clast supported cong.
-  Grits/sandstones
-  Massive sandstones
-  Dike

Two major mining operations are located in the proximal sediments of the Banket Formation. At Iduapriem, a total of 11 million metric tons of proven and probable ore reserves at an average grade of 2.7 ppm have been established, and in the Teberebie area, approximately 18 million metric tons of ore at a grade of 1.7 ppm are known.

In the northern portions of the Tarkwa basin where Banket Formation consists of a package of mature sediment, most gold is concentrated in conglomerate bands (reefs) totalling 3 to 5 meters thick and occurring near the base of the Formation (Fig. 2.10 and 2.6a). An average grade of 9 ppm was obtained for 1131 samples of mature conglomerates taken from Akoon, Apinto and Fanti mines (Fig. 2.2 and 2.11). Assay data on these distal facies sediments indicate that higher gold grades occur in clast supported conglomerate bands within the reef horizon, whereas lower grades comparable to gold levels in the immature proximal sediments are common in loosely packed matrix supported conglomerates. Gold grades in 423 samples of well packed conglomerates averaged 15.41 ppm in contrast to an average of 5.57 ppm obtained for 708 samples of matrix supported conglomerate from the same locale. Zones with grades exceeding 300 ppm are encountered in hematitic bands, locally referred to as washed out zones, that are laterally continuous with well packed conglomerate reefs (Fig. 2.6d).

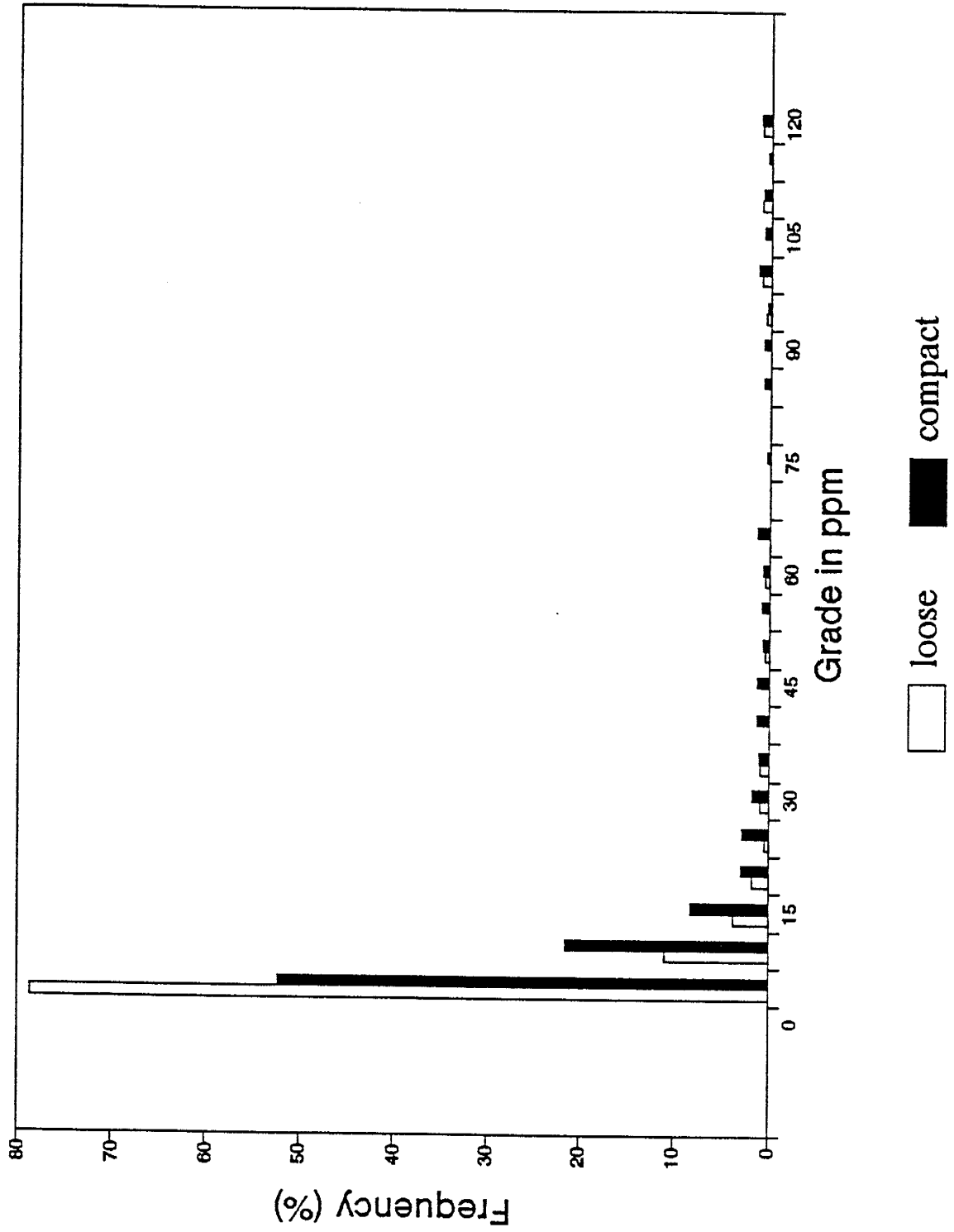
FIG. 2.11 Histogram of gold values in Banket sediments. Proximal sediments are debris flows deposited in basin margins; distal sediments are relatively reworked and mature sediments in distal parts of the basin.

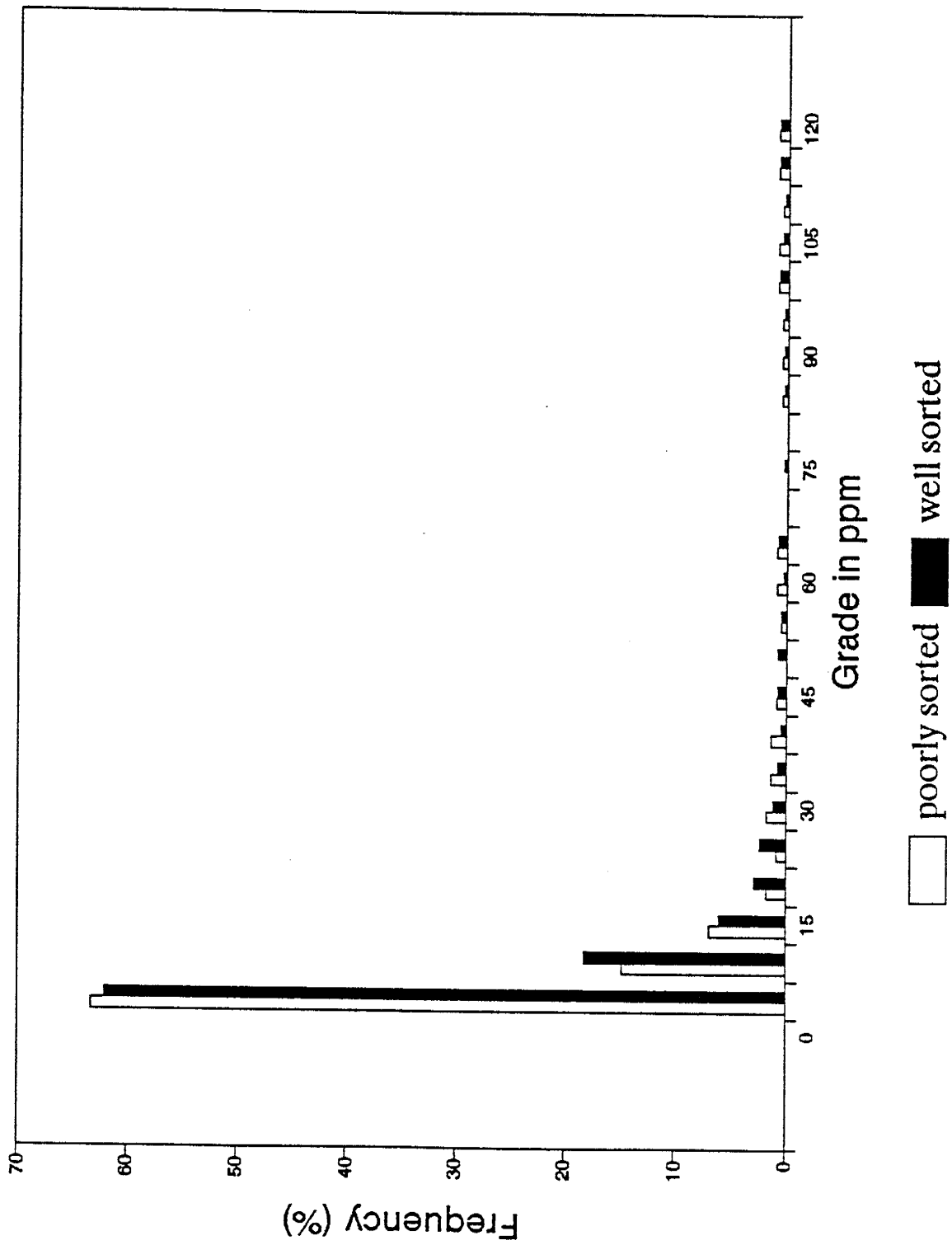


The effect of packing on gold content of conglomerates in Akoon, Apinto and Fanti areas are shown on Figure 12a. The data is consistent with earlier observation by Sestini (1973) and indicates that packing is an important sedimentological factor governing the concentration of gold in the reefs. Sorting is also a factor but to a much lesser degree (Fig. 2.12b). Total gold production of mines located in this package of mature distal facies sediments exceed 8 million ounces.

The common size range of detrital gold grains in the Banket reefs is 20 to 50 microns (Fig. 2.7). Larger grains up to 300 microns were observed in the less mature proximal facies sediment, and grains 5 to 10 microns in size occur in the quartz-pebble conglomerates in the northern portions of the basin. Visible gold grains were commonly found in hand specimens obtained from high grade areas in the Akoon mines. Hand specimens from the Apinto and Fanti mines rarely contain any visible gold. The observation indicates a progressive decrease in grain size of gold north-northeastward in the Tarkwa basin.

FIG. 2.12 Histogram showing gold grades in samples of loose versus compact reefs at AVS, Apinto and Fanti Mines.
(b) A comparison of gold grades in poorly sorted and better sorted reefs at AVS, Apinto and Fanti Mines.





Gold composition

Compositions of 2 gold samples from a mature conglomerate at Akoon, and of 3 samples of primary gold from mesothermal quartz veins within the Birimian were determined by instrumental neutron activation analysis (INAA). Data on the paleoplacer gold indicate less than 4 wt. % Ag, minor Hg and trace levels of Sc, Co, Sr, Sb, Hf, Th and Ce. The primary gold, on the other hand, contain 13.6 to 20.4 wt. % Ag, minor Sb and no detectable amounts of Co or Sc (Table 2.2). The types and levels of minor and trace elements in gold from the Tarkwa paleoplacer are similar to those of gold from deeply weathered lateritic terranes (Boadi and Norman, 1991; Boadi et al., in prep.) (Fig. 2.13) and suggest a common origin for gold in these two deposit types.

Table 2.2. Instrumental neutron activation analysis of primary gold (p) and gold from the Tarkwa paleoplacer deposit (t)

(ppm)	1p	2p	3p	4t	5t
Sc	0	0	0	0.43	0.28
Cr	0	0	0	0	0
Co	0	0	0	652	210
Sr	0	0	0	0	739
Zr	0	0	6862	0	0
Sb	744	743	974	59	0
Ce	66	0	0	170	67
Nd	0	0	0	0	0
Eu	0	0	0	0	0
Tb	0	0	0	0	0
Yb	0	0	0	0	0
Hf	0	0	31	12.2	21
Th	15	0	0	7	48
Fe*	0.00	0.00	1.71	0.00	0.00
Hg*	0.05	0.03	0.04	0.03	0.04
Ag*	20.42	20.30	13.63	3.48	2.32

* values given in wt. %

FIG. 2.13a Composition of Tarkwa gold shown on a Sc - Ag plot. Concentrations of Ag, Sc and other minor and trace elements in the gold were obtained by instrumental neutron activation analysis.

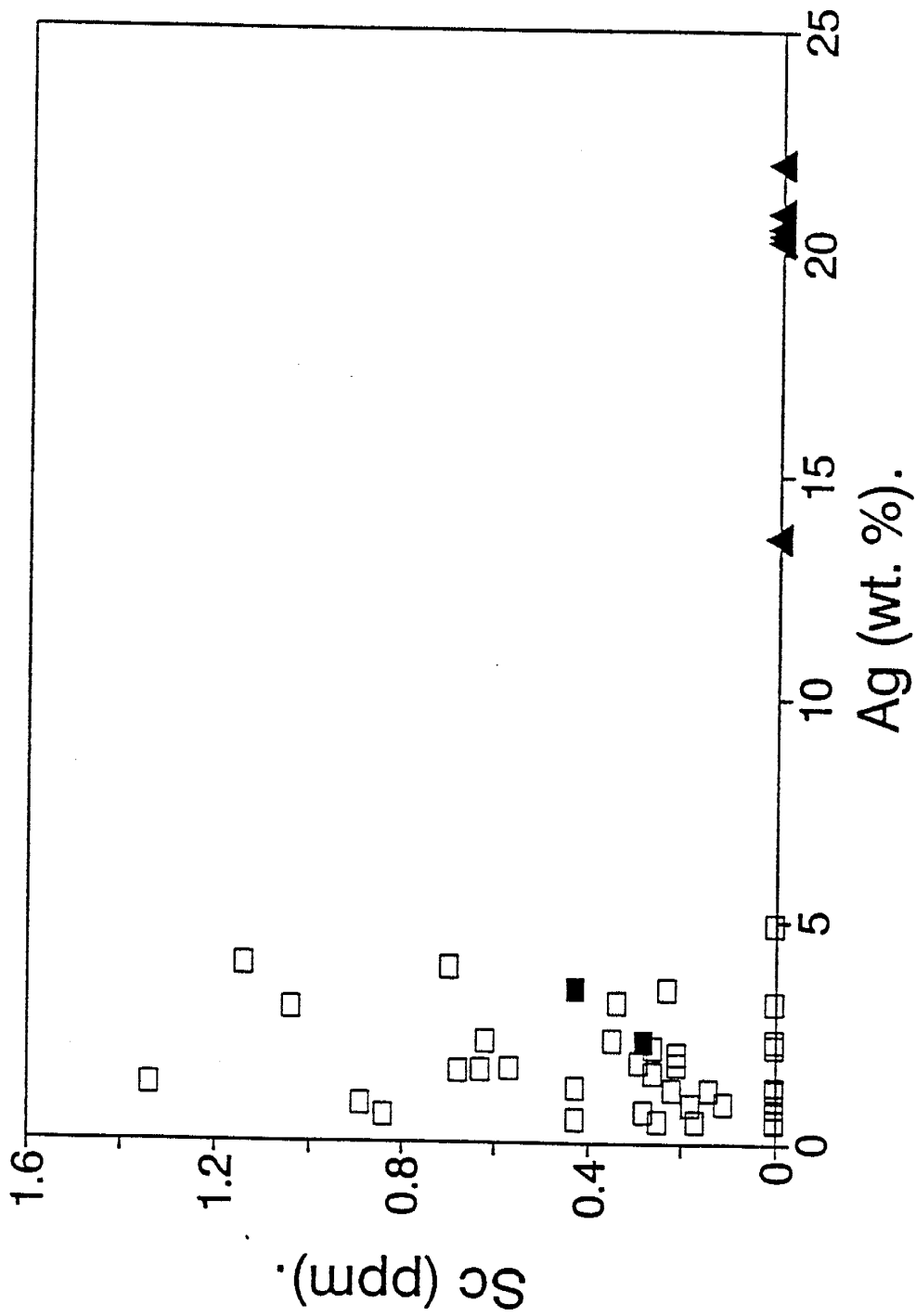
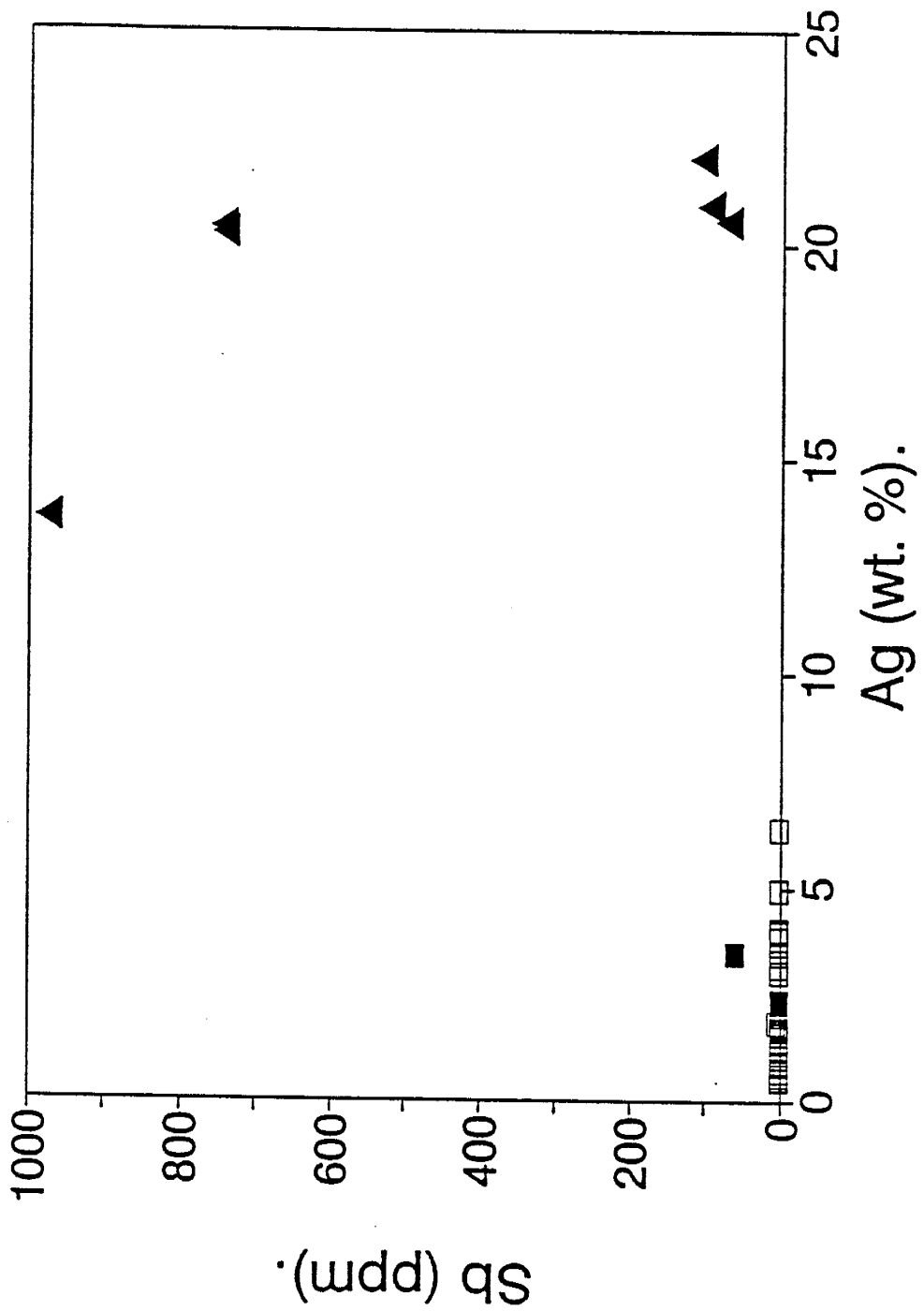


FIG. 2.13b Composition of Tarkwa gold shown on a Sb - Ag plot.



□ LATERITE ▲ PRIMARY ■ TARKWA

LITHIC FRAGMENTS

A total of 18 lithic fragments of the Kawere (2) and Banket Formations (16) obtained from Abooso, Agona Wassa, near Bonsaso, Teberebie and Iduapriem (Fig. 2.2) were studied by petrographic and geochemical methods. The lithic fragments are samples of source rocks that furnished gold into Tarkwa basin. They thus provide important clues on the origin of the Tarkwa paleoplacer, particularly the nature of its source terrane.

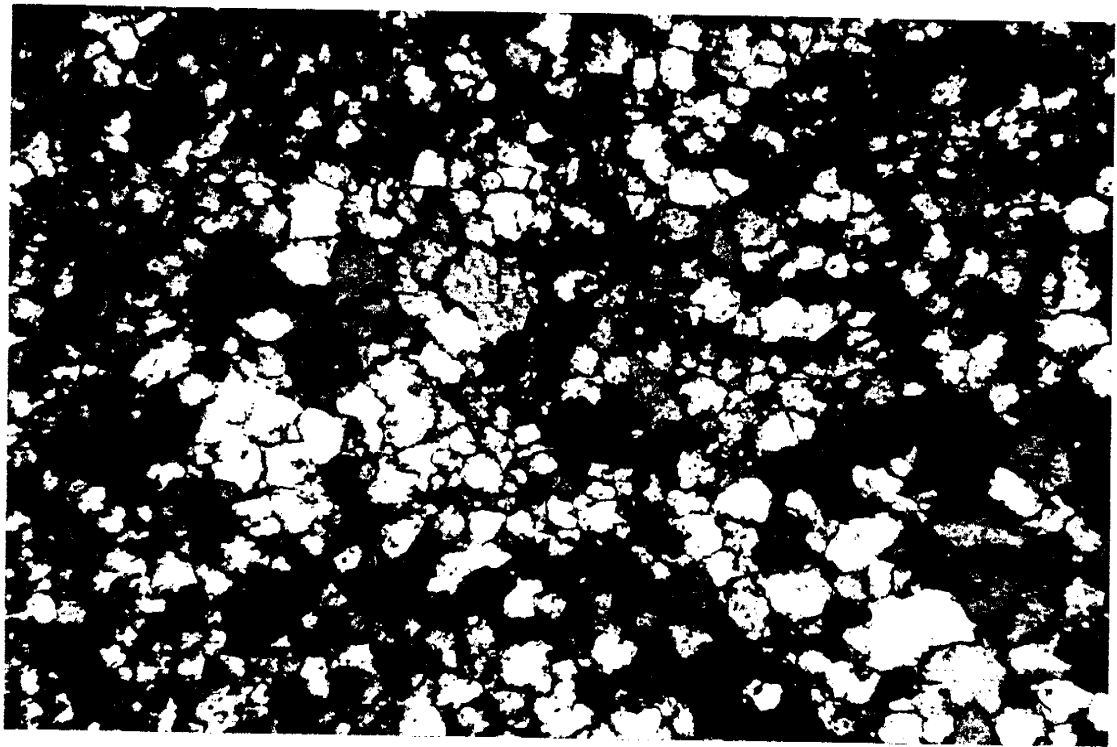
Petrography

The mineralogy of lithic fragments from the Kawere consists of quartz, sericite and chlorite with minor to accessory amounts of tourmaline and magnetite. Some opaque minerals have shapes reminiscent of arsenopyrite crystals observed in the Birimian rocks. These are commonly leached out leaving behind euhedral rhombic cavities. Others are variably oxidized, are opaque to translucent in transmitted light and surrounded by an iron oxide halo. Under reflected light, the opaque phases were found to be largely magnetite and hematite. Coarse chlorite flakes form at the margins of magnetite and other opaque crystals.

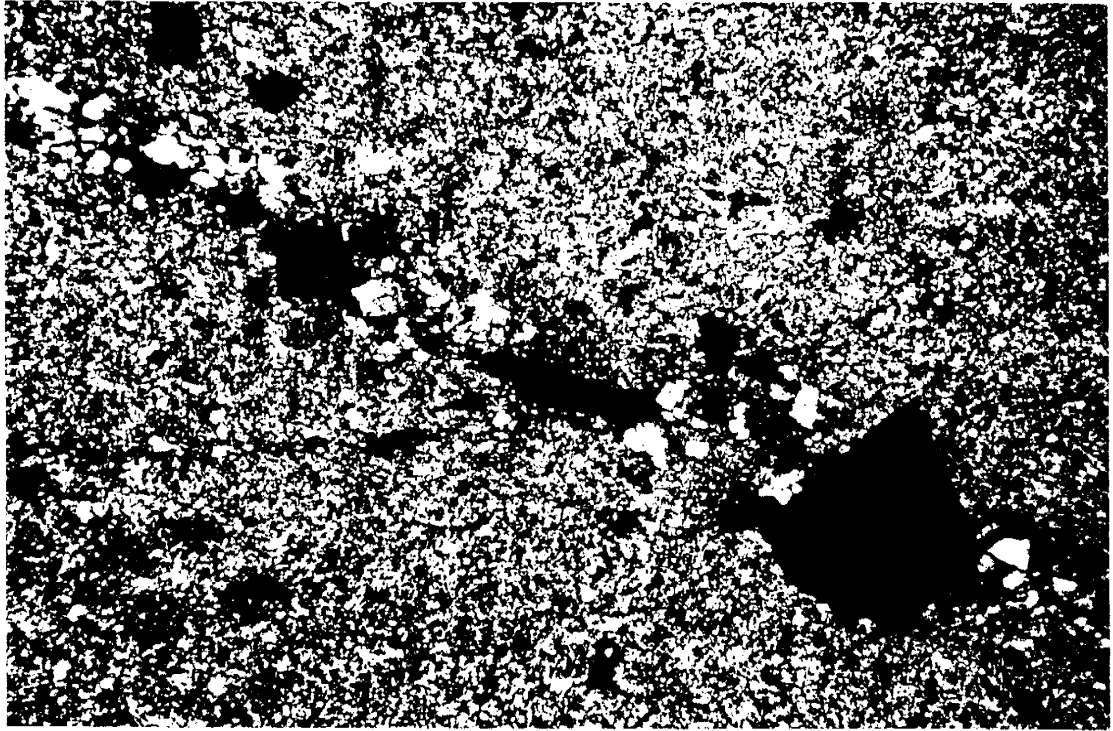
Lithic fragments of the Banket Formation studied include volcanic fragments and chert. The volcanic fragments have a simple mineralogy consisting essentially of quartz and

sericite. Broken quartz crystals with non-undulose extinction and lathes of feldspars now altered to sericite are common in these fragments and indicate relict eutaxitic textures. Coarse muscovite flakes occur in the volcanic fragments in addition to the fine sericite. Together, these micas constitute the dominant assemblage in the fragments. Iron oxides occur as an accessory dispersed phase and with an earthy appearance that suggest they probably formed by supergene processes. Euhedral casts after arsenopyrite crystals are present in the fragments associated with minute quartz veins or as disseminations (Fig 2.14). Mineralogy and texture observed in the volcanic fragments, in particular the high content of sericite and coarse muscovite, indicate their protolith was an altered, felsic tuff. Minerals such as chlorite and carbonates common in altered Birimian rocks, and epidote and actinolite in unaltered Birimian (Senger, 1984; Junner, 1932; Hirdes and Leube, 1989) were not observed in any of the Banket fragments examined indicating that the volcanic fragments differ in composition from volcanic rocks in exposed Birimian terranes adjacent to the Tarkwa basin. Other thin sections of Banket fragments show rocks composed almost entirely of polygonal equigranular quartz and accessory hematite. These fragments are interpreted to be recrystallized cherts.

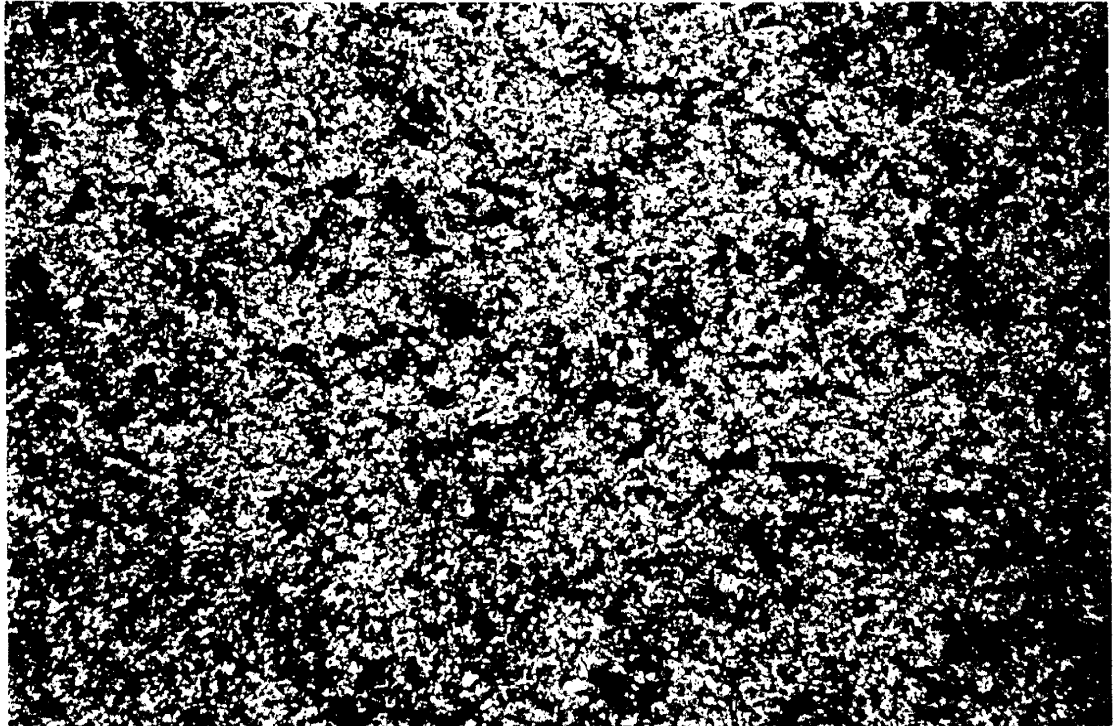
FIG. 2.14 (a) Photomicrograph of recrystallized chert fragment in the immature Banket sediments at Teberebie. (b) Volcanic fragment from the Banket Formation at Iduapriem; mineralogy: quartz and sericite. Mineralized quartz stringer with casts of arsenopyrite reflects nature of mineralization in source terrane. (c) Volcanic fragment from Iduapriem. Consists mainly of quartz and sericite with acicular minerals that appear to be pseudomorphous after arsenopyrite. Field of view is 1.0 mm for a-c.



(a)



(b)



(c)

Geochemistry

Data on major and trace element analyses of basement Birimian metavolcanic and volcanoclastic rocks, and of lithic fragments from the Banket and Kawere Formations are in Appendix 2-A. Representative analyses are given in Table 2.3.

Major element chemistry of volcanic lithic fragments from the Banket Formation indicates they are highly aluminous with normative corundum values of 5 to 15 wt. %, compared with 0 to 2 wt. % for samples from the adjoining Birimian metavolcanic terrane. The Kawere fragment is less aluminous with 2.38 wt % normative corundum. Volcanic fragments from the Banket show a marked depletion in Ca, Na and Mg, and have low loss on ignition values (0.1 - 3.5 wt. %). The moderate to high contents of chlorite and carbonates minerals in most of the Birimian samples is reflected in their major element chemistry by higher loss on ignition values of up to 31 wt. %.

Trace element contents of the volcanic and volcanoclastic rock fragments from the Banket and Kawere Formations, and samples from the basement Birimian greenstone terrane are compared with those of Phanerozoic volcanic rocks on a Zr/TiO₂ versus Nb/Y variation diagram after Winchester and Floyd (1977). The lithic fragments are indicated on this immobile element plot to have protoliths with dacite to rhyodacite compositions.

Table 2.3 Selected geochemical data on Birimian metavolcanic (#), volcanoclastic (*) rocks, and volcanic fragments (Lf) from the Basket Formation.

%	CBR-3*	N-3*	-64AR1#	-65AR3#	Lf-1	Lf-11
SiO ₂	56.80	59.02	45.69	56.66	65.41	76.03
TiO ₂	0.57	0.45	1.12	0.46	0.55	0.28
Al ₂ O ₃	16.87	15.10	11.14	12.26	21.09	14.07
Fe ₂ O ₃	6.29	4.97	12.51	6.48	2.79	2.99
MnO	0.07	1.26	0.22	0.14	0.01	0.10
MgO	2.96	2.67	5.24	2.91	0.41	0.14
CaO	1.29	2.81	4.62	6.21	0.02	0.02
Na ₂ O	4.32	1.95	2.08	2.25	1.10	0.65
K ₂ O	2.44	2.38	0.35	0.91	4.03	3.44
P ₂ O ₅	0.12	0.11	0.14	0.11	0.09	0.04
LOI	7.44	7.86	15.25	10.68	3.48	1.77
Total	99.19	98.59	98.36	99.07	98.99	99.54

(ppm)

Pb			10		19	16
Th						
Rb	91	65	13	25	111	86
U					5	
Sr	247	163	186	522	274	135
Y	18	17	30	9	54	13
Zr	145	123	100	75	256	140
Nb	8	5	4	5	8	7
Mo	1	1	1			
Ga	20	19	16	14	23	17
Zn	77	68	97	45		
Cu	30	31	39	31		
Ni	39	55	26	20	24	14
Nb/Y	0.44	0.29	0.13	0.56	0.05	0.05
Zr/TiO ₂	0.03	0.03	0.01	0.02	0.15	0.54

Q	14.24	28.66	12.14	24.22	44.31	59.23
C	5.54	4.95			15.63	9.51
Or	15.81	15.57	2.55	6.12	25.00	20.85
Ab	40.04	18.26	21.41	21.65	9.80	5.65
An	6.18	14.63	24.35	23.55		
Di				8.89		
Hy	14.06	14.61		12.66	2.72	2.78
Ol			2.05			
Mt	2.65	2.11	29.24	1.63	1.32	1.38
Il	1.19	0.95		1.00	1.10	0.55
Ap	0.30	0.28		0.28	0.05	0.48

FIG. 2.15 Zr/TiO_2 versus Nb/Y variation diagram (after Winchester and Floyd, 1977) for samples of Birimian meta-volcanic rocks (\blacktriangle), Birimian volcanoclastic rocks (\triangle) and volcanic fragments from the Banket Formation (\circ).

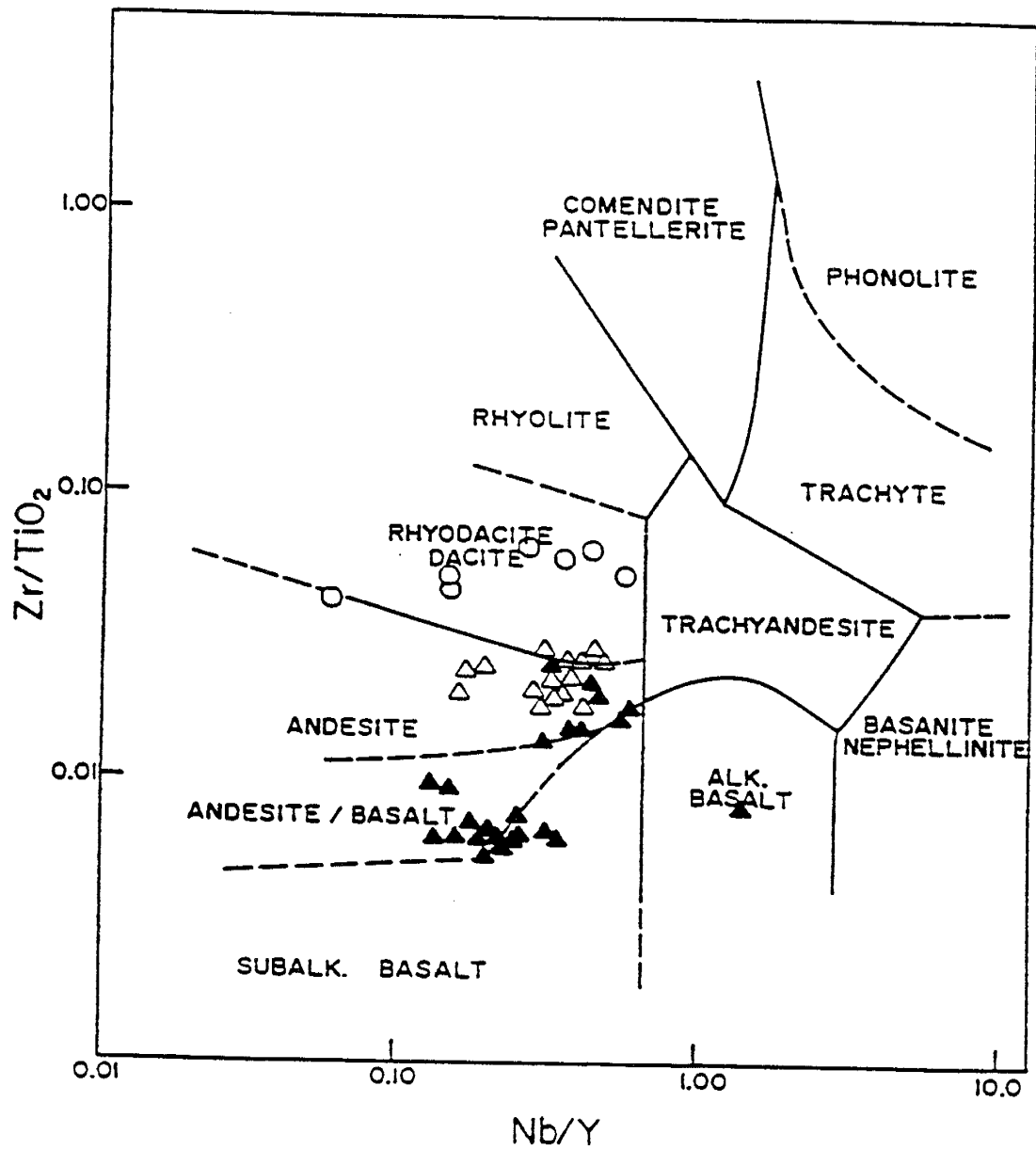


Table 2.4. Instrumental neutron activation analysis of lithic fragments from proximal sediments.

Sample ID	ppb			ppm			
	Au	Ag	Cu	Zn	As	Sb	W
IBL-1	3330	0.3	-	4	3	0.8	-
IBL-2	150	0.2	15	10	2	0.6	4
IBL-3	230	-	2	2	1	-	-
IBL-4	65	-	38	136	2	1.5	-
IBL-5	-	-	16	42	-	1.8	-
IBL-6	48	-	14	8	2	0.5	3
IBL-7	340	-	7	7	1	0.8	6
IBL-8	340	-	6	4	3	1.4	5
IBL-9	5660	-	29	11	3	0.9	4
IBL-10	869	-	-	-	-	0.9	-
IBL-11	97	-	15	7	2	0.6	2

Analysis performed at Bondar-Clegg Geochemical Laboratory, North Vancouver, B.C. Samples IBL-4 and IBL-5 were obtained from the Kawere Formation. All other samples are from the Banket Formation.

Samples of the basement Birimian rocks are, however, indicated to have protoliths whose composition range from subalkaline- and alkaline-basalts to andesites (Fig. 2.15).

Samples of lithic fragments were analysed for gold and other trace elements by INAA (Table 2.4). Nine of the samples were obtained from the Banket Formation at the Iduapriem and Teberebie areas, two others (IBL-3 and IBL-5) were from outcrops of the Kawere Formation at Abosso and Agona Wassa. One sample from the Kawere Formation contained less than 5 ppb gold. All of the other samples, however, contained elevated levels of gold ranging from 48 to 5660 ppb. Gold levels in the lithic fragments are comparable to the range of values in the immature sediments that host the fragments. The levels are also similar to the range of values obtained on Birimian samples from zones of disseminated sulphide ore adjacent to the mineralized vein systems at Prestea, and to values in meta-volcanic and -volcaniclastic rocks bordering the Buesi-chem or crush zone type mineralization in the Bogosu area (Mumin et al., 1988). Drill core data from both areas indicate that zones of sulphide mineralization with such elevated gold levels are discontinuous and generally less than 200 meters wide (Flach, personal comm. 1989). Lithic fragments analysed in this study were collected from a geographically wide area. Their occurrence in the Banket formation, with gold grades

comparable to gold levels in zones of sulphide mineralization within exposed Birimian terranes indicate the presence of similar but much broader primary gold mineralization in the source terrane of the Banket Formation.

Rubidium - Strontium isotopic systematics

Rb-Sr isotopic analyses were performed on 7 samples of Birimian metavolcanic rocks from the Prestea area, and on 6 volcanic fragments from Teberebie and Iduapriem (Table 2.5). Rb and Sr concentrations were determined by XRF, and $^{87}\text{Sr}/^{86}\text{Sr}$ ratios obtained by isotope dilution thermal-ionization mass spectrometry at the University of New Mexico Geochronology laboratory. Analytical procedure given in Ward (1986) was followed in preparing samples for isotopic analysis. Samples weighing between 95 and 120 mg (crushed to -100 mesh using a swing or Tema mill) were digested in 5 ml HF (reagent grade) and 5 ml HNO_3 (vycol distilled) at 140°C in teflon jars. After two days, they were evaporated to dryness. Residue from each sample was dissolved in 2.5 ml of 2.5 N HCl (distilled) and spun for 20 to 40 minutes at 2300 rpm in centrifuge tubes. Sr^{2+} was separated from other cations by ion exchange chromatography using Dowex AG50W-X8 resin and 2.5 N distilled HCl eluant. Sr fractions collected were evaporated to dryness, redissolved in 1 ml 2.5 N HCl and again evaporated to dryness. Three microliters of fuming HNO_3 were added to the residue at this point, to destroy any organic matter picked up from exchange column. Residues were each dissolved in 3 microliters of 2.5 N HCl; 0.75 to 1.5 microliters of resulting solutions were loaded on tantalum filaments and analysed. Isochrons were calculated using a computer program, Isochron v. 4.0, based on York (1969) algorithm (Ward, 1990).

Birimian metavolcanic samples define an isochron with a date of 2.15 +/- 0.11 Ga and an initial $^{87}\text{Sr}/^{86}\text{Sr}$ ratio of 0.70057 +/- 43 at 95% confidence level (Fig 2.16a, Table 2.5). The low initial isotopic ratio of Birimian samples indicate they represent a new crust derived from a mantle source (Taylor et al., 1988). Isotopic data on samples of the lithic volcanic fragments scatter between the 2.15 Ga isochron and a 1.968 Ga isochron obtained by Taylor et. al. (1988) for post Tarkwaian granitoids (Fig. 2.16b). The data suggest that the volcanic fragments have similar isotopic systematics as the Birimian metavolcanics. The scatter in the data on the volcanic fragments may be the result of one or a combination of the following: a) weathering in source area, b) hydrothermal alteration associated with mineralization in the fragments and c) post depositional interaction of the fragments with fluids in the permeable Tarkwa sedimentary units.

The initial $^{87}\text{Sr}/^{86}\text{Sr}$ ratio obtained for the the Birimian samples overlap with calculated $^{87}\text{Sr}/^{86}\text{Sr}$ ratio of 0.7008 for depleted mantle at 2.15 Ga. The isotopic data thus indicate derivation of Birimian metavolcanic rocks from a depleted mantle. The isochron age of 2.15 +/- 0.11 Ga and depleted mantle source for Birimian metavolcanic rocks agree with Sm/Nd age of 2.166 +/- 0.066 Ga and an initial epsilon-value of +2.0 for the Birimian rocks (Taylor et al., 1988; Hirdes et al., 1987).

Table 2.5. Rb-Sr isotopic analysis of Birimian meta-volcanic rocks, and lithic volcanic fragment (with LF prefix) from the Tarkwa basin.

ID	Rb ppm	Sr ppm	$^{87}\text{Sr}/^{86}\text{Sr}$	$^{87}\text{Rb}/^{86}\text{Sr}$
LF-12	12	62	0.71643	0.56046
LF-11	86	135	0.75360	1.85138
LF-1	111	274	0.73565	1.17529
LF-10	32	163	0.71986	0.56867
LF-17	23	63	0.73140	1.05871
Lf-21	42	66	0.75158	1.84906
-65AR2	57	336	0.71564	0.49120
-64AR6	32	500	0.70652	0.18514
-67AR1	94	608	0.71413	0.44759
-64AR10	30	261	0.71105	0.33266
CBR-4	63	296	0.71734	0.61637
-64AR1	13	186	0.70660	0.20219
-65AR4	37	429	0.70833	0.24955
-67AR3	38	336	0.71094	0.32731

FIG. 2.16a Whole rock Rb-Sr isochron diagram of Birimian
metavolcanic rocks from Prestea.

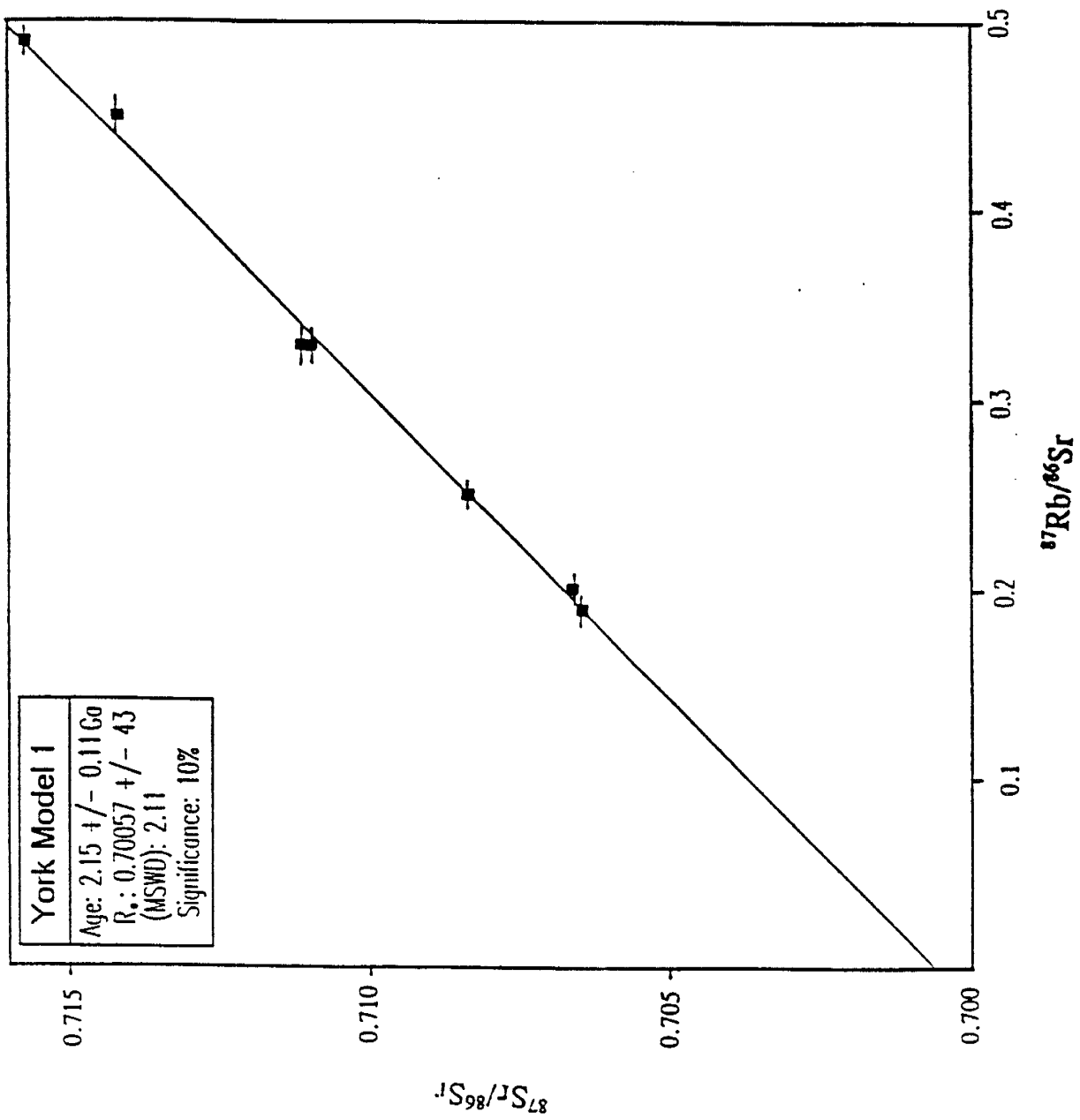
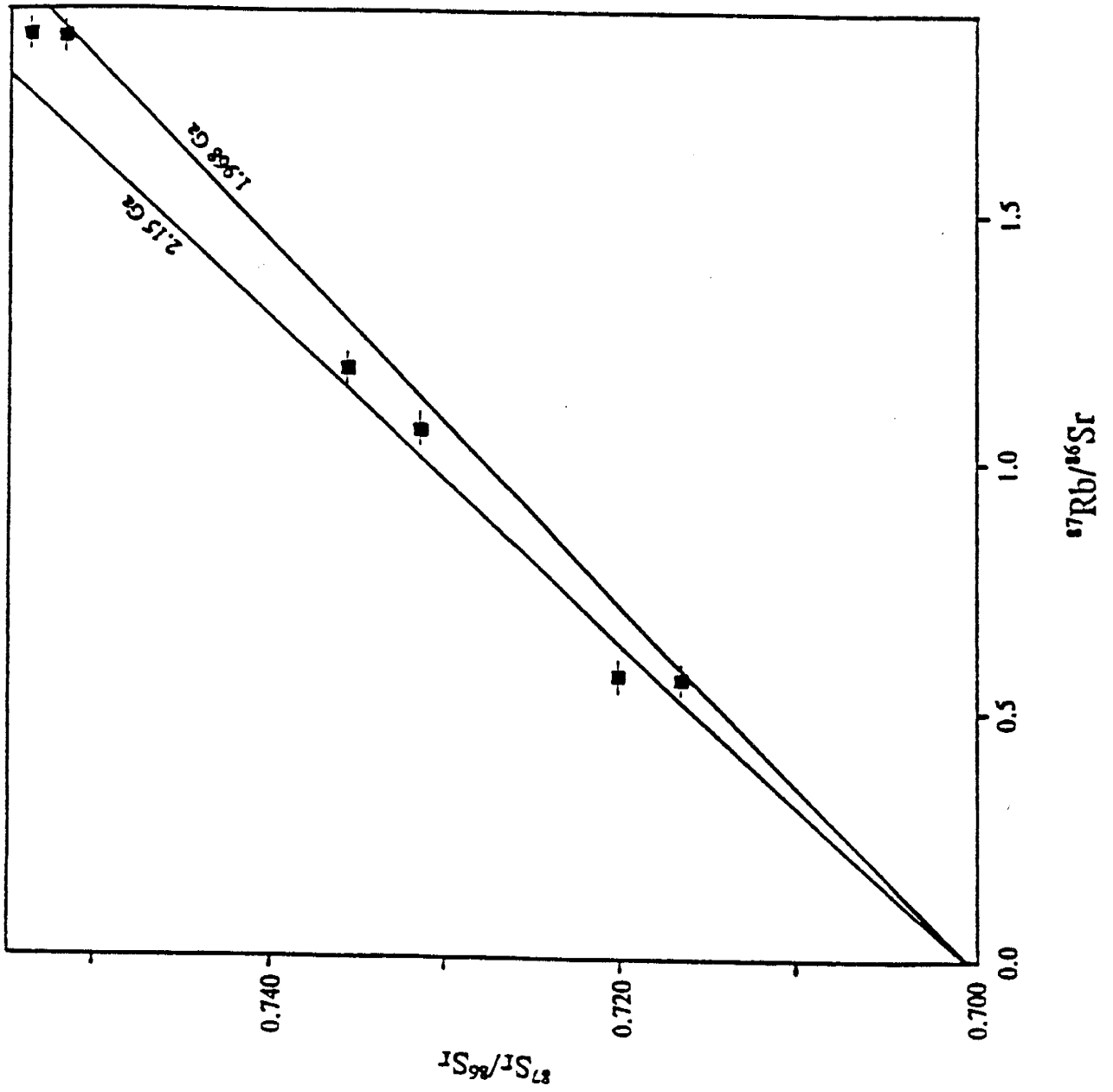


FIG. 2.16b Isotopic data on volcanic fragments from the Banket Formation compared with 2.15 Ga isochron for Birimian metavolcanic rocks, and with 1.968 Ga isochron of Taylor et al., (1988) for post Tarkwaian granitoids.



DISCUSSION

Source of gold

Evidence that formations comprising the Birimian Supergroup are the source of gold and sediments in the Tarkwa basin is compelling. The angular pelitic and volcanic fragments in immature Banket sediments could not have survived much transport and are clearly proximal to the sediment source. In southwestern Ghana, the Birimian Supergroup is the only rock unit older than the Tarkwaian sediments (Taylor et al., 1988) and as a consequence the only possible sediment source, at least, for the immature sediment that are indicated to be locally derived. Similar isotopic systematics for volcanic fragments from the Banket Formation and for Birimian meta-volcanic rocks support derivation of the fragments from the Birimian Supergroup.

Composition and nature of source terrane

Petrographic and trace element data indicate a source terrane with abundant felsic volcanic rocks for the Banket sediments in contrast with the metamorphosed mafic to intermediate volcanic and volcanoclastic rocks that now flank the Tarkwaian sediments and constitutes the bulk of exposed Birimian terrane. The association of cherts and volcanic fragments in proximal facies of the Banket Formation suggest their deriva-

tion from a submarine volcanogenic package of rocks. Cherts with minor sulphides and gold contents averaging 108 ppb occur within exposed Birimian rocks in southwestern Ghana (Hirdes and Leube, 1989). The chert-felsic volcanic fragment association in the Banket sediments is interpreted to indicate a source area underlain by the felsic component of the same submarine volcanogenic package present in exposed Birimian terranes.

Several lines of evidence suggest that the source terrane of Banket sediments was weathered. The quartz - sericite assemblage of lithic volcanic fragments from the Banket indicate either chemical weathering or a pervasive alteration of feldspars in the fragments. Depletion in Ca, Na and Mg in the fragments and their aluminous nature are both indicative of weathering (Robb and Meyer, 1990). Chemical weathering in humid tropical environments result in the alteration and subsequent break down of feldspars with removal of silica in ground water and concentration of alumina (Krauskopf, 1979; Thomas, 1974). Abundant hematite in matrix of Banket sediments compared with a magnetite rich matrix for modern placers suggest a prolonged period of oxidizing (weathering) conditions at the source area of the sediments. Small angular fragments in debris flow units of the Banket support this interpretation as do the chemical data on gold grains from Tarkwa indicating compositions similar to that of gold from

lateritic soils developed over deeply weathered Proterozoic bedrock. The chemical data indicate gold in the Banket Formation was once dissolved and reprecipitated in soils to include mineral grains such as zircon, monazite and sphene found in soils (Boadi and Norman, 1991; Boadi et al., in prep.). Further evidence for weathering in source area is provided by rounded quartz pebbles in the debris flows. The pebbles suggest drainages were well established in source area; pebbles from gravel deposits were incorporated as debris flows accessed the basin along the drainages.

Nature of mineralization in source terrane

The broad areal distribution of auriferous sediments in the Tarkwa basin at uniform grades over large areas in proximal portions of the basin, suggests a basin that was fed by an network of gold-bearing streams draining a large catchment area with anomalous to ore grade levels of gold (0.1 - 6.0 ppm). Mineralized chert and volcanic fragments occurring over a wide geographic area in the basin are further indications of the extensive nature of mineralization in source terrane. The package of submarine volcanogenic rocks indicated for the source terrane of the Banket sediments, and constituting the Birimian Supergroup (Leube et al., 1990) are good hosts for large exhalative deposits (Franklin et al., 1981). Broadly disseminated mineralization of the type envisaged for the

source of deposits in the Tarkwa basin occur in similar package of rocks in the Abitibi and Matagami greenstone belts, Ontario and Quebec, respectively, Canada (Walker et al., 1975; Ridler, 1976), in the United Verde deposit at Jerome, Arizona (Dewitt and Waegli, 1989) and in the Bukon Jedeh area of eastern Liberia where gold is in lateritic soils and in deeply weathered basement rocks (Boadi and Norman, 1990; Boadi et al., 1992). Disseminated auriferous sulphides and cherts with sub-economic gold mineralization in the Birimian Supergroup (Hirdes and Leube, 1989) are manifestations of exhalative deposits that were better developed in the upper and more felsic members of the Birimian.

Placer Formation and concentration of gold in basin

Important factors necessary for the formation of large gold placers include rapid sedimentation from a mineralized source into a basin, and the contemporaneous or subsequent concentration of gold by mechanical processes (Sutherland, 1985; Henley and Adams, 1979). Concentration (reworking) involves removal and transportation of certain mineral fractions downstream until a hydraulic equivalence of light and heavy minerals is obtained (Force, 1991; Buck and Minter, 1985). Rapid sediment supply into the Tarkwa basin is indicated by debris flows in proximal sediments. The indicated weathered sediment source would erode readily following uplift and development of the basin. Concentration of gold in the sediments commenced in

source area with weathering. Mass solutional loss of up to 40 % of bedrock can occur during chemical weathering resulting in substantial enrichment of gold and other resistant minerals (Thomas, 1974; Sutherland, 1985). Mineralized lithic fragments and concentration of gold in debris flows reflect levels of gold in sediments supplied to the Tarkwa basin. Lenses of mature conglomerates, hematitic cross-bedded sands, and erosional surfaces in debris flows indicate periods of low sediment supply from source area; sediments already in the basin were reworked during such intervals resulting in more mature units and concentration of gold (Sutherland, 1985; Yeend, 1974). Alternation in supply may be due to uplift or tilting associated with a high tectonic or igneous activity. A high igneous activity and tectonically unstable history during deposition of the Tarkwa sediments are indicated by mafic and felsic dykes and sills, and by the deformation of the succession (Junner et al., 1942; Leube et al., 1990). Measured paleocurrent directions in the Tarkwa basin (Sestini, 1973; Norman, personal comm.) are consistent with derivation of the mature conglomerate units from the debris flows. A trend towards sediment maturity with a corresponding increase in gold values within the basin is further indicated by the change in facies type north-northeastward and suggest reworking of sediments was more prevalent in the distal areas and progressed along axis of the basin.

Average gold content of 9 ppm in mature conglomerate bands from distal portion of the basin represents approximately six times enrichment over the average gold content in sediments to the south, or up to twenty times enrichment over values in unworked sediments. In the northern parts of the basin, the Basket Formation averages 120 meters thick. Most gold here is concentrated within a total of 4 meters of this thick column of sediment. If an average gold grade of 0.05 ppm is assumed for the remaining 116 meters of the basket sediments, an overall average of the Basket sediments is 0.35 ppm¹. This simple calculation serves to illustrate the fact that the high levels of gold present in reefs at Akoon, Apinto and Fanti areas can be adequately explained by reworking of low grade proximal sediments whose gold is dispersed through a thick column of immature sediments and concentrating the gold, in thin workable zones represented by the reefs.

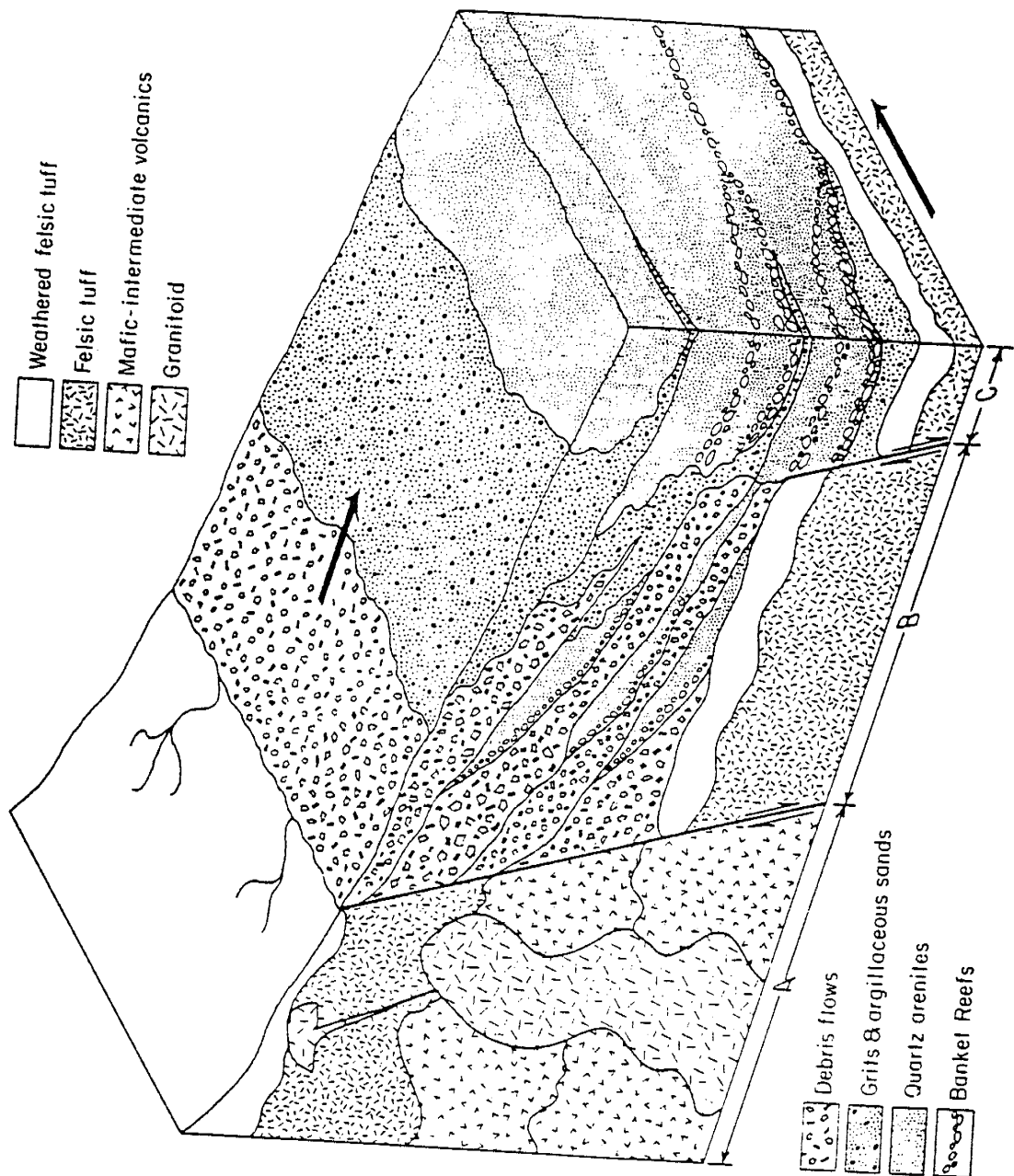
Model

The Tarkwa deposit is envisioned to have formed as the result of the following events. Gold was derived from a source terrane with regionally extensive anomalous gold concentrations. It was first liberated from associated sulphides and pre-concentrated in soils by chemical weathering. Enriched

¹Overall average grade of Basket sediments in the northern portion of the Tarkwa basin is given by: $\{(9\text{ppm} \cdot 4\text{m}) + (0.05\text{ppm} \cdot 116\text{m})\} / 120\text{m} = 0.35\text{ppm}$

soils and regolith material with grades of 0.1 - 6 ppm gold were rapidly shed into a basin as debris flow during uplift, in response to a high tectonic and igneous activity associated with the Eburnean event, to form the immature sediments at the entry points of the basin. Reworking by removal of light mineral fraction and its transport downstream resulted in mature conglomerates in which gold and other detrital heavy minerals were concentrated (Fig. 2.17).

FIG. 2.17 Schematic representation of a model for the formation of mega-gold placers. Essential factors in this model are (a) a deeply weathered source terrane with regional scale mineralization, (b) rapid sedimentation into an adjacent basin and (c) extensive reworking of sediments and mechanical concentration of gold in mature sedimentary units within basin.



CONCLUSIONS

1. The source material for the Tarkwa deposit contained elevated levels of gold ranging from 0.1 to 6 ppm and was shed into the basin as debris flows.

2. Gold was derived from soils and regolith mantle developed over broad low grade disseminated mineralization in predominantly felsic Birimian rocks.

3. Gold in proximal areas of the basin is dispersed through a thick unworked sedimentary column with grades that reflect gold contents in sediments at source. These immature sediments were reworked in distal portions of the basin to form the more productive mature conglomerates. The generally higher content of gold in mature conglomerates in these ancient deposits is the result of extensive reworking over a prolonged period of time, of sediments whose initial concentrations of gold were similar to levels obtainable in modern placers. The reefs thus represent several orders of magnitude enrichment of gold out of enormous quantities of much lower grade auriferous sediments.

4. Volcanic fragments from the Banket Formation represent an upper felsic component of the Birimian Supergroup in which gold mineralization was broadly distributed. Indicated source

rocks of the Banket Formation were extracted from a depleted mantle source at about 2.1 Ga.

5. The data on Tarkwa suggest that promising areas to explore for this type of deposits are enclosed tectonic basins in terranes with broad disseminated gold mineralization and paleoclimatic conditions, at time of sedimentation, favoring deep chemical weathering.

REFERENCES CITED

- Amanor, J.A and Gyapong, W.A, 1988, The geology of Ashanti Gold fields (Ashanti Goldfields Corporation unpublished report).
- Appiah, H., Norman, D. I. and Boadi, I., 1991, The geology of the Prestea and Ashanti goldfields: a comparative study. In Brazil Gold '91, E. A. Ladeira, ed. p. 247-255.
- Armstrong, G. C., 1966, Sedimentological control on gold mineralization in the Kimberley reefs of the East Rand goldfield: Univ. Witwatersrand Econ. Geol. Res. Unit Inf. Circ. 47, 24 p.
- Bateman, J. D., 1958, Uranium bearing auriferous reefs at Jacobina, Brazil; Econ. Geol., v. 53, p. 417-425.
- Boadi, I. O. and Norman, D. I., 1990, Formation of gold nuggets in laterite soils, Bukon Jedeh, Liberia, West Africa, in Geological Society of America abstracts with programs, vol. 22, No. 7, p. A43.
- Boadi, I. O. and Norman, D. I., 1991, Source terrane for the Tarkwa paleoplacer deposit, Ghana, in Geological Society of America abstracts with programs, vol. 23, No. 5, p. A 419.
- Boadi, I. O., Norman, D. I. and Kyle, P. R., in prep., Formation of gold nuggets in lateritic deposits, Bukon Jedeh, eastern Liberia.
- Bonhomme, M., 1962, Contribution a l'Etude Geochronologique de la Plate-forme de l'Quest Africaine, These Clermont. Ann. Fac. Sci. Univ., Clermont-Ferrand, 5 Geol. Mineral. 62 pp.
- Bowell, R. J., Gize, A. P., Hoppis, H. A., Laffoley, N. A., and Rex, A. J., 1991, Mineralogical and chemical characteristics of a tropical weathering profile in Ghana: Implications for gold exploration, in Brazil Gold '91, E. A. Ladeira, ed. p. 713-719.
- Boyle, R. W., 1979, The Geochemistry of Gold and Its Deposits: Geological Survey of Canada Bulletin 280, 584 p.
- Buck, S. G. and Minter, W. E. L., 1985, Placer formation by fluvial degradation of an alluvial fan sequence: carbon leader placer, Witwatersrand Supergroup, S. Africa. J. geol. Soc London, 142, p. 757-764.
- Cooper, W. G. G., 1934, The geology of the Prestea gold field. Gold Coast geol. surv. Mem. 3, 20 pp.
- Davidson, C. F., 1953, The gold - uranium ores of the Witwa-

- tersrand; Mining mag., v. 88, p. 73-85.
- 1964, The mode of origin of banket orebodies; Trans. Inst. Min. Metall. v. 74, pt. 6, p. 319-338.
- Dobkins, J. E. Jr. and Folk, R. L., 1970, Shape development on Tahiti-Nui; Jour. Sed. Petr. v. 40, No. 4, p. 1167-1203.
- Eales, H. V. and Reynolds, J. M., 1983, Factors influencing the composition of chromite and magnetite in some southern African rocks. Spec. publ. Geol. Soc. S. Africa, 7, 5-20.
- Erasmus, C. S., Sellschop, J. R. P. and Hallbauer, D. K., 1982, Major amounts of mercury in native gold from Upper Witwatersrand sediments: Council for Mineral Technology (MINTEK) Rep.M 54, 18 pp.
- Force, E. R., 1991, Placer deposits, Reviews in Econ. Geol. vol. 5, p. 131-140.
- Franklin, J. M., Lydon, J. W., and Sangster, D. F., 1981, Volcanic-associated massive sulfide deposits: Econ. Geol., 75th Anniversary vol. p. 485-627.
- Graton, L. C., 1930, Hydrothermal origin for the Rand gold deposits; Econ. Geol., v. 25, suppl. to No. 3, 185 p.
- Gyapong, W. A., 1980, Factors controlling ore localization at Ashanti Mine, Ghana, MSc thesis, Imperial coll. London, 182 p. (unpubl.).
- Henley, R. W. and Adams, J., 1979, On the evolution of giant gold placers. Trans. Instn. Mining Metall. 88, B41-50.
- Hirdes, W. and Leube, A., 1989, On gold mineralization of the Proterozoic Birimian Supergroup in Ghana, West Africa. Rep. on Technical Cooperation Project No. 80.2040.6, Ghana-German Mineral Prospecting Project.
- Hirdes, W. Saager, R. and Leube, A., 1987, The Tarkwaian Group of Ghana: New aspects relating to its tectonic setting, structural evolution, gold mineralization and provenance area; Int. conf. on metallogeny related to tectonic, Arusha, pp. 19-20 (abstract).
- 1988, New structural, radiometric, and mineralogical aspects of the gold-bearing Tarkwaian group of Ghana (abs.): Proc. vol., Int. conf. on the geology of Ghana with special emphasis on gold. Comm. 75th Anniversary of Ghana Geol. Surv. Dept.

- Junner, N. R., 1932, Geology of the Obuasi goldfield. Gold Coast Geol. Surv. Mem. 2, 71 pp.
- 1935, Gold in the Gold Coast. Gold Coast Geol. Surv. Mem. 4, 67 pp.
- Junner, N. R., Hirst, T., and Service, H., 1942 The Tarkwa goldfield. Gold Coast Geol. Surv., Mem., 6, 75pp.
- Kesse, G. O ., 1982, The occurrence of gold in Ghana: Gold 82, R. P. Foster ed. p. 645-659.
- Kesse, G. O., 1985, The mineral and rock resources of Ghana: 624 pp.
- Kitson, A., 1930, Gold resources of the Gold Coast, British W. Africa; in Gold resources of the world; 15th Int. Geol. Congress, Pretoria, p. 161-168.
- Krauskopf, K. B., 1979, Introduction to geochemistry, 617 pp.
- Leube, A., Hirdes, W., Mauer, R. and Kesse, G.O., 1990, The Proterozoic Birimian Supergroup of Ghana and some aspects of its associated gold mineralization: Precambrian Res. 46 : 139-165
- Levin, V. I., 1970, Stratigraphic position and lithogenetic characteristics co gold bearing conglomerates from the Proterozoic of the Davangra - Khugdinsk graben, Aldan Plateau, USSR; in Sostoyaniye i zadachi, Sovetskoy litologii. Vses. Litol. Soveshch., 8th. Dokl., vol. 2, p. 213-219
- Mellor, E. T., 1916, The conglomerates of the Witwatersrand; Inst. Min. Metall., Trans., v. 25, p. 226-348.
- 1931, The origin of gold in the Rand banket: discussion on Professor Graton's paper; Geol. Soc. S. Africa, Trans. (Annex.), v. 34, p. 55-69.
- Meyer, M., Oberthuer, T., Robb, L. J., Saager, R. and Stupp, H. D., 1985, Ni, Co, and gold contents of pyrites from Archean granite-greenstone terranes and early Proterozoic sedimentary deposits in southern Africa: Univ Witwatersrand Econ. Geol. Res. unit, Inf. Circ. 176, 11 p.
- Minter, W. E. L., 1978, A sedimentological synthesis of placer gold, uranium and pyrite concentrations in Proterozoic Witwatersrand sediments: Canadian Soc. Petroleum Geologists, Mem. 5, p. 801-829.
- 1979, Sedimentological approach to mapping and assess

- ment of the Witwatersrand sequence: Univ. Western Australia Geology Dept., Univ. Ext. Pub. 3, p. 89-102.
- 1988, Comments on "Problems with the placer model for Witwatersrand gold": Geology, v. 16, p. 1153-1154.
- Mumin, H. A., Clarke, G. A., Flach, G. A. and Badu, F., 1988, Geology and mineralogy of gold mineralization at the Bogosu concession, Western Region, Ghana: Proc. vol., Int. conf. on the geology of Ghana with special emphasis on gold. Comm. 75th Anniversary of Ghana Geol. Surv. Dept.
- Nunoo, B. and Tsiriku, A., 1988, A brief description of the geology of the Tarkwa Goldfield (SGMC unpublished report).
- Phillips, G. N. and Myers, R. E., 1989, The Witwatersrand gold fields: Part II. An origin for Witwatersrand gold during metamorphism and associated alteration: ECON. GEOL. MON. 6, p. 598-608.
- Pretorius, D. A., 1964, The geology of the Central Rand gold field; in The geology of some ore deposits in southern Africa, v. 1, S. H. Haughton, ed., Geol. Soc. S. Africa, Johannesburg. p. 63-111.
- 1976, Gold in the Proterozoic sediments of South Africa: Systems, paradigms, and models, in Wolf, K.H., ed., Handbook of stratabound and stratiform ore deposits: Amsterdam, Elsevier, p. 1-27.
- Reinecke, L., 1927, The location of payable orebodies in the gold-bearing reefs of the Witwatersrand; Geol. Soc. S. Africa, Trans. v. 30, p. 89-119.
- 1930, Origin of the Witwatersrand System; Geol. Soc. S. Africa, Trans., v. 33, p. 111-133.
- Ridler, R. H., 1976, Stratigraphic keys to the to the gold metallogeny of the Abitibi Belt. Can. Min. J. 97(6):81-88.
- Robb, L. J. and Meyer, M., 1985, The nature of the Witwatersrand hinterland: conjectures and source area problem: Univ. Witwatersrand Econ. Geol. Research Unit Inf. Circ. 178, 25p.
- 1990, The nature of the Witwatersrand hinterland: conjectures and source area problem. Econ. Geol. vol. 85 pp 511-536.
- 1991, A contribution to recent debate concerning epigenetic versus syngenetic mineralization processes in the

- Witwatersrand basin. Econ. Geol. v. 86, p. 396-401.
- Sestini, G., 1970, Sedimentological study of the Tarkwaian gold deposits, Ghana; Univ. Leeds, Res. Inst. Afr., Geol. Dep. Earth Sci., v. 14, p. 23-26.
- 1973, Sedimentology of a paleoplacer: The gold-bearing Tarkwaian of Ghana. In ores and sediments, Amstutz, G>C and Bernard, A.J (eds.)
- Smirnov, V. I., 1969, Problem of the occurrence of metals in ancient conglomerates in the territory of the Soviet Union, "Nauka" Moscow, 192 p.
- Shand, S. J, 1947, Eruptive rocks, their genesis, composition, classification and their relation to ore deposits. 3rd Edition, 488 p. Woodbridge Ltd., Guildford.
- Strogen, P., 1988, The structure and sedimentology of the Tarkwaian, and its relevance to gold mining, exploration and development: in Proc. vol., Int. conf. on the geology of Ghana with special emphasis on gold. Comm. 75th Anniversary of Ghana Geol. Surv. Dept.
- Sutherland, D. G., 1985, J. Geol. Soc. London, v. 142, pp 727-737.
- Taylor, S. R. and McClennan, S. M., 1985, The continental crust: Its composition and evolution. An examination of geochemical record preserved in sedimentary rocks, 312 p. Blackwell Scientific Publications.
- Taylor, P. N., Moor bath, S., Leube, A. and Hirdes, W., 1988, Geochronology and crustal evolution of early Proterozoic granite-greenstone terrains in Ghana, W. Africa: in Proc. vol., Int. conf. on the geology of Ghana with special emphasis on gold. Comm. 75th Anniversary of Ghana Geol. Surv. Dept.
- Thomas, M. F., 1974, Tropical geomorphology. MacMillan, London.
- Utter, T., 1978, Raster-elektronenmikroskopische und geochemische Untersuchungen an Erzminerale aus dem Oberen Witwatersrand und Ventersdorp-System des Klerksdorp-goldfeldes, Südafrika: Unpub. PhD thesis, Univ. Frankfurt am Main, 159 p.
- Viljoen, R. P., Saager, R. and Viljoen, M. J., 1970, Some thoughts on the origin and processes responsible for the concentration of gold in the early Precambrian of South Africa: Mineralium Deposita, v. 5 p. 164 - 180.

- Ward, D. B., 1990, Rubidium-Strontium geochronology of Proterozoic rocks from the Pecos and Truchas metamorphic terranes, north-central New Mexico: in New Mexico Geological Soc. guide book, 41st Field Conf. Southern Sangre de Cristo Mountains, New Mexico.
- Winchester, J. A. and Floyd, P. A., 1977, Geochemical discrimination of different magma series and their differentiation products using immobile elements: Chem. Geol., v. 20, p. 325-343.
- Wronkiewicz, D. J. and Condie, K. C., 1987, Geochemistry of the Archean shales from the Witwatersrand Supergroup, South Africa: source-area, weathering and provenance: Geochim. et Cosmochim. Acta, v. 51, p. 2401-2416.
- Yeend, W. E., 1974, Gold-bearing gravels of the ancestral Yuba River, Sierra Nevada, Ca. : Prof. pap. U.S Geol. Surv. 772.
- York, D., 1969, Least square fitting of a straight line with correlated errors: Earth and Planetary Science Letters, v. 5, pp. 320-324.

APPENDIX 2-A

Geochemical analysis of Birimian metavolcanic (mv) and volcaniclastic (vc) rocks, and lithic volcanic fragments (lvf) from the Basket Formation.

wt. %	67AR3 mv	61CR4 mv	SML-4 vc	SML-2 mv	64AR1 mv	58DR2 mv	65AR6 mv	57AR1 mv
SiO ₂	40.40	57.41	49.80	39.77	45.69	48.19	33.07	67.53
TiO ₂	0.81	0.89	0.89	0.91	1.12	0.85	0.64	0.42
Al ₂ O ₃	11.55	7.67	17.95	14.65	11.14	15.19	11.62	15.36
Fe ₂ O ₃	11.96	8.57	12.60	10.12	12.51	12.02	10.10	3.11
MnO	0.11	0.11	0.09	0.13	0.22	0.18	0.21	0.04
MgO	6.17	2.93	5.29	5.31	5.24	8.88	6.94	1.37
CaO	6.23	5.23	6.13	7.70	4.62	10.89	13.39	2.55
Na ₂ O	3.47	4.33	0.49	3.31	2.08	2.18	2.27	4.54
K ₂ O	0.87	0.17	0.07	1.45	0.35	0.12	0.92	3.07
P ₂ O ₅	0.03	0.09	0.09	0.03	0.14	0.08	0.05	0.20
LOI	15.85	11.10	6.43	14.15	15.25	1.72	21.23	0.51
Total	97.46	98.48	99.83	97.53	98.36	100.30	100.44	98.70

(ppm)

Pb	15			10	10	17		23
Rb	38	5		63	13	3	34	100
U								4
Sr	336	900	137	423	186	108	534	1097
Y	16	16	24	22	30	19	16	7
Zr	48	58	51	57	100	51	39	159
Nb	3	4	4	4	4	4	3	7
Mo	1	1	1	1	1	1	1	1
Ga	12	7	16	4	16	16	11	20
Zn	94	51	67	90	97	95	52	58
Cu	94	156	92	143	39	107	79	11
Ni	82	43	128	211	26	158	77	17
Nb/Y	0.19	0.25	0.17	0.18	0.13	0.21	0.19	1.00
Zr/TiO ₂	0.01	0.01	0.01	0.01	0.01	0.01	0.01	0.04

CIPW MINERAL NORMS (WT. %)

Q		20.73	22.11		12.14			21.89
C			6.64					0.41
Or	6.38	1.15	0.42	10.39	2.55	0.71		18.52
Ab	31.73	42.24	4.52	18.85	21.41	18.90		39.23
An	16.52	1.14	32.26	25.22	24.35	32.07	23.96	11.58
Lc							5.45	
Ne	2.55			8.14			13.27	
Di	17.63	23.29		16.98	2.05	18.42	27.01	
Hy		5.85	27.27		29.24	18.85		5.66
Ol	18.05			13.98		4.94	15.76	
Cs							8.40	
Mt	5.15	3.43	4.73	4.26	5.29	4.28	4.47	1.43
Il	1.91	1.94	1.82	2.10	2.60	1.64	1.55	0.81
Ap	0.10	0.24	0.23	0.08	0.38	0.19	0.14	0.47

wt. %	64AR2 mv	64AR8 mv	65AR3 mv	64AR13 mv	58DR1 mv	64AR10 vc	SML-1 ¹ v	87CR1 mv
SiO ₂	45.77	25.08	56.66	42.07	52.54	42.10	56.36	40.60
TiO ₂	1.25	0.16	0.46	0.68	0.77	0.92	0.89	1.91
Al ₂ O ₃	12.19	4.75	12.26	12.54	14.48	15.46	17.04	12.42
Fe ₂ O ₃	13.15	13.31	6.48	9.41	11.35	14.24	10.71	14.37
MnO	0.20	0.28	0.14	0.15	0.18	0.15	0.07	0.20
MgO	4.92	25.15	2.91	6.09	7.17	6.21	5.24	5.32
CaO	5.56	2.45	6.21	8.82	11.02	2.70	0.14	6.50
Na ₂ O	2.42	0.27	2.25	2.35	1.53	3.25	2.80	2.55
K ₂ O	0.18	0.16	0.91	0.38	0.14	0.81	0.24	0.23
P ₂ O ₅	0.15	0.01	0.11	0.06	0.07	0.09	0.06	0.18
LOI	16.36	31.27	10.68	16.42	1.71	13.86	4.96	16.47
Total	102.16	102.90	99.07	98.98	100.96	99.78	98.51	100.77

(ppm)

Pb		12				14		
Th								
Rb	6	5	25	14		30	8	7
U								
Sr	133	28	522	206	93	261	62	189
Y	33	3	9	16	20	15	20	30
Zr	108	13	75	43	47	53	54	121
Nb	5	4	5	4	5	5	5	10
Mo	1	1	0	1	1	1	1	1
Ga	16	3	14	13	18	17	14	17
Zn	97	142	45	54	74	117	77	107
Cu	38		31	69	23	81	86	92
Ni	32	1649	20	95	138	103	150	55
Nb/Y	0.15	1.33	0.56	0.25	0.25	0.33	0.25	0.33
Zr/TiO ₂	0.01	0.01	0.02	0.01	0.01	0.01	0.01	0.01

CIPW MINERAL NORMS (wt. %)

Q	8.99		24.22		7.72		27.64	
C						5.35	13.02	
Or	1.29		6.12	2.78	0.83	5.64	1.51	1.66
Ab	24.14		21.65	24.34	13.21	32.51	25.58	25.98
An	25.79	16.00	23.55	27.54	32.78	15.12	0.36	26.18
Lc								
Ne		1.76						
Kp		12.99						
Di	4.61		8.89	20.92	18.35			9.30
Hy	26.59		12.66	15.28	22.92	27.31	27.37	22.93
Ol		81.13		4.86		8.05		5.25
Cs		0.34						
Mt	5.39	4.18	1.63	2.55	2.56	3.72	2.56	3.83
Il	2.80	0.43	1.00	1.59	1.48	2.07	1.83	4.36
Ap	0.41	0.05	0.28	0.16	0.16	0.24	0.14	0.51

¹weathered metavolcanic rock from the Konongo area.

wt. %	87DR2 mv	59DR vc	64AR6 mv	CBR-3 vc	61CR2 mv	67AR1 mv	SML-3 vc	N-3 vc
SiO2	44.47	69.30	46.28	56.80	43.87	38.87	48.54	59.02
TiO2	0.96	0.45	0.58	0.57	1.05	0.72	1.09	0.45
Al2O3	10.60	14.15	11.25	16.87	10.40	11.60	19.68	15.10
Fe2O3	11.83	4.96	8.19	6.29	13.27	10.58	14.23	4.97
MnO	0.17	0.05	0.16	0.07	0.19	0.23	0.13	1.26
MgO	4.59	1.44	3.17	2.96	4.91	4.56	4.27	2.67
CaO	8.27	0.42	9.68	1.29	6.32	9.34	4.19	2.81
Na2O	1.74	4.24	2.26	4.32	2.21	0.57	0.51	1.95
K2O	0.60	1.23	0.97	2.44	1.14	2.56	0.07	2.38
P2O5	0.11	0.08	0.17	0.12	0.27	0.02	0.11	0.11
LOI	17.01	1.81	14.91	7.44	14.90	18.67	7.59	7.86
Total	100.35	98.13	97.61	99.19	98.54	97.71	100.41	98.59

(ppm)

Pb	12	11				34		
Th								
Rb	28	45	32	91	51	94	3	65
U								
Sr	298	243	500	247	653	608	75	163
Y	18	14	15	18	22	22	32	17
Zr	60	117	27	145	66	43	62	123
Nb	4	6	3	8	5	3	5	5
Mo	1		1	1	1	6	1	1
Ga	13	15	12	20	14	18	19	19
Zn	69	45	60	77	113	103	90	68
Cu	33		35	30	50	48	67	31
Ni	39	32	13	39	50	70	204	55
Nb/Y	0.22	0.43	0.20	0.44	0.23	0.14	0.16	0.29
Zr/TiO2	0.01	0.03	0.00	0.03	0.01	0.01	0.01	0.03

CIPW MINERAL NORMS (wt. %)

Q	8.72	36.64	8.65	14.24	4.73		26.33	28.66
C		5.50		5.54			12.45	4.95
Or	4.29	7.56	6.96	15.81	8.13	19.31	0.48	15.57
Ab	17.90	37.39	23.32	40.04	22.68	6.21	4.67	18.26
An	23.46	1.64	21.56	6.18	18.23	27.51	21.85	14.63
Di	21.05		29.45		14.56	26.06		
Hy	17.09	8.21	4.79	14.06	22.92	12.87	26.30	14.61
Ol						1.56		
Mt	4.98	1.98	3.47	2.65	5.58	4.70	5.39	2.11
Il	2.22	0.90	1.33	1.19	2.42	1.75	2.27	0.95
Ap	0.30	0.19	0.48	0.30	0.76	0.05	0.28	0.28

wt. %	56AR4 mV	CBR-4 vC	56AR5 vC	55CR2 vC	87DR1 vC	58BR1 vC	NGST1 mV	64AR9 vC
SiO2	61.66	56.11	55.01	57.05	56.53	60.70	63.87	59.89
TiO2	0.60	0.56	0.72	0.74	0.58	0.70	0.60	0.58
Al2O3	14.94	14.50	17.77	18.50	15.19	19.46	13.89	16.12
Fe2O3	4.40	7.67	9.01	9.03	11.27	6.02	8.92	7.18
MnO	0.07	0.10	0.06	0.07	0.25	0.05	0.18	0.06
MgO	2.40	2.84	3.31	3.06	1.54	1.97	3.33	2.19
CaO	2.66	2.40	1.62	0.32	0.14	0.85	1.48	0.75
Na2O	4.55	2.30	2.13	1.82	1.37	2.48	4.55	1.79
K2O	1.59	1.74	2.55	2.86	2.14	2.62	0.40	2.41
P2O5	0.17	0.15	0.18	0.16	0.04	0.10	0.11	0.09
LOI	5.46	10.79	7.99	6.65	9.67	4.60	3.41	7.81
Total	98.50	99.16	100.36	100.26	98.72	99.54	100.74	98.87

(ppm)

Pb	13		16	16	10	13		12
Th								
Rb	61	63	93	101	83	75	15	76
U								
Sr	258	296	250	285	205	177	132	176
Y	22	23	25	25	41	29	13	17
Zr	141	126	145	154	130	131	83	124
Nb	8	8	8	8	7	8	5	6
Mo	1	1	1		1	1	1	1
Ga	16	17	23	22	19	23	17	18
Zn	75	103	110	87	165	71	76	68
Cu	43	46	67	28	48	74	22	28
Ni	47	54	67	50	92	34	73	41
Nb/Y	0.36	0.35	0.32	0.32	0.17	0.28	0.38	0.35
Zr/TiO2	0.02	0.02	0.02	0.02	0.02	0.02	0.01	0.02

CIPW MINERAL NORMS (wt. %)

Q	19.89	26.84	22.77	28.63	36.65	30.87	24.61	35.77
C	1.40	5.52	9.83	13.15	11.85	11.89	3.67	10.42
Or	10.12	11.70	16.43	18.17	14.32	16.40	2.45	15.76
Ab	41.56	22.16	19.63	16.59	13.16	22.20	39.84	16.71
An	13.06	12.43	7.46	0.58	0.54	3.80	6.86	3.43
Di								
Hy	10.86	17.05	18.90	17.99	18.20	11.26	18.29	14.02
Mt	1.46	2.69	3.03	3.00	3.94	1.97	2.85	2.45
Il	1.22	1.21	1.49	1.51	1.24	1.40	1.18	1.22
Ap	0.43	0.40	0.47	0.40	0.10	0.23	0.26	0.24

wt. %	65AR4 mv	56BR2 vc	N-5 mv	56AR3 vc	CBR-1 mv	63BR1 mv	56AR1 vc	65AR2 mv
SiO2	52.00	54.10	46.64	50.40	59.16	44.20	59.93	61.22
TiO2	0.61	0.75	0.39	0.53	0.44	0.85	0.63	0.58
Al2O3	16.28	17.51	11.52	12.73	14.06	16.78	14.65	14.86
Fe2O3	7.42	6.86	4.29	15.23	5.65	9.33	6.42	5.25
MnO	0.10	0.12	8.81	0.06	0.07	0.14	0.15	0.07
MgO	3.25	2.26	2.81	1.75	2.89	4.15	2.22	2.38
CaO	4.17	2.80	5.75	1.46	3.34	5.01	2.73	3.17
Na2O	4.40	1.04	1.08	1.65	3.71	1.34	1.94	3.31
K2O	1.13	3.61	1.56	2.45	1.75	2.92	2.05	1.76
P2O5	0.05	0.08	0.12	0.10	0.07	0.14	0.15	0.14
LOI	9.51	8.98	16.02	12.10	8.79	13.54	7.89	6.63
Total	98.92	98.11	98.99	98.45	99.94	98.40	98.76	99.39

(ppm)

Pb		41	12	41				10
Th								
Rb	37	173	43	104	64	155	70	57
U				8				
Sr	429	296	172	218	420	502	340	336
Y	14	24	7	36	12	20	19	14
Zr	86	179	67	122	91	108	140	110
Nb	5	9	4	7	5	6	8	6
Mo		1	1	5	1	1		1
Ga	18	37	15	23	17	21	16	16
Zn	67	93	88	341	63	77	51	51
Cu	51	43	52	873	35	39	24	43
Ni	25	54	74	137	27	47	35	37
Nb/Y	0.36	0.38	0.57	0.19	0.42	0.30	0.42	0.43
Zr/TiO2	0.01	0.02	0.02	0.02	0.02	0.01	0.02	0.02

CIPW MINERAL NORMS (wt. %)

Q	5.64	24.87	12.20	21.76	18.73	5.29	32.20	24.83
C	0.39	7.89		5.82	0.19	3.14	5.11	2.24
Or	7.52	24.06	11.16	16.98	11.41	20.53	13.42	11.29
Ab	41.92	9.98	11.07	16.39	34.63	13.45	18.18	30.36
An	22.94	15.06	26.58	7.75	17.73	28.47	13.94	16.06
Di			6.01					
Hy	17.59	13.92	30.28	24.36	14.30	23.39	13.25	11.94
Mt	2.58	2.39	1.60	5.52	1.92	3.42	2.19	1.75
Il	1.32	1.62	0.90	1.17	0.92	1.93	1.34	1.19
Ap	0.12	0.21	0.34	0.26	0.19	0.38	0.38	0.35

%	22 lvf	23 lvf	1 lvf	9 lvf	3 lvf	10 lvf	21 lvf	5 lvf
SiO2	90.62	60.69	65.41	84.97	93.53	76.52	84.80	78.13
TiO2	0.07	0.21	0.55	0.13	0.02	0.40	0.34	0.18
Al2O3	4.53	21.90	21.09	1.89	1.02	12.20	7.12	11.85
Fe2O3	0.71	3.39	2.79	9.94	2.74	4.06	1.07	1.52
MnO	0.01	0.01	0.01	0.02	0.01	0.05	0.00	0.06
MgO	0.14	0.45	0.41	0.12	0.00	0.12	0.00	0.31
CaO	0.01	0.02	0.02	0.03	0.00	0.05	0.00	0.06
Na2O	0.25	0.64	1.10	0.21	0.18	0.73	0.36	5.41
K2O	0.87	5.93	4.03	0.21	0.08	1.21	1.65	0.57
P2O5	0.04	0.02	0.09	0.04	0.03	0.23	0.05	0.05
LOI	0.57	3.13	3.48	0.10	0.04	2.91	0.94	0.66
Total	97.82	96.39	98.99	97.66	97.65	98.48	96.33	98.81

(ppm)

Pb		19	19	11	27	36		
Th		9				9	11	
Rb	22	146	111	6		32	42	14
U			5				6	
Sr	33	136	274	18		163	66	170
Y	9	12	54	4	4	100	18	19
Zr	36	126	256	20	11	159	188	111
Nb	4	5	8	4	3	6	6	5
Mo							1	
Ga	6	28	23	3	3	21	9	9
Zn						43		11
Cu						28		
Ni	5	15	24	9	8	14		
Zr/TiO2	0.05	0.06	0.05	0.02	0.06	0.04	0.06	0.06
Nb/Y	0.44	0.42	0.15	1.00	0.75	0.06	0.33	0.26

CIPW MINERAL NORMS (wt. %)

Q	87.84	34.83	44.31	81.39	93.49	69.34	79.96	44.35
C	3.27	15.51	15.63	1.36	0.65	10.17	4.98	2.38
Or	5.29	37.64	25.00	1.28	0.49	7.52	10.23	3.44
Ab	2.18	5.83	9.80	1.83	1.56	6.49	3.20	46.70
Hy	0.90	4.07	2.72	9.19	2.47	3.48	0.40	1.97
Mt	0.33	1.64	1.32	4.62	1.27	1.92	0.51	0.70
Il	0.14	0.43	1.10	0.26	0.04	0.80	0.68	0.35
Ap	0.05	0.05	0.05	0.10	0.05	0.24		0.28

%	7 lvf	17 lvf	11 lvf	CBR-2 vc	55BR4 vc
SiO2	92.74	83.65	76.03	56.34	57.38
TiO2	0.06	0.17	0.28	0.65	0.78
Al2O3	2.72	4.82	14.07	17.04	18.00
Fe2O3	1.00	7.39	2.99	8.06	7.13
MnO	0.01	0.08	0.10	0.10	0.10
MgO	0.00	0.29	0.14	2.23	2.22
CaO	0.02	0.02	0.02	0.19	1.72
Na2O	0.26	0.49	0.65	1.66	2.70
K2O	0.43	0.84	3.44	2.30	2.56
P2O5	0.02	0.06	0.04	0.13	0.16
LOI	0.28	0.70	1.77	10.28	6.54
Total	97.54	98.52	99.54	98.98	99.30

(ppm)

Pb			16	12	13
Rb	13	23	86	85	90
Sr	29	63	135	291	324
Y	3	6	13	23	23
Zr	26	39	140	137	183
Nb	4	3	7	8	9
Mo		1		1	1
Ga	4	8	17	19	22
Zn				114	84
Cu				74	33
Ni	6	8	14	76	38
Zr/TiO2	0.04	0.02	0.05	0.35	0.39
Nb/Y	1.33	0.50	0.54	0.02	0.02

CIPW MINERAL NORMS (wt. %)

Q	91.79	76.30	59.23	34.95	24.07
C	1.88	3.19	9.51	13.37	8.73
Or	2.61	5.10	20.85	15.45	16.40
Ab	2.26	4.26	5.65	15.93	24.78
An				0.13	8.12
Hy	0.83	7.32	2.78	15.60	13.51
Mt	0.46	3.42	1.38	2.82	2.38
Il	0.12	0.33	0.55	1.41	1.62
Ap	0.05	0.38	0.48	0.33	0.40

This dissertation is accepted on behalf of the faculty
of the Institute by the following committee:

Joseph M. Hornon 9 Dec. 1991
Adviser

Philip R. Kyle 9 Dec '91

Andrew R. Campbell Dec. 10, 1991

Jan M. Rhee Dec 10, 1991

Joseph O. Kene
Date